(P)

ProQuest LLC.
789 East Eisenhower Parkway
P.O. Box 1346
Ann Arbor, MI 48106 – 1346

UniS

The Mathematical Model of *Schizosaccharomyces pombe*. Batch and Repeated Batch Simulations

by

Ruben Dario Rodriguez Quintero

Submitted for the degree of Doctor of Philosophy in Chemical Engineering

Department of Chemical Engineering
School of Engineering
University of Surrey
August 2004

ABSTRACT

Mathematical models are playing an important part in the current developments in engineering, science and biotechnology. Within this field the most fashionable and representative organisms are the ones who are genetically and physiologically tractable. Since the fission yeast *Schizosaccharomyces pombe* plays a role model among them and its behaviour has medical, genetic and industrial links (related to cancer research, metabolic pathways and beer production), this makes it a particularly interesting organism for study.

This dissertation presents the first physiological model ever developed for the yeast *S. pombe.* The model allows for the simulation and prediction of batch and repeated batch experiments which are an important engineering tool in terms of optimization of industrial processes improving yield in bioreactors by predicting precise values of harvest fraction (HF) and dilution cycle times (DCT).

The model has been developed within the generic modelling framework of CelCyMUS (Cell Cycle Model University of Surrey). As part of the research being carried out CelCyMUS has been up-dated by introducing the new Fortran 95 features and utilities in order to exploit its powerful new features and to keep the generic model in pace with technological software advancements.

The model is a one-dimensional age-based population balance for the fission yeast *S. pombe.* It includes the four typical phases (S, G2, M and G1) with the G2 phase divided into two phases (G2A, G2B) and two checkpoints that govern the movement of cells between G1 and S, and G2B and M phases. The transitions (movement of cells between phases) are determined by a probability function related to the consumption of glucose. The G2B-M transition is also dependent on cell size, but since individual growth of cells is related to the consumption of the carbon source (in this case glucose), cell size is dependent upon the amount of glucose consumed per cell.

The model also includes a phase for cells facing starvation before going into a meiotic cycle, with some chance of coming back to the mitotic cycle, and a death phase that accounts for cells dying with no chance of recovering at all.

Parameters in the *S. pombe* model have been gathered from experimental data in batch culture reported in literature. Data generated from this specific model have been compared with data from experiments (Fotuhi, 2002) in batch and repeated batch cultures of *S. pombe* following the behaviour of population balance, consumption of nutrients, and production of metabolites.

The new code was tested by successfully reproducing data from mm-321 hybridoma cell line, the first specific model of a cell line developed in CelCyMUS. As a new feature a model of mass transfer has been incorporated in the generic framework. This mass transfer module accounts for interactions of metabolites (oxygen and carbon dioxide) in the gas and liquid phase of bioreactors. The new *S. pombe* model was fitted to the experiments of Creanor (1992) on synchronised cultures where the consumption of oxygen was being measured. Such experiments identify two points (G2B and G1) where the rate of oxygen uptake increased in the cycle, doubling the consumption at the end of every cycle. With the model fitted to experimental results in synchronised cultures of *S. pombe* the model was then used to simulate desynchronised cultures. *S. pombe* was successfully tested when reproducing experimental data generated by Fotuhi (2002) in *S.pombe* for batch and repeated batch bioreactors. The *S. pombe* model was able to simulate cell number, oxygen and glucose consumption. Carbon dioxide and ATP production were predicted by the model however there was no experimental data to compare with.

Now that the *S. pombe* model has been tested against experimental data it will be applied in a model-based observer strategy for the online control of bioreactors. This research is actually being carried out at University of Surrey and some suggestions and recommendations about future experiments are presented in this dissertation.

Acknowledgements

First and foremost I would like to thank with all my heart, the greatest respect and love to the one who has always been there for me in my life . . . to you God my Lord.

And now I would like to thank all the ones God has put on my way:

To the one who never doubted me and fed my dreams with strength, unconditional love and words of genuine support . . . To my grandmother (r. i. p)

To the ones who gave me everything I needed to be where I finally am . . . To my parents and my brothers.

To Maria Lucia for the love she gives me and her support. To Daniela, Nathalie, Santiago and Juan Diego a strong reason to keep my chin up looking at the skies.

To my supervisors: Dr. Dave Faraday, thanks for trusting me, giving me your support and for believing in what I am capable of, that was my main motivation.

Dr. Norman Kirkby thanks for teaching me, thanks for your guidance and for keeping my feet on the ground.

To Bryan Underwood: thanks for his support, advice and encouragement and for filling up my engineering orientated mind with knowledge in microbiology.

To my friends in the research group, Gemma, Tigran, Hamid for keeping me up all the time, and to all my friends in the department for sharing with me in the good and hard times.

CONTENTS

Page No.

Page No.

GLOSSARY

Anaphase: consist of the segregation of the sister chromatids at the metaphase plate and their subsequent movement pole ward along microtubules toward the spindle pole.

Ascus: Elongated spore case containing 4 or 8 haploid sexual ascospores of ascomycete fungi (which include most yeasts).

Cdc2: is a protein kinase, which phosphorylates key proteins leading to major events in mitosis (nuclear envelope breakdown, golgi body disassembly etc). Activation of cdc2 protein kinase is dependent on cell size and the completion of S phase. To activate the protein kinase involves association with cyclin B (forming Mitosis Promoting Factor - MPF) and a change in the phosphorylation state of cdc2.

Cdc25: A protein phosphatase that dephosphorylates Y15. Cdc25 removes the inhibitory Y15 phosphorylation, and activates cdc2. Cdc25 removes the inhibitory Y15 from the cdc2/cyclinB complex. This then allows the initiation of key events leading to mitosis. Mutations in cdc25 cause cells to arrest before mitosis, giving elongated phenotypes. Cells continue to grow but cannot enter mitosis as cdc2 is never activated. Where DNA damage is detected (by CHK1) cdc25 will be phosphorylated, the gene product of Rad24 will recognise this phosphorylated form of cdc25 and it will transport the protein phosphatase out of the nucleus. Thus mitosis cannot proceed until the DNA damage has been repaired.

Cell death: Cells die (non-accidentally) either when they have completed a fixed number of division cycles (around 60; the Hayflick limit) or at some earlier stage when programmed to do so, as in digit separation in vertebrate limb morphogenesis. Whether this is due to an accumulation of errors or a programmed limit is unclear; some transformed cells have undoubtedly escaped the limit.

Cyclin B: Cyclin B complexes with cdc2 forming MPF (Mitotic Promoting Factor). Levels of cyclin fluctuate during the cell cycle. Cyclin is gradually produced throughout interphase, and then degraded prior to exit from mitosis. This breakdown of cyclin occurs at metaphase and is required indirectly for the segregation of the two sister chromatids and the progression of the cell into anaphase. Active Anaphase Promoting Complex (APC) is required both for the ubiquitination/degradation of cyclin, and the breakdown of cut2 (the protein controlling the cohesion of the two chromatids). The actual breakdown of cyclin however is not necessary for separating the chromatids. Complete degradation of cyclin is required later for exit from mitosis, here MPF must be completely inactivated or the cell cannot leave mitosis.

Cytokinesis: is the final stage of mitosis. The material within the parent cell is cleaved equally into two daughter cells through contraction of a ring of actin and myosin around the equator of the cell.

Flow cytometry: Slightly imprecise but common term for the use of the Fluorescence Activated Cell Sorter (FACS). Cells are labelled with fluorescent dye and then passed, in suspending medium, through a narrow dropping nozzle so that each cell is in a small droplet. A laser-based detector system is used to excite fluorescence, and droplets with positively fluorescent cells are given an electric charge. Charged and uncharged droplets are separated as they fall between charged plates, and so collect in different tubes. The machine can be used either as an analytical tool, counting the number of labelled cells in a population, or to separate the cells for subsequent growth of the selected population. The great strength of the system is that it looks at large numbers of individual cells, and makes possible the separation of populations with, for example, particular surface properties.

Haploid: Describes a nucleus, cell or organism possessing a single set of unpaired chromosomes. Gametes are haploid.

Hybridoma: A cell hybrid in which a tumour cell forms one of the original source cells. In practice, confined to hybrids between T- or B-lymphocytes and appropriate cell lines.

In vitro: In an unnatural position (e.g., outside the body, in the test tube). "*In vitro*" is Latin for "in glass." For example, the testing of a substance, or the experimentation in (using) a "dead" cell-free system.

In vivo: Latin for "*in living*" (e.g., the testing of a new pharmaceutical substance or experimentation in (using) a living, whole organism. An *in vivo* test is one in which an experimental substance is injected into an animal such as a rat in order to ascertain its effect on the organism.

Interphase: is defined as the stages preceding mitosis in the cell cycle. During interphase the cell will grow and replicate the genetic information it contains.

Meiosis: A specialized form of nuclear division in which there are two successive nuclear divisions (meiosis I and II) without any chromosome replication between them. Each division can be divided into 4 phases similar to those of mitosis (pro-, meta-, ana- and telophase). Meiosis reduces the starting number of 4n chromosomes in the parent cell to n in each of the 4 daughter cells. Each cell receives only one of each homologous chromosome pair, with the maternal and paternal chromosomes being distributed randomly between the cells. This results in the recombination of genes. Meiosis occurs during the formation of gametes in animals, which are thus haploid and fertilization gives a diploid egg. In plants meiosis leads to the formation of the spore by the sporophyte generation.

Metaphase: When all the chromosomes have formed bipolar attachments and are oscillating about an equatorial position (the metaphase plate) **metaphase** has been

reached. Metaphase is a transient stage, as the cell will progress rapidly into anaphase soon after metaphase is reached.

Prophase: is the first stage after commitment to mitosis. The mitotic spindle is beginning to form, but as the nuclear envelope has yet to break down there is no contact between the chromosomes and microtubules

Spore: Highly resistant dehydrated form of reproductive cell produced under conditions of environmental stress. Usually have very resistant cell walls (integument) and low metabolic rate until activated. Bacterial spores may survive quite extraordinary extremes of temperature, dehydration or chemical insult. Gives rise to a new individual without fusion with another cell.

Telophase: the chromosomes will recondense, and the nuclear envelope will reform around the genetic material. The plane of cytokinesis will have been defined, and the separation of the parent cell into two identical daughter cells will follow.

Wee1: Protein kinase that phosphorylates Y15. Wee1 suppresses cdc2 activity and stops entry into mitosis. Cells with a wee1.50 mutation divide at a smaller size than the wild type cell. The cells are still viable at this size, indicating that some other size threshold checkpoint acts before wee1. Mik1 (mitotic inhibitory kinase) is closely related to wee1, and is thought to have some Y15 phosphorylation activity. Redundancy in the function of wee1 and mik1 means that to an extent there is an overlap of function. Therefore a mutation in either wee1 or mik1 will not be lethal, only a mutation of both wee1 and mik 1 is lethal to the cell, as all Y15 phosphorylation activity is lost.

From the wee1 ts mutant phenotype it is possible to deduce that wee1 acts as a brake on mitosis. Mitosis can proceed faster than the cell can complete growth and DNA replication, therefore wee1 is required to slow entry into mitosis and allow these other targets to be reached.

LIST OF GRAPHS

APPENDIX A

APPENDIX B

APPENDIX C

GRAPH 1 - Oxygen consumption. Simulations from Creanor experiments

GRAPH 2 – Oxygen consumption. Comparison between Creanor experimental data and simulated experiments

GRAPH 3 – Cell number. Comparison with Fotuhi's experiments. Batch with 2% Glucose, 19.2 Million cells.

GRAPH 4 – Glucose concentration. Comparison with Fotuhi's experiments. Batch with 2% Glucose, 19.2 Million cells.

GRAPH 5 - Cell number. Comparison with Fotuhi's experiments. Batch with 2% Glucose, 8.8 Million cells.

GRAPH 6 - Glucose concentration. Experimental and simulated consumption of glucose, Fotuhi experiments. 8.8 Million Cells.

GRAPH 7 – Cell number. Comparison with Fotuhi's experiments. Batch with 2% Glucose, 1.2 Million cells.

GRAPH 8 – Glucose concentration. 2%Glucose. Experimental and simulated consumption of Glucose, 1.2 Million cells.

GRAPH 9 – Variation in Glucose consumption rate.Concentration. 2%Glucose. Comparison between experimental and simulated consumption rate of Glucose, 1.2 Million cells.

GRAPH 10 – Variation in Glucose consumption rate.Concentration. 2%Glucose. Comparison between experimental and simulated consumption rate of Glucose, 8.8 Million cells.

APPENDIX D

GRAPH 1 - Studying possible chaotic growth kinetics. 100 Batches. Initial cell number = 17.5 Millions/ml. DCT = 18hr. HF = 80%. First 25 Batches.

GRAPH 2 - Studying possible chaotic growth kinetics. 100 Batches. Initial cell number = 17.5 Millions/ml. DCT = 18hr. HF = 80%. 25 – 50 Batches.

GRAPH 3 - Studying possible chaotic growth kinetics. 100 Batches. Initial cell number = 17.5 Millions/ml. DCT = 18hr. HF = 80%. 50 – 75 Batches.

GRAPH 4 - Studying possible chaotic growth kinetics. 100 Batches. Initial cell number = 17.5 Millions/ml. DCT = 18hr. HF = 80%. 75 - 100 Batches.

GRAPH 5 - Studying possible chaotic growth kinetics. 200 Batches. Initial cell number = 20 Millions/ml. DCT = 18hr. HF = 80%. 40 Batches.

GRAPH 6 - Studying possible chaotic growth kinetics. 200 Batches. Initial cell number = 20 Millions/ml. DCT = 18hr. HF = 80%. 40 – 80 Batches.

GRAPH 7 - Studying possible chaotic growth kinetics. 200 Batches. Initial cell number = 20 Millions/ml. DCT = 18hr. HF = 80%. 80 - 120 Batches.

GRAPH 8 - Studying possible chaotic growth kinetics. 200 Batches. Initial cell number = 20 Millions/ml. DCT = 18hr. HF = 80%. 120 – 160 Batches.

GRAPH 9 - Studying possible chaotic growth kinetics. 200 Batches. Initial cell number = 20 Millions/ml. DCT = 18hr. HF = 80%. 160 – 200 Batches.

LIST OF FIGURES

LIST OF TABLES

Appendix D

CHAPTER 1

INTRODUCTION

Mathematical modelling is a well-established, powerful and reliable option for many scientists who work in simulating different sort of industrial and biotechnological processes. For decades research has been carried out on the modelling of growth kinetics of cells and micro-organisms in bioreactors so that these processes might be optimised. More recently the concept that an apparently homogeneous cell culture is in fact a mixture of sub-populations of cells has greatly added to the understanding of the problems involved in modelling these systems.

The underlying biology responsible for the behaviour of these cultures is the cell cycle which will be defined as the sequence of events whereby a living cell (mother cell) duplicates its essential components and distributes them at division to a daughter cell which is capable of repeating the sequence itself for a number of times until it finally dies. It is central to this dissertation that any mathematical model of these processes integrates or takes account of current research in this area to produce an effective model.

In this chapter mathematical modelling in general, its importance, uses and links will be discussed. An introduction to modelling in biological processes will be presented. The importance of the cell cycle and its generalities are also included, giving an overview of the internal processes that generate the cycle of life in a cell, setting the scene for what it will be the main goal of this dissertation: developing a mathematical model for the fission yeast ***Schizosaccharomyces pombe*** *(S. pombe).* Other main goals and objectives will also be put forward.

1.1 MATHEMATICAL MODELS USES AND LINKS

Mathematical models encapsulate the order in a given natural system, playing a fundamental role in science, allowing quantitative and qualitative analysis using

mathematical tools, and allow workers to relate theory with empirical data; furthermore they can be use for various ends:

1. Simulation; when studying a system behaviour by simulating experimental conditions in the real world using a model with the possibility of simulating beyond what is feasible in the real world, for example testing a new design when it would be expensive to run in a pilot plant or under experimental conditions i.e. On-line control in fermentors can be tested first (Araujo, 1998) by using a model of the process to be controlled.

2. Evaluating experimental conditions; checking how various parameters and variables of the system influence its behaviour. Running a model in scenarios that otherwise would be difficult to be carried out or difficult to observe under different experimental conditions or moving beyond the boundaries of real life in order to explore new untested experimental conditions.

3. Predictions; when giving estimates from real systems behaviours in systems that have not yet been tested with a good degree of accuracy. Prediction helps to set up changes in the experimental set up avoiding undesirable results, cost cutting and to verify assumptions made when simulating a system.

Mathematical models have been used in optimisation of processes, where once a process has been established and by manipulating parameters in the system (simulated by the model) the overall efficiency of the process or of one desired part is improved. Industrial applications would be related to optimising yields and controlling bioreactors using model based observer (M.B.O.) control systems (Araujo, 1998), a field which is still being developed. Mathematical models have been used in environmental studies when separating organic compounds in residual waters using granular activated carbon beds (Friedrich G., Helfferich, 1996) and in the use of permeable reactive barriers for remediating contaminated groundwater

(Jefferis, Norris, 1998) and many other areas of environmental research. Medicine is an area of public interest where mathematical modelling is used in simulating and predicting behaviour of cancer (Wegener, Nusslin, 2000) and tumour cells populations. Economics, when forecasting tendencies in markets in different countries and continents, and many other areas of engineering such as civil engineering, aerodynamics (i.e. wings design in airplanes), fluid dynamics, particle technology, social behaviour, and physical science in general.

1.2 MATHEMATICAL MODELLING IN BIOLOGICAL PROCESSES

With the explosion in experimental data within biology, there are many attempts to develop mathematical models for the description of cellular functions, either overall functioning (cell population) or individual cell behaviour. In biotechnology there is an especial focus on the cellular metabolism, as this may be exploited for the production of compounds that might find application as materials, pharmaceuticals, food additives, and so on. Besides featuring very complex networks, with interconnecting pathways that consist of hundreds of reactions, the metabolism of a cell is also subject to control and regulatory mechanisms. These regulatory mechanisms are not completely elucidated and are therefore very difficult to quantify. Thus the establishment of fully mechanistic, empirical, probabilistic, and deterministic models to describe cellular behaviour in terms of its metabolism and population growth is not completely possible and most models are therefore based on significant simplifications.

In this context mathematical models play a crucial role in hypothesis testing, they can serve as a guide to choosing amongst different possible regulatory structures for a specific cellular process. In traditional studies of cell cultures growth in bioreactors, extra cellular metabolites (such as substrates and products) have been measured, as well as the biomass concentration and the relationship between these metabolites and the behaviour of the cell population has been linked through regulatory mechanisms (check points). The models that can be based on these types of measurements are structured models that have increased the possibility for interpretation and prediction of cell physiology. Besides, the versatility of computer

programs allow including more features in more structured models of different cells cultures.

To understand the behaviour of a cell culture, it is appropriate to look in detail at the metabolic processes, physiological changes and regulatory controls in an individual cell. There follows an overview of the cell cycle, the activities carried out for the cells throughout the different phases of the cycle and the regulatory mechanisms that control the transition between them.

1.3 GENERALITIES OF THE CELL CYCLE

The cell cycle can be seen as the sequence of events that makes two nearly identical cells from an original mother cell. Within this process it is very important to carry out three main tasks, the synthesis of DNA, its replication to transfer a copy of genetic information from a mother cell to a new daughter cell and the precise partitioning (cytokinesis) giving birth to a new cell. The cell cycle as such is divided in four phases, G1 and G2 phases, or 'gap phases' due to their timing depends on the duration of the S phase where the cell synthesises DNA and M phase prepares to give birth to a daughter cell respectively. The cell using checkpoints regulates the transition between one phase and another.

One of the approaches to understanding checkpoints is through the dishwasher analogy (Alberts *et al.*, 1994). Cell cycle regulation is like the control dial on a dishwasher. The dial turns clockwise from one checkpoint to the next. The phases of the cell cycle are like the soak, wash, rinse and dry phases of the dishwasher cycle. The dishwasher control has at least one checkpoint at the end of the cycle; to make sure that the door is opened and closed before a new cycle starts.

A second form of looking at checkpoints is the one used by those authors who see the cell cycle as a sequence of transitions from one (pseudo) steady state to another. Cells remain in a stable steady state at every checkpoint of the cell cycle, cells progress through these states depending upon chemical signalling. The signals that relay information about cellular factors, cell size, DNA damage etc. impinge on the

parameters of the control system, favouring either stability of the steady state (if the answer is 'stop') or passing the check point (if the answer is 'go'), if the conditions are given to overcome the steady state. These signals are a manifestation of the interaction of the components of the enzymes cyclin – CDK machinery. As CDK/cyclin activities rise and fall, the cell is driven through four phases of the cell cycle in order. The phases of the cycle are the stages where a whole population of cells carries out the same set of activities in order to achieve a common goal (DNA synthesis, cell size etc.) and with control mechanisms (checkpoints) to assure all tasks in a phase have been complete before moving to the next phase.

In eukaryotic cells, DNA replication and sister chromatid separation are temporally separated into distinct phases of the cell cycle: S phase (for DNA synthesis) and M phase (for mitosis). A general description of the checkpoints in the eukaryotic cell cycle can be given as follows:

1. G1/S checkpoint. Before entering the S phase, the cells check that they have divided once since the previous round of DNA replication, cells make sure that they are large enough (cell size) to guarantee another round of successful replication, and that environmental conditions are suitable for (or permissive of) mitotic reproduction. There are genes (such as cdc2) which encode proteins (p34 protein kinase) and cdc13 encoding p56 B-type cyclin, which move the cells forward to a new phase in the cycle.

2. G2/M checkpoint. Cells check that they have finished replicating their DNA, that they have repaired any DNA damage that might has occurred, and that they are large enough to divide even though cell size has been previously revised in G1/S. DNA damage can cause cell cycle delay before S-phase, during replication and before mitosis. This involves a number of highly conserved proteins (kinases) that sense DNA damage and signal to the cell cycle machinery. Kinases that were initially discovered in yeast model systems have recently been shown to be in charge of regulating the production of cyclin dependent kinases and other proteins in charge of

repairing damages in DNA chains. This illustrates the importance of checkpoints for maintaining genome stability (repairing DNA).

3. Metaphase checkpoint. Metaphase is the moment during mitosis when all the chromosomes have formed bipolar attachments and are oscillating about an equatorial position. This occurs before initiating anaphase (the separation of sister chromatid to the poles of the mitotic spindle) the cell checks that all the chromosomes are properly aligned with each kinetochore (point where microtubules of the spindle apparatus are attach) in place.

Clearly there is a regulatory system of signals that co-ordinate growth, DNA synthesis and division. The details of this control system have been widely researched in molecular biology through study of the interactions between proteins and genes which rule the restrictions imposed at different checkpoints between phases.

1.4 MATHEMATICAL MODELS AND THE CELL CYCLE

One current approach used in mathematical modelling is to use a population balance model to explain the behaviour of the cells. These models together with sets of equations to account for different features of the bioreactor such as flow rates of nutrients; air and other variables coming in and out of the bioreactor have proved effective in describing the behaviour of micro-organisms and cell cultures.

Studying the cell cycle has become a useful tool to understand and predict not just the behaviour of populations of eukaryotic and mammalian cells but also cancer and tumour cells. Based on biological observations and cell kinetic data, models of radiogenic responses have already been developed. These models predict cell growth and cellular as well as cell population responses to irradiation (Wegener, Nusslin, 2000).

The main principle for this type of model is the function carried out by kinases which recently have been shown to regulate the behaviour of cyclin-dependent

kinases and to control the stability of p-53 (Transcription factor, required for the G1/S checkpoint). In other words they are in charged with repairing the possible damage in the DNA during the G2 phase prior to mitosis.

The knowledge of the kinetics of these proteins, have been combined with models describing the growth of rapidly proliferating normal cells and those of growth of tumours in order to predict the minimum amount of radiation required for killing the maximum number of tumour cells.

Another important topic of study is the property eukaryotic cells have of not dividing continuously. Under certain environmental conditions they stop cell division, leave the cycle, and enter a stable quiescent state (Nurse, 1987). Quiescent cells remain viable for extended periods of time and are much more resistant to thermal heat shocks than actively cycling cells. For most eukaryotic cells, environmental signals cause growth arrest resulting in cells arrested in the G1 phase of the cell cycle. These arrested cells enter a quiescent state referred to as G_0. A notable exception to this is found in the yeast *S. pombe* where entry to a quiescent phase can happen from any phase (facing starvation, chemical blocks etc.). Even though the mechanisms involved in the entering and exiting the quiescent phases are not clear yet, these findings are already important for clinical oncology in cases where tumour cells escape from the effect of chemotherapeutic agents. The escape from the effect of these drugs is due to tumour cells entering quiescent states at points in the cycle other than G1 phase.

A number of issues have arisen about the uses of modelling cell cycle has in engineering, industrial applications and medicine, now an overview of the different experimental approaches that have been used by researches will be presented.

1.5 EXPERIMENTAL APPROACHES TO STUDYING CELL CYCLE

To study the cell cycle is necessary to follow behaviour of a cell at all times in every single phase of the cell cycle. This is achieved by means of synchronisation of cultures which is obtained by arresting cells in a particular phase by using physical

means such as centrifugation or chemical blocking using products to inhibit cell division such as hydroxiurea. Once cells are 'trapped' in a desired phase they are released in fresh medium to start cycling again. Such a process is known as synchronisation of cells.

Most of the studies carried out in cell cycle of different cells are experiments done in batch cultures. A batch culture is a closed system culture of micro-organisms with specific nutrient types, temperature, pressure, aeration, and other environmental conditions, where only a few generations are allowed to grow, before all nutrients are consumed. One of the main objectives of batch reactor engineering is the optimization of reactor operation, striving for higher productivity, a shorter reaction time, higher product quality, good reproduction of results from batch to batch, etc. Once a performance index is defined and some constraints are fixed, involving a dynamic model and other physical limitations, a way to determine the best operational conditions is then introduced, which results in control actions for implementation in an open-loop scheme (mathematical models with no action upon controllers in the system) or close-loop in the case of on-line controllers. The practical implementation of these strategies involves many challenges that arise mainly due to the lack of knowledge of the true behaviour of the process and of the cell culture in use. Sometimes an optimal strategy determined in a simulation study results in a complete failure when experimentally implemented due to batch processes that favour manual operation, which are highly dependent on the abilities of a "specialist".

In order to solve the proposed problem, a mathematical model for the process is implemented. This is the first and most important challenge. Construction of reliable models for bioprocesses is a difficult task due to the complex nature of microbial metabolism and the nature of its kinetics. For these processes, the development of detailed models based on fundamental principles of the cell cycle of a particular cell, its kinetics and metabolic behaviour are of great importance due to the overall effect of the cycle in the results of a batch or continuous batch experiment. At the University of Surrey a research group has been working on the solution of this particular problem and the development of a framework that is able to cope with

specific modules for different types of micro-organisms and the simulation of batch and repeated batch cultures.

1.6 THE RESEARCH GROUP

At the University of Surrey a generic model framework for the study of cell populations through out the cell cycle known as Cell Cycle Model, University of Surrey (CelCyMUS) has been developed. CelCyMUS was born 18 years ago, it is a model capable of predicting kinetics, physiological state of the cell (inter and extra-cellular), consumption of nutrients, production of metabolites, population distribution of cells in different phases. The generic framework was then used to develop a mathematical model for the mm321 hybridoma cell line based on experimental data gathered in the lab. The results were successful in predicting the behaviour of the mm321 cell line population and its particular features within the cycle, such as: the consumption of glutamine and production of antibody to paraquat.

The model could be used to control of bioreactors online. CelCyMUS was then used in virtual control of batch bioreactors as part of MBO (Model Based Observed) control techniques, by simulating a real process with a copy of the program. Once again the results achieved were successful (Araujo, 1998) allowing the team to control errors and to increase them until the system failed. This part of the experiment was done as a pre-test of online control in a real system with CelCyMUS.

More recently research has been carried out on a particular kind of cell: the fission yeast *S. pombe.* The reason why this especial type of cell has been chosen relies on its similarities with more developed organisms. *S. pombe* is a eukaryotic cell, which divides as mammalian cells do having a way of division similar to the way cells from higher organisms divide. It is much easier to handle in the lab, faster growing than mammalian cells and cheaper in terms of cost. Furthermore, a large number of scientists are working on *S. pombe* and there is a vast scientific literature.

Experiments on growing this cell culture in batch reactors using repeated and periodical fed batch fermentation have been carried out in other projects. In this project a mathematical model for describing the *S. pombe* has been developed as another module in the generic framework of CelCyMUS. Throughout this chapter the main features of the cell cycle as a subject have been described as being of huge importance and use at all levels of industry, medicine, biology, and genetics. All of these points make cell cycle modelling an important subject of study and are the main reasons for this research. Next the aims and objectives of the research are stated below.

1.7 AIMS AND OBJECTIVES

The aims of this dissertation are:

1) To develop a specific mathematical model for the *Schizosaccharomyces pombe* (*S. pombe*) yeast cell. The model will be the first ever physiological model of *S. pombe*.

2) To update the generic framework of CelCyMUS and introduce a mass transfer module that accounts for exchange of materials such as oxygen and carbon dioxide within the cell (internally) and interaction with the medium.

3) To simulate experimental data and predict results for the cell cycle of *S. pombe* in batch and repeated batch bioreactors using the smallest number of parameters possible. The model will be able to predict optimum values of harvest fraction (HF) and dilution cycle time (DCT) in order to improve yield in bioreactors.

In order to complete the model, the research presented here has sought to achieve some specific objectives:

1. The generic framework CelCyMUS was to be updated with the new Fortran 95 utilities and features to make it portable as a program more robust and more flexible as a model.

2. To develop a specific mathematical model for the *S. pombe* cell line, defining phases of the *S. pombe* cycle, transition rules, death rules, rates of consumption and production of different metabolites.

3. To link the model to the simulation of batch bioreactors using batch and repeated batch experiments carried out on *S. pombe* cell cultures by Fotuhi (2002).

The structure of this dissertation and the general issues presented in each chapter is as follows:

A literature survey is presented in Chapter 2 on yeast *S. pombe* models particularly those which describes the population balances in a similar fashion to the one being used in CelCyMUS. Genetic models will be mentioned since they have also been developed to predict and to simulate the behaviour of *S. pombe.*

Chapter 3 describes the core theory of CelCyMUS as a generic framework that supports a new module for *S. pombe.* The numerical methods used to solve the model are also described here explaining why the technique was chosen. Then transforming the theory into code will be described. Finally the specific module for *S. pombe,* to be installed into CelCyMUS is outlined presenting the main features of this model and the assumptions that have been considered within it. A mass transfer module to account for the exchange of oxygen and CO_2, is introduced as a new feature for CelCyMUS.

Chapter 4 shows the results achieved by the new code based on experimental data developed for batch bioreactor cultures (Fotuhi, 2002) for *S. pombe* and introduces the main features of the new module for the *S. pombe* yeast indicating the parameters chosen for it. Chapter 4 also describes the research carried out in order to simulate the behaviour of repeated batch cultures based in Fotuhi's experiments. The *S. pombe* model, involves experimental work to determine fix parameters within the model such as glucose and oxygen consumption and research on data gathered from other sources on metabolite production in this particular case.

Finally Chapter 5 includes a discussion of the information presented in the dissertation report concluding on the main tasks completed throughout. Chapter 6 presents recommendations and future work, commenting on the analysis of the goals that have been achieved and viable applications of the model in real systems, such as control on line M.B.O. (Model Based Observed) of experimental processes and optimisation of the existing model for *S. pombe*. Recommendations on introducing new features with regards to metabolites in intra-cellular pools when cells are facing low levels of carbon source and possible applications of the model in study of periodic feeding are also presented.

CHAPTER 2

LITERATURE SURVEY

2.1 INTRODUCTION

The most relevant research on *S. pombe* will be reviewed, a description of the importance of this particular cell will be given and the different approaches taken by different authors to look at *S. pombe* as an easily manageable micro-organism will be presented. Concentrating on the literature on models is a priority here since one will be developed, especially for models of biological processes in batch and repeated batch cell culture. The models are:

a) those based on metabolic pathways and genetic control and,
b) those that approach the cell cycle as a population balance following probabilistic transitions despite the fact that they are not specific *S. pombe* models.

2.2 MATHEMATICAL MODELLING IN CELL CULTURES

Model equations can be obtained in several ways: using theoretical concepts, through direct experimental observation or by using the equations of a system believed to be analogous to the one under analysis. In general, considerable effort is required to establish useful models. Modelling can thus only be justified if the models are less complicated than the processes they represent and lead to significant advantages. Process models have been widely used in the chemical industry, from the design phase to plant maintenance. However, these models have limited use as they often lack robustness due to the processes not being fully understood.

This review is focused on mathematical models that describe the cellular metabolism, as these models play a central role in the rapid developing field of metabolic engineering (Bailey 1991, Stephanopoulos 1999). In this discussion, the

models are grouped according to their structure: firstly, stoichiometric models, which are based on the time invariant characteristics of metabolic networks; and secondly, kinetic models, which are usually based on both stoichiometry and enzyme or microbial kinetics.

2.2.1 STOICHIOMETRIC MODELS

Metabolic flux analysis (MFA) has been widely used for the quantification of the intracellular fluxes in the central metabolism of bacterial, yeast, filamentous fungi and animal cells. In MFA, mass balances over all the intracellular metabolites are used to calculate the fluxes through the different branches of the network. Hereby it is possible to get an understanding of the metabolism under a particular condition. The fluxes can be calculated by combining measurements of a few fluxes either with linear algebra or linear optimisation (Varma and Palsson, 1994). More recently, the use of labelled substrates combined with the measurement of the labelling state of intracellular metabolites, either by NMR (Marx, De Graaf, Wiechert, 1996) or by gas chromatography/mass spectrometry (GC-MS) (Christensen and J. Nielsen, 1999) has been used to estimate the fluxes. When the material balances used in traditional MFA are combined with balances of the labelling pattern of the metabolites, the models become non-linear (Wiechert, De Graaf, 1997, Christensen and J. Nielsen 1999). The additional information supplied by measurements of the labelling pattern of the metabolites do, however, allow for a more reliable estimation of the fluxes, as well as the analysis of the pathway structures and possible reversibility. These new features make it possible to speculate about some key points in cell metabolism, such as pathway identification and compartmentation of enzymes and metabolites, which lead to the use of the term 'metabolic network analysis' (MNA) (Christensen and J. Nielsen, 1999).

Besides being applied to the investigation of cells under different environmental conditions and for studying different mutants of a particular cell, these stoichiometric models have also been applied with the aim of predicting the genotype–phenotype relationship, in order to fill in the gap that exists between DNA sequence data and functional information. Schilling *et al.* 1999, have constructed a

stoichiometric model describing all known reactions in *Escherichia coli*, and have analysed the phenotypes of different deletion mutants, using linear optimisation. The predictions made by using this approach were in agreement with 60 of the 66 mutants examined. Furthermore, it was proposed that by identifying a proper set of vectors of the stoichiometric matrix or by determining the elementary flux modes by convex analysis, it is possible to assess all the capabilities of a metabolic genotype (Schuster, T. Dankekar, 1999).

Stoichiometric models are clearly very powerful, but their main drawback is the limited predictive power, which is due to the lack of regulatory information in the model formulation.

2.2.2 KINETIC MODELS

When detailed information is available about the kinetics of specific cellular processes (e.g. enzyme-catalysed reactions, protein–protein interactions, or protein–DNA binding) it is possible to describe the dynamics of these processes by combining kinetics with the known stoichiometry of metabolic pathways. Rizzi *et al.* (1997) have applied this methodology to model glycolysis in *Saccharomyces cerevisiae*. The model includes reactions of the Embden–Meyerhof–Parnas (EMP) pathway, tricarboxylic acid (TCA) cycle, glyoxylate cycle, and respiratory chain (22 material balances around metabolites and 23 rate equations for enzymes have been included) and has been successfully applied to predict the levels of intracellular and extracellular metabolites after a glucose pulse in a continuous culture of the *S. cerevisiae*. The model has only been applied to a 120 s timescale, however, and phenomena such as enzyme synthesis and degradation — which would be important in larger timescales — have not been included. Besides this, regulation has only been included at the level of individual enzymes and all the kinetic parameters for enzymatic activities are taken from *in vitro* experiments, which probably do not reflect the *in vivo* situation. Vaseghi *et al.* (1999) have applied the same strategy to investigate the pentose phosphate (PP) pathway in *S. cerevisiae*. The concentrations of some intracellular metabolites, such as glucose-6-phosphate and 6-phosphogluconate, as well as of the co-enzyme NADPH predicted by the model

were in agreement with experimental results. By using the model, some kinetic rate equations and parameters were identified — as they could not be found directly in the literature — and it was suggested that the split ratio between the PP and the EMP pathways is related to the intracellular concentration of $MgATP^{2-}$.

Kinetic modelling has also been applied to the investigation of the penicillin biosynthetic pathway in *Penicillium chrysogenum* (Pissara, Nielsen, 1996). The model was used for calculating the fluxes through this pathway (enzyme kinetics for 10 reactions were included), as well as the concentrations of the metabolites involved, which were in agreement with experimental results. In these studies (Pissara, Nielsen 1996), the models have been applied to analysis of the flux control in the pathway, which demonstrates the use of kinetic models in the field of metabolic engineering. Van Riel *et al.* (1998) have established a kinetic model for the central nitrogen metabolism in *S. cerevisiae*, including variables that account for regulatory aspects. These variables represent the concentration of regulators and may indicate a way — though non-mechanistic means — of accounting for the control aspects of metabolism.

Another way of accounting for the regulatory aspects of cell metabolism is by applying cybernetic principles (Varner and D. Ramkrishna, 1999). In this case, cybernetic variables are introduced into a kinetic model with the aim of substituting the unknown mechanistic details of the cell regulatory architecture by an objective function by supposing that the metabolism of a cell operates with a specific overall goal, such as the optimisation of growth. This approach has been used to predict the increase in flux towards threonine formation in *Corynebacterium lactofermentum*, as a consequence of genetic modifications (Varner and D. Ramkrishna, 1999). Cybernetic models will be explained later in this chapter. A further way of including regulatory aspects in a mathematical model is the approach presented by Hatzimanikatis *et al.* (Hatzimanikatis, Floudas, 1996), which formulates the model as a `mixed integer linear programming' (MILP) optimisation problem. In this case, the presence or absence of different possible regulatory loops is represented by discrete variables. This approach has been applied to the investigation of genetic alterations in recombinant high-ethanol-producing *E. coli* (Hatzimanikatis, M. Emmerling, 1998). By using a log- linear approximation for a non-linear model, the

authors verified a qualitative agreement between the predictions of the model and experimental results. When mechanistic details are missing, neural networks (Hellinga, Luyben, 1997) or fuzzy logic-based models (Lee, Yen, Yang, 1999) can be used with the aim of simulating metabolic behaviour; however, the amount of experimental data required to generate these models is usually very high and also less insight into the underlying mechanisms is gained. To illustrate the difficulty in mechanistically modelling particular aspects of metabolism, Wong *et al.* (P. Wong, S. Gladney, 1997) presented a model for aspects such as catabolite repression and inducer exclusion that required several assumptions to be made. Thus, even in this very well studied system there are still some mechanistic aspects that have not been fully elucidated.

If information on all the enzymatic reactions (both equations and parameters) of the whole metabolism of an organism were available, it would in principle be possible to apply detailed modelling to interpret experimental results and predict the dynamic behaviour of cells when subjected to a determined shift in the environmental conditions and the consequences of specific genetic changes. The limitation of this approach, however, is the lack of information on general regulatory aspects, as well as the fact that normally only *in vitro* parameters are available for the enzyme kinetics. *In vivo* perturbation experiments could be a way of fine-tuning these parameters, as illustrated by Rizzi *et al.*1997.

Mathematical modelling of regulatory phenomena, such as heat-shock regulation (Peper, C.A. Grimbergen, 1998), synergistic eukaryotic gene activation (Wang, Ellwood, 1999), regulation of the G1/S transition of eukaryotic cells (Hatzimanikatis, Lee and Bailey, 1999), signal transduction pathways (Bhalla and R. Iyengar, 1999), and gene expression in a complex (Agger and Nielsen, 1999), can serve as a tool — which should be used together with experimental investigation — in clarifying the molecular mechanisms behind these phenomena. This may lead to combining modelling of the metabolism with modelling of signal transduction pathways.

With the aim of trying to interpret the genotype–phenotype relationship, Hatzimanikatis *et al.* (1999) propose the dynamic analysis of the protein levels of an

organism instead of using a set of metabolic fluxes as the output of a non-dynamic model. As it is not possible to correlate mRNA and protein levels directly (Franza and R. Aebersold, 1999), the sole information on gene expression generated by hybridisation on a solid surface (such as from DNA microarrays) cannot account for the functional assignment of the genome sequence of an organism. In order to illustrate the need for combining mRNA and protein levels, Hatzimanikatis and Lee (Hatzimanikatis and K.H. Lee, 1999) applied a continuous dynamic model to describe circadian rhythmicity that agrees with experimental observations. In spite of being incipient as a result of limitations that still exist in proteome analysis, this kind of functional modelling is promising and focuses on the protein which is the final product of the gene.

2.2.3 CYBERNETIC MODELS

Cybernetic modelling involves the identification of:

a) The kinetics of enzyme syntheses and growth processes as a function of relevant concentrations and cybernetic variables, and
b) An optimality criterion that assigns optimal values for the cybernetic variables at each instant. The cybernetic variables represent the cellular regulatory processes of induction or repression and inhibition or activation, respectively.

These models have described the growth of *Escherichia coli* on mixtures of glucose and organic acids such as pyruvate, fumarate, and succinate showing both diauxic and simultaneous uptake. Batch fermentation kinetics of *Lactobacillus bulgaricus* were examined in detail using cybernetic modelling methodology. The original cybernetic framework was expanded by Straight and Ramkrishna so that it can also offer solutions to problems associated with predicting and understanding microbial growth limited by complementary substrates, by expanding kinetic models with simple representation of established regulatory processes. Cybernetic modelling can also be applied to antibiotic production, activated sludge and wastewater treatment systems.

2.3 ALTERNATIVE APPROACHES FOR MODELLING CELL CULTURES

Models may be used to estimate process information on-line and continuously (Stephanopoulos *et al.*, 1999; Bastin and Dochain, 1990; Montague *et al.*, 1992). Data-based and simple qualitative models, such as artificial neural network (ANN) models and fuzzy models, have been receiving considerable attention in the last decade. Although introduction of such models has increased the possibilities to describe biological processes, the models developed are simple descriptions and cannot be classified according to the method proposed by Fredrickson and Tsuchiya (Fredrickson and Tsuchiya, 1966).

ANNs are computational instruments that try to emulate the topology of the human brain, on an extremely simplified scale (Gomm *et al.*, 1995; Zorzetto, 1995; Montague, 1992). They are also referred to as connectionist models because they are composed of a set of interconnected process units, called neurones or nodes (Zorzetto, 1995). ANNs have the potential to identify and learn correlative patterns between sets of input data and corresponding target values; the latter are usually key process variables, which are difficult to measure (Montague and Morris, 1994). Although a reasonable amount of representative data is required, ANNs offer a 'black-box' approach, being able to model relationships in a process with no knowledge of its mechanism. ANNs are thus very attractive when dealing with biological processes (Lant *et al.*, 1990; Bulsari and Saxén, 1994) as these are often not well understood and normally result in a large amount of reliable process data, albeit mostly off-line data.

Further modelling alternatives include fuzzy logic and neurofuzzy models. Fuzzy logic attempts to represent reality by introducing the idea of gradations of truth, or falseness (Postlethwaite, 1996); it thus 'humanises' conventional logic (Lübbert and Simutis, 1994). Fuzzy models are useful for non-linear processes (Sanders, 1998), where human experience outbalances mathematical modelling (Rhinehart and Murugan, 1997). Neurofuzzy models offer the precision and learning capability of ANNs, whilst being easy to understand, like fuzzy models (Lübbert and Simutis, 1994). Although widely used in fields such as robotics and financial markets,

application of these models to biological systems is yet scarce (Frank and Köppen-Seliger, 1997).

Combination of ANNs and fuzzy principles with poor process models provides an intermediate solution to modelling. These combined models are often referred to as hybrid or 'grey-box' models and have been successfully applied to biological systems (Gehlen *et al.*, 1992; Wu and Joseph, 1992; Zorzetto, 1995; Fu and Barford, 1996; Shimizu, 1996; Groep, 1997).

2.4 POPULATION BALANCES IN MODELLING BIOLOGICAL PROCESSES

By viewing a microbial culture as a homogeneous mixture of identical cells, experimental results and mathematical models representative of average cell behaviour are readily scaled to the cell population level. However, individual cells exhibit heterogeneity as a result of small differences in their cellular metabolism and cell cycle dynamics. Repeated movement through the cell cycle yields a heterogeneous population in which individual cells differ according to their size and intracellular state. Unless a synchronous population is established by exploiting natural mechanisms (Zamamiri, Birol and Hjortso, 2001) or through artificial means (B. Futcher, 1999), the average cell behaviour is only partly representative of the entire population. This motivates the development of experimental and modelling techniques that account for heterogeneities present at the single-cell level.

Cell heterogeneities can have a significant impact on microbial culture dynamics and the production of key metabolites and several examples are given below.

Yeasts can exhibit glycolytic oscillations at the single-cell level owing to the autocatalytic activity of the enzyme phosphofructokinase. In the absence of a synchronization mechanism, random variations in energy metabolism would cause individual cells to oscillate out of phase. Instead, secreted acetaldehyde causes dynamic synchronization of the individual cells and results in sustained oscillations at the cell population level (S. Dano, P. Sorensen, 1999).

Continuous yeast cultures can exhibit oscillations of a much longer period, which are related to the asymmetric nature of the budding cell cycle. Normally random variations in cellular metabolism and cell-cycle regulation produce a heterogeneous population in which individual cells are dispersed throughout the cell cycle. Under aerobic and glucose-limited growth environments, a synchronization mechanism yet to be fully understood causes cell subpopulations to move simultaneously through the cell cycle and leads to sustained oscillations in extracellular measurements (Birol, Zamamiri and Hjortso, 2000).

Secretion rates of microbial products can be affected by the cell-cycle position of individual cells and therefore on the degree of heterogeneity. Synchronous cultures of the budding yeast *Saccharomyces cerevisiae* have been used to investigate the secretion rates of various proteins as a function of the cell-cycle phase. Studies have shown that significant protein secretion rates are obtained only as the synchronized cells approach mitosis (Frykman and Srienc, 2001).

To develop fundamental understanding of cell heterogeneities and their effects on microbial population dynamics, biochemical analysis methods, which provide information at the single-cell level, are required. Flow cytometry has emerged as a very powerful method for measuring the distribution of cellular properties across large cell populations. By combining cell staining techniques and analysis of light scattering and fluorescence signals, individual cells can be differentiated with respect to their size, protein content, DNA content and other intracellular properties (Rieseberg, Kaspar, 2001). Recently, flow cytometry has been combined with flow injection techniques to produce automated systems that provide on-line measurements of cell distribution properties (Abu-Absi, A. Zamamiri, 2003). When combined with suitable cell population models, on-line flow cytometry will enable the development of computer-based systems that provide real-time monitoring and control of cellular distributions in microbial fermentations.

Two general approaches are discussed: population balance equation (PBE) models, in which the intracellular state is characterized by a single variable such as cell age or mass, and cell ensemble models constructed from single-cell models that have more detailed descriptions of cellular metabolism and/or cell-cycle progression.

Applications of these cell population models for predicting culture dynamics and designing feedback control strategies are described.

2.4.1 Different Types of Population Balance Models

Population balance models range from simple empirical descriptions of growth curves to models that include numerous, and sometimes complex, partial differential equations. The latter are potentially capable of accounting for behaviour under a much wider variety of conditions (Fredrickson *et al.*, 1967), but require detailed knowledge of the process. Fredrickson and Tsuchiya were the first to categorise models according to the detail included in the system representation. These workers classified models into four distinct categories: unstructured, structured, unsegregated and segregated (Fredrickson and Tsuchiya, 1963). Unstructured models describe the biophase only in terms of its quantity and not of its quality, whilst structured models require some qualitative description of the biophase (Harder and Roels, 1982). Unsegregated models consider the population of cells or micro-organisms to be a single, uniform, lumped biophase (Fredrickson *et al.*, 1970; Ramkrishna, 1979); these models are also called continuum or distributed models (Harder and Roels, 1982). Segregated models consider the existence of discrete, heterogeneous cells (Bailey and Ollis, 1986). Both unstructured and structured models may assume a segregated or unsegregated viewpoint. It is obvious that the 'real' situation is a structured, segregated system.

The simplest models are unstructured, distributed models (Harder and Roels, 1982) and are usually empirical descriptions of growth curves. A growth curve for a cell population in a conventional batch bioreactor usually exhibits four distinct periods (Bailey and Ollis, 1986):

- a lag period, during which very little or no growth occurs;
- an exponential period, during which rapid growth occurs, with the number of cells increasing exponentially with time;
- a stationary period, during which no growth occurs; and
- a decline period, during which the population dies.

The simplest model is known as Malthus' Law and describes the exponential period only (Bailey and Ollis, 1986). This law assumes that the rate of increase of biomass is directly proportional to the current biomass. Although simple, it leads to the definition of the specific growth rate that is of paramount importance in the description of biological processes. Modifications to Malthus' Law have been proposed in order to incorporate other periods of the batch growth curve (Velhurst, 1838; Pearl, 1924, Volterra, 1959). Other workers suggested that the specific growth rate could be related to the concentration of a particular substrate in the growth medium (McKendrick and Pai, 1910; Monod, 1942; Monod, 1949). Monod adopted this approach to propose an empirical description of exponential growth in a fermentation process (Monod, 1942). This model is referred to as the Monod Equation and has been applied to the growth kinetics of many biological systems. Several modifications to the Monod Equation have been introduced to account for further features, e.g., the effect upon specific growth rate of cell concentration (Contois, 1959), substrate inhibition (Andrews, 1968; Aiba *et al.*, 1968) and multiple growth limiting substrates (Megee *et al.*, 1972; Ryder and Sinclair, 1972).

Unstructured, distributed models include two limiting assumptions: an 'average cell' approximation and an average biophase state approximation. As a result, it has been suggested that the use of these models should be restricted to situation of balanced growth situation (Bailey and Ollis, 1986). This is a growth state in which every extensive property of the growing system changes by the same factor (Campbell, 1957). The most successful application of these models has been observed in chemostats (Monod, 1950; Herbert *et al.*, 1956; Powell, 1958); under steady state conditions, balanced growth seems as a viable option (Harder and Roels, 1982). The major advantage of unstructured, distributed models is that they generally give rise to relatively simple, linear differential equations, which can either be solved analytically or by simple numerical techniques (Faraday, 1994).

Structured models can generally be divided into two types (Harder and Roels, 1982): those, which simply consider the primary metabolism and those that attempt to model the internal biochemistry in some detail. The former type can still be sub-divided into compartmental and cybernetic models. Compartmental models

define a number of internal pools or compartments (Williams, 1967; Harder and Roels, 1982). Cybernetic models assume that through 'natural selection' microbes have developed the ability to control their regulatory processes and, as a result, they are able to optimise their growth patterns (Ramkrishna, 1982; Ramkrishna *et al.*, 1987). Structured models, which describe the internal biochemistry, are less common than compartmental or cybernetic models due to the large number of equations and parameters, which may have to be considered (Harder and Roels, 1982).

Segregated models consider cells as individual and heterogeneous entities (Bailey and Ollis, 1986). As a result, segregation enables uncoupling reproduction from growth, i.e., whereas unsegregated models consider the biophase as a lump, which 'grows', segregated models consider that the biophase changes due not only to cells growing, but also to cells reproducing. Thus these models are, more complicated than unsegregated models and require the numerical solution of more complex differential equations involving quite computationally intensive methods (Fredrickson *et al.*, 1967; Ramkrishna, 1979; Faraday, 1994).

Reproduction may be described either deterministically or stochastically. The deterministic approach considers cell division to be an explicit function of the state of the system, only independent of time, whereas the stochastic approach considers cell division to be a partly random process (Faraday, 1994).

2.4.2 Specific Population Balances in Microbial Growth

For the purposes of this dissertation modelling in microbial cell population will be restricted to those models that describe cell populations as a set of subpopulations in different phases. Cells are distributed into several discrete cell populations due to the transitions that make a cell change from one phase to another. This has caught the attention of industrial biotechnologists and mathematical modellers who agree that a population balance model can be linked with a kinetic model for cell reactions and a model for the characteristics of the bioreactor in use which together constitute a good combination for a cell cycle framework model.

Initially, the models of growth of microbial populations were of the non-segregated or continuum type (Friedrickson, 1970). Such models were based on the assumption that cells were identical and that the septation process was random. Nowadays it has been established that these processes depend on the physiological state of the cell and models must account not just for the segregated nature of the cell population but also for the individual state of the cell. Since properties such as cell size, consumption of nutrients etc. influence cell growth and division, the state of individual cells can be specified by an abstract collection of state properties, the physiological state vector (Friedrickson, 1971; Kirkby and Faraday, 1988). The population balance equations are in fact a number balances on individual phases of a population, which follow cell division, death and the continuous changes in physiological growth processes.

Fredrickson (1967) proposed one of the first equations formulated:

$$\frac{\partial n(X,t)}{\partial t} + \nabla x.\left[\dot{X}(x)n(x,t)\right] = 2\int_{x}^{\infty}\Gamma(\dot{x})P(x,x')n(x',t)dx' - \Gamma(x)n(x,t) \qquad 2.1$$

Here, $\dot{X}(x)$ is the rate of change of cellular properties, $\Gamma(x)$ is the time specific division rate function, and $P(x,x')$ is the partitioning function, which specifies the probability that a mother cell with state vector x' gives birth to a daughter cell with state vector x.

This equation accounts for the material balance for a well-mixed batch bioreactor, cells reproducing by binary division, no cell death occurs with environmental conditions of the cell culture such as temperature, pH value, and nutrient concentration assumed to be constant.

Fredrickson (1996), has used this type of population balance with different approaches, such as the successive generations approach trying an age structured model where:

$$\frac{\partial n_k(a,t)}{\partial t} + \frac{\partial n_k(a,t)}{\partial a} = -\Gamma(a) n_k(a,t), k \geq 2 : \qquad 2.2$$

With boundary condition:

$$n_k(0,t) = 2\int_0^\infty \Gamma(a) n_{k-1}(a,t) da \qquad 2.3$$

are the equations for an age structured population balance in a well-mixed bioreactor. Here $n_k(a,t)$ is the number density function of the *k*th generation, so that n(a,t)da is the number of cells which have age between a and a+da, $\Gamma(a)$ is the conditional probability density function which specifies the rate of cell division. The boundary condition expresses the physical meaning that new-born cells have age zero. The equations are solved by converting them into integral equations following the method of characteristics (Ramkrishna, 1979) and then solved numerically using the method of successive approximation (Guenther and Lee, 1988).

Following exactly the same pattern (structured model) for mass and growth rate, Fredrickson put together a model that can compute the propagation of the age distributions of individual generations and of the entire microbial culture. The cell division function $\Gamma(a)$, which depends on cell age, is the only factor, which controls the rate of dispersion of a synchronised culture. $\Gamma(a)$ can be calculated using the probability density function of the generation time distribution (Eakman *et al.*, 1966):

$$\Gamma(a) = \frac{g(a)}{1 - \int_0^a g(\dot{a}) d\dot{a}} \qquad 2.4$$

Where g(a) is the probability density function which takes g(a)da to be the probability of a cell to divide aged between a and a+da.

Mass structured cell population balance model in an environment of changing substrate concentration has also been developed (Mantzaris, Liou, Friedrich, 1998).

Generally the main problem with population balance models is that some of them are extremely difficult to be solved. Some others are very time consuming such as the Monte-Carlo method used by several authors (Baron, Krabben, 1997) to describe development of populations. This Monte-Carlo algorithm is called a discrete-event simulation algorithm because it keeps track of the timing of individual transition events by monitoring the state of the overall population instead of directly tracking the growing of individual cells. To carry out such simulations is need to be determined the laws that govern the distributions for the different arrival times and of the variables which identify the transition event and the cell undergoing the transition.

These distributions depend on the assumptions embedded in the population balance model and they can be derived from the same arguments used to derive the original partial integro-differential equations (Equation 2.1). The different types of modelling approaches in growing of cell cultures have been explained. Particular emphasis has been given to describing cell population balance models since this dissertation presents one. There follows an introduction to the main process that influence of all cell cultures behaviour is presented; the cell cycle.

2.5 INTRODUCTION TO THE CELL CYCLE

The fundamental process underlying all biological growth and reproduction in eukaryotic cells is the cell division cycle, which is the periodic repetition of three main events: mitosis and cytokinesis DNA synthesis. These events transform a single cell into two daughter cells. All of this cycle is 'controlled' by a complex and effective genetic mechanism that orchestrates the fluctuation of cyclin-dependent protein kinases.

In most eukaryotic cells this co-ordination of events is carried out at three checkpoints. A checkpoint is a stage of the cell cycle where progress is halted until certain signals indicate that conditions are suitable to continue through the cycle. A typical example is at the end of the G1-phase (Forsburg and Nurse, 1991) where cells evaluate their external environmental conditions (for growth factors, nutritional

status etc.) and their internal state (cell size) before going into replication of DNA (S phase).

G2-phase cells make sure that the synthesis and repair of DNA is completed and that cells are large enough to divide. At metaphase they ensure that all chromosomes are aligned in the right position before the order is given to segregate sister chromatids to opposite poles of the mitotic spindle.

Given the information gathered on the molecular details on these control systems, it is possible to translate the biochemical mechanisms into systems of non-differential equations (Ramkrishna, Varner, 1999). In this approach, a checkpoint is interpreted as a 'stable steady state solution' of the equations that best described the system. These steady states are established by particular conditions (such as consumption of nutrients, cell size, DNA replication etc.). These checkpoints have been widely discussed by many authors from different point of views, (genetic, probabilistic, deterministic etc.) the most important approaches to them will be covered together with an introduction to the approach taken in this work for a particular micro-organism: *S. pombe.*

2.6 *S. pombe*

The yeast, *S. pombe* is a simple single fungal eukaryote with a DNA content only four to five times greater than that of *Escherichia coli* (Nurse, 1992). *S. pombe* is becoming increasingly popular as a model organism for molecular genetics studies. *Pombe* means "beer" in Swahili. It was originally isolated from the East African millet beer known as pombe. It probably diverged from the budding yeast *Saccharomices cerevisiae* 1000 million years ago (Sipiczki, 1989).

The strains used in the laboratory today are derived from a Swiss isolate called *Schizosaccharomices liquifaciens* Oswalder now called *S. pombe.*

S. pombe was developed as a genetically tractable organism in the early 1950s by Urs Leupold (Leupold, 1989). He isolated a homothallic strain h^{90} (so called because

90% of the cells could form spores) and two heterothalic strains of opposite mating types, h^+ and h^-, which were derived from the h^{90} strain. It is from these original isolates that all present day *S. pombe* strains used for genetic analysis are derived.

S. pombe cells contain three chromosomes that condense during mitosis, and can be distinguished by light microscopy. The nuclear envelope remains intact throughout mitosis (closed mitosis) unlike many other eukaryotes where the nuclear envelope fragments (open mitosis). *S. pombe* is an haploid cell (only one copy of each chromosomes), they are rodlike and are 7-14μm in length and 3-4μm in diameter.

The haploid cells will divide asexually through mitosis. This involves growth by elongation at the cell tips, usually called NETO (new end takes off) followed by nuclear division and septa formation and cytokinesis (binary fission). The *S. pombe* yeast is an ideal organism for the study of the cell cycle because it grows rapidly on simple media, each haploid cycle takes around 3 hours. In rich medium they grow as a rod-shaped cell of constant diameter, which divides by septation and medial fission (Nurse, 1992). When starved, cells enter a stationary phase either from G1 or G2 phases depending on which nutrient becomes limiting. Cells starved of nitrogen arrest predominantly in G1 and if cells of both mating types are present they conjugate, forming a diploid zygote that undergoes meiosis and sporulates to generate four haploid spores contained within an ascus. *S. pombe* is normally haploid but can be induced to undergo a diploid mitotic cycle if cells are re-fed with nitrogen after conjugation but before meiosis has been initiated. Yeast cells can also exit the cycle at any phase to enter a quiescent phase where they become resistant to thermal heat shocks (Nurse, 1993).

2.6.1 Cell Cycle Control in *S. pombe*

In *S. pombe* as in most of the eukaryotic cells there are three main events to be controlled within the cell cycle (Novak, 1999) as follows:

1) G1/S checkpoint
2) G2/M checkpoint

3) Metaphase checkpoint.

The presence of these checkpoint controllers within the cell and their mechanisms has been studied in *S. pombe* through three main sources of information about the cell cycle control in fission yeast: 1) the kinetics based on consumption of nutrients through out the cycle or the production of metabolites such as carbon dioxide (CO_2), oxygen (O_2), etc. 2) The genetics (Novak, 1996) because *S. pombe* is an easily tractable organism (Mitchinson, Tyson and Novak, 1998) and 3) an indirect method by using population balances with experimental parameters linking genetics and kinetics (Friedricson, 1996).

2.7 MODELLING APPROACHES TO *pombe's* CELL CYCLE

The majority of the models created to describe the *S. pombe* cell cycle rely heavily on the kinetics of the genetics controllers and the interactions of proteins and genes described before. There are a few authors (Friedrickson, 1996; Kirkby and Faraday, 2001) who worked with population balances that could be used (as will be explained) in building a model for *S. pombe*, although they were written for different kinds of micro-organism.

2.7.1 The Kinetic Approach in *S. pombe*

Observation of the production of metabolites or consumption of nutrients throughout the cell cycle in synchronised cultures was one of the first techniques used to look for specific patterns that would lead to information about the existence of internal controls in or between phases of the fission yeast cycle.

CO_2 evolution was measured in synchronous cultures of *S. pombe* and a periodic change in the rate of evolution once per cycle was found, (Creanor, 1978). When the DNA division cycle was blocked with chemical inhibitors it was found that periodic changes continued for one to two cycle times after the blocks. These findings were one of the earliest unequivocal demonstrations that periodic cell cycle events can continue in growing eukaryotic cells after a block to DNA synthesis and division.

Novak and Tyson, (1988) continued and extended the research by Creanor following CO_2 production by manometry in synchronous and asynchronous cultures of *S. pombe* prepared by elutriation from the same initial culture. The rate of production follows a linear pattern in synchronous cultures with a rate change per cycle at the time of cell division. The association between the rate of change and the time of division is maintained during growth speeded up in rich medium and slowed down in poor medium or at lower temperature. The association is also maintained after an increase in temperature. Results with wee mutants (*S. pombe* mutants with small cell size) suggest that the association is with the S phase rather than division itself. The rate of CO_2 production is approximately proportional to cell size (protein content) in asynchronous cultures.

When synchronous cultures of the temperature-sensitive mutants cdc 2.33 and wee1.6 are brought up to the restrictive temperature (the temperature at which cells stop dividing), the DNA division is blocked. The oscillatory pattern of CO_2 production however continues for one or two cycles until the acceleration (change of rate of CO_2 production) reaches a constant value, after which the oscillations are undetectable.

These studies were a base to determine whether or not the transition (movement of cells between phases) was promoted by cell size due to nutrients consumption. Since the rate of CO_2 is proportional to cell size in asynchronous cultures, this points to cell size as one of the 'indicator signals' (G1/S and G2/M checkpoints) in *S. pombe.*

Similar research has been carried out in cells such as mm321 hybridoma cell line (Hayter, 1987), where the rate of consumption of glutamine in a synchronised culture throughout the cycle was measured. The rate of consumption of glutamine was then used as a measure of the cumulative content of glutamine being taken up in G1 phase to determine the probability of transition to the S phases (Faraday, 1988). If the kinetics of the cell cycle gives an idea of the physical and palpable changes in the cell and population dynamics, genetics may eventually provide the understanding of the internal mechanisms that determine this behaviour.

2.7.2 The Genetic Approach in *S. pombe*

The genetic approach is consider in depth by Tyson and Novak (1998) where they established that the cell cycle for fission yeast is controlled by a single CDK, namely Cdc2 (protein encoded by the gene $cdc2^{+}$) in combination with three B-type cyclins (Cdc13, Cig1, and Cig2). Genes have the information on how to produce proteins; such information will be picked up for a ribosome in-charge of the actual synthesis of proteins. The most important partner of Cdc2 protein is Cdc13. The complex of Cdc2 and Cdc13 is known as M-phase promoting factor (MPF) and is fundamental to initiate mitosis, in the absence of other complexes, this complex can trigger the S phase as well.

The Cdc13 level fluctuates dramatically during the cell cycle, reaching a maximum as cells enter mitosis, dropping precipitously as cell exits mitosis, and reappearing after cells enter S phase. The activity of Cig-2 dependent kinase peaks at M-phase even though its physiological role is not known.

The Cdc2 catalytic subunit of the heterodimer (A dimer in which the two subunits are different. Heterodimers are relatively common, and the arrangement has the advantage that, for example, several different binding subunits may interact with a conserved signalling subunit), is present at a constant level throughout the cell cycle. Its catalytic activity is determined not only by the availability of cyclin partners but also by phosphorylation at two specific amino-acids: Thr-167 and Tyr-15. Phosphorylation of Thr-167, which is necessary for Cdc2 kinase activity, happens rapidly after cyclin binding.

Tyr-15 phosphorylation, which inhibits S and early G2-phases, decreases dramatically as cells enter M-phase. Phosphorylation of Tyr-15 is carried out by Wee1 and Mik1 kinases and dephosphorylation by Cdc25 phosphatase. Phosphorylation by active MPF-inhibits wee1 and activates Cdc25, and these two positive feedback loops are responsible for the abrupt activation of MPF as cells enter M-phase.

The genetic approach is not of great use amongst modellers yet due to the tiny amount of quantitative information available in the literature and the experiments carried out in regarding this issue. However the focus of this research will be orientated towards the development of a structured model within the generic framework CelCyMUS for *S. pombe*.

2.7.2.1 G2/M Checkpoint

Wild type yeast cells have short durations of G1, S and M-phases, and a long G2 phase. Tyr-15 phosphorylation is used to stop cells at the G2 checkpoint. Two requirements must be met to start dephosphorylation of Tyr-15 residues:

1) Cells must reach a critical size and
2) The chromosomal DNA must be fully replicated.

Comparing cells of different sizes at birth, Fantes and Nurse (1977) found that larger cells grow less during their division cycle (same growth rate but shorter cycle time), proving that cell size has a strong effect on progress through the cell cycle (see fig.1). Using nutritional shifts it was proven that, in wild type fission yeast cells do not pass the size-control checkpoint until shortly before mitosis (Fantes and Nurse, 1977).

Novak and Mitchinson (1998) established that there is a marker in G2 in (WT) cells provided by a rate change point (RCP) where the linear rate of length growth increases by approximately 30%. The period before RCP is dependent on size and can be called a 'sizer'. The period after the RCP is nearly independent of size and can be called a 'timer'. The achievement of a threshold critical size is either at or near RCP, which is on average at about 0.3 of the cycle (halfway through G2). The RCP is about the time when H1 histone kinase activity and the B type cyclin, cdc13, start to rise in preparation for mitosis.

Molecular genetics studies implicated Cdc25 and wee1 in the G2 size control mechanism. When cells are sufficiently large, the positive feedback loops engage, activating MPF and driving cells into mitosis.

The surveillance mechanism for unreplicated DNA also seems to work through wee1 and Cdc25, by activating phosphates opposing the MPF dependent phosphorylation of these enzymes. As a consequence, MPF cannot turn on the positive feedback loops, and CD 13/Cdc2 dimers are kept in their inactive, tyrosine-phosphorylated forms.

2.7.2.2 G1 Checkpoint

Fantes and Nurse (1978) produce evidence that wee1$^+$ was an essential element of the mitotic size control and that in its absence the mitotic size control was abolished and it was replaced by a G1/S size control. The G1/S transition (Start) is controlled by antagonistic interactions between Rum1 and cyclin/Cdc2 dimers (Cig2/Cdc2 and Cdc13/Cdc2): Rum1 binds to and inhibits the dimers, whereas the dimers phosphorylate Rum1, making it more susceptible to proteolysis. Below the critical size, Rum1 is predominant and progress through the cell cycle is stalled. Above the critical size, Rum1 inhibition is removed and cyclin/Cdc2 dimers drive the cell into S-phase. Recently, Novak and Tyson (1998) have turned these ideas into a mathematical model, which describes the behaviour of these interactions

2.7.2.3 Mitotic Checkpoint

The mitotic size control in fission yeast ensures that cells large at birth will have shorter than average cycle times, and vice versa for small cells. Fantes (1977) demonstrated this negative correlation between cycle time and birth length.

At the end of mitosis, MPF is inactivated by degradation of its Cdc13 subunits. The degradation step is mediated by a multi-enzyme complex, called the anaphase promoting complex (APC), which attaches ubiquitin labels to cyclin molecules and renders them susceptible to proteolysis.

In addition to cyclin B molecules, the APC also induces degradation of the tether molecules that hold the sister chromatids together. The mitotic checkpoint ensures that APC is activated only after all chromosomes are properly attached to the bipolar mitotic spindle.

It is important to notice that APC activity and cyclin B accumulation seem to be mutually exclusive: in budding yeast and fission yeast the APC is active during G1-phase, when B-type cyclins are absent, and is inactive during S+G2+M, when B-type cyclins are present. These facts led scientists to propose that B-dependent kinase activity must be a potent inactivator of the APC as well.

2.8 CONCLUDING COMMENTS

This review has presented an overview on modelling on biological processes, cell cultures and the different approaches (Kinetic, genetic, cell population balances etc.) taken by different authors regardless of the type of micro-organism. Then a review on mathematical models for the *S. pombe* cell has also been introduced following the same modelling approaches that were followed for other authors in other eukarotic micro-organisms.

The introductory chapter described the cell cycle setting the scene for the *S. pombe* model. A review of the literature has now been done. Different approaches to modelling of the cell cycle in general and to modelling of *S. pombe* in particular were presented. Previous work in CelCyMUS as a generic framework and its development are explained in the theory chapter, the theory chapter will also be used to show what the *S. pombe* model will look like from the particular point of view of this research group. In order to do that it is important to know the generic framework CelCyMUS and why it has been chosen for this task. All the new features such as mass transfer modules and the new modules for the particular organism of study *S. pombe* are introduced. The approach on segregated populations for the *S. pombe* model is new and differs from the existing genetic model accounting for the kinetics of proteins activity.

CHAPTER 3

Schizosaccharomyces pombe MODEL

3.1 INTRODUCTION

A mathematical model is a representation of the essential aspects of a real system. It is mainly constituted of a set of mathematical relationships which describe the behaviour of a real system at a reasonable level of detail and with an acceptable degree of accuracy.

Throughout this chapter the definition of a mathematical model will be applied to the yeast; *S. pombe*. This is a deterministic model, which means each variable, and parameter takes fixed values for some given conditions. However, despite being deterministic this model has a representation of events that may be stochastic in reality.

The model has been built as a module within the generic framework of the updated CelCyMUS model coded in Fortran 95. The model takes into account the population balance of fission yeast, the phases of the cell cycle including phases where the cells exit the cycle due to external damage and environmental factors. Consumption of nutrients (glucose), probability transitions, production of catabolites (CO_2, glucose) will also be considered. The basic theory that supports CelCyMUS will be explained. The main equations which are included in the program and the assumptions made to derive the generic framework of the model for *S. pombe* are introduced.

3.2 CelCyMUS

A one-dimensional age-based population balance model of the cell cycle known as **CelCyMUS** (Kirkby and Faraday, 2001) has been developed. This is a fully deterministic model, which can describe changes in the cell age distribution,

interactions of the cell population with a multi-component medium and changes in cytological state. It defines a phase as the state in which all cells obey the same set of transition rules, share the same forms of interaction with the environment and are performing the same internal functions. Changes in cell age distribution are also accounted for by describing how cells move from one phase to another by undergoing a 'transition' between phases.

The model accounts for cells in any phase at any time following one of these three main mutually exclusive events:

a) The cells get older ('flow')
b) Cells leave this current phase ('transition')
c) Cells leaving the system ('washout')

CelCyMUS counts with a population density function (number of cells per unit volume per unit biological age) represented in the population balance below:

$$\frac{\partial n_X(t,\tau_X)}{\partial t} = \frac{F(t)}{V(t)} n_X(t,\tau_X) - \sum_{j=1}^{G_x} r_{jx}(\tau_X, n_X(t,\tau_X), C_c(t,\tau_X), C(t)) - \frac{\partial n_X(t,\tau_X)}{\partial \tau} \qquad (3.1)$$

Where: τ is the biological age (hr); F is the feed flow rate to the system (m^3h^{-1}); V is the volume of the system (m^3); r_{jx} is the rate at which cells undergo transition as a result of the J^{th} transition rule in phase X (cells m^{-3} hr^{-2}); G_x is the number of transition rules which apply to phase X; C_c is the cytological state vector, accounting for the concentrations of all the intra-cellular components of interest (kg $cell^{-1}$) and C is the medium state vector, accounting for the concentrations of all the medium components of interest (kg m^{-3}).

Within the model each phase has a finite maximum duration and, in all cases, the first transition rule is used to account for this fact. Therefore, for any phase X the following is true:

$$\Upsilon_{1x}(\tau_x, n_x(t,\tau_x), Cc(t,\tau_x), C(t)) = 0 \qquad 0 \le \tau_x < T_x \qquad (3.2)$$

$$\Upsilon_{1x}(\tau_x, n_x(t,\tau_x), Cc(t,\tau_x), C(t)) = n_x(t,T_x) \qquad 0 \leq \tau_x < T_x \qquad (3.3)$$

Where T_x is the maximum duration of phase X (hr). However, there may be any number of other transition rules, which also apply to this phase.

Each phase also has boundary conditions, which will depend on the kind of micro-organism, is being dealt with. The boundary conditions have to be defined for each phase (as will be shown for the *S. pombe* module) depending upon the transitions between phases and these play an important role on the solution technique employed to solve the equations in the model.

The model of mm321 has been proved to be a successful specific model and was included as a module within CelCyMUS. Based on data of Dr. Paul Hayter who studied the behaviour of synchronised cultures of a mouse-mouse hybridoma cell line (mm321) producing Immunoglobulin G antibody to paraquat, a module to simulate this particular type of cell was developed by Faraday. The mm321 module has successfully tested CelCyMUS as a generic framework inviting the study of other micro-organisms. It has also been used as part of a M.B.O. (Model Based Observer) controller model for the same cell line, in a theoretical way (Araujo, 1998) with promising results for a real application.

A brief description of the generic framework of CelCyMUS has been outlined, the equations and numerical methods used to solve them were studied in order to choose a method accurate, stable and fast enough to solve the system as discussed below.

3.3 MATHEMATICAL SOLUTION TECHNIQUE

The population balance equations (Equation 3.1) are first order, quasi-linear hyperbolic partial differential equations and may be solved by a variety of numerical techniques. By considering the total derivative and the method of characteristics this expression may be rewritten as an ordinary differential equation along characteristics trajectories given by $dt/d\tau = 1$.

By applying the boundary conditions as will be mentioned for the *S. pombe* module (Equations 3.8 to 3.15) these ordinary differential equations can also be solved by using Euler integration. A step length of 1 minute has deliberately been chosen to match the biological age in the program to give simplicity in the handling of the code program. Such step length proved to be most appropriate since this is the equivalent unit use to divide the array for biological age.

The object of the Euler method is to obtain an approximation to the solution y(t) to the initial value problem:

$$\frac{dy}{dt} = f(t,y), \quad a \le t \le b, \quad y(a)=\alpha \tag{3.4}$$

The technique consists in generating approximations to y(t) that will be generated at various values, called mesh points, in the interval [a,b]. Once the approximate solution is obtained at the points, the approximate solution at other points in the interval can be obtained by interpolation if required. The values for initial conditions are set up for the user of the program through the initial number of cells for the population distribution balance at time t=0. The Euler integration technique was built into CelCyMUS in such a way that the program itself contains Euler method in the backbone of the code.

The original version of CelCyMUS was written in Fortran 77 code. As part of the research, one of the tasks carried out has been to update the CelCyMUS code to Fortran 95 taking advantage of the new features this programming language has incorporated. Such features and a brief description of the language will be given as follows.

3.4 SOFTWARE FORTRAN 95

Most of the major languages are particularly suited to a particular class of problems; often this class is very wide. Fortran is one such language, and is particularly well suited for almost all scientific and technological problems as well as to a wide range of other problems areas especially those with a significant numerical or

computational content. All of these together with the powerful utilities are described as follows.

3.4.1 New Features and its Implementation

As follows some of the new Fortran 95 features and how they have been exploited will be introduced. Every application will be supported by an example of its functionality in the program that appears in the form of F.95 files enclosed in a CD with this thesis.

3.4.2 Modules

A form of program unit, which did not exist in FORTRAN 77, is a module. The purpose of a module is quite different from a function or subroutine. Quite simply, a module exits in order to make some or all of the entities declared within it accessible to more than one program unit, as an extension and replacement for common blocks.

Perhaps the most important use of a module is the global accessibility to variables, constants and derive type functions. This utility gives the opportunity of using common variables, which are going to be used through out the program. Even assigning initial values by declaring subroutines within them since a module itself cannot be used to execute statements. However, modules can contain complete subroutines and functions, which are known as module procedures. These procedures are accessed as part of the other program units by including a *USE* statement containing the module name in the program unit.

Procedures which are included within a module must follow any data objects declared in the module and must be preceded by a *CONTAINS* statement. Such feature is applied in various parts of our program; the module initialising is one of them.

3.4.3 Making the Code Portable: Derive Data Type

Parameterised numeric data types, which permit control over range and precision in a portable manner, are available in Fortran 95. The range of values that may be stored in an integer will vary according to how many bits are used to represent it in a computer's memory, while both the range and the precision of real values can vary enormously depending on how they are actually represented by the computer being used. This presents considerable numerical difficulties when attempting to write portable programs.

Fortran 95 overcome these problems by allowing all the intrinsic types (other than double precision) to have more than one form, known as different *kinds*, and provides the means for a program to define which kind of variables and constants it wishes to use. Each implementation of Fortran 95 will provide at least one kind of each intrinsic data type, known as default kind, and may provide as many other kinds as it wishes. The non-default kinds are identified by means of *kind type parameters*.

User define types give to the user flexible programs with robust data structures ideal for age distribution data. A single module stating the *type kind* of the integer and real variables can be seen in the derive type module.

3.4.4 Dynamic Memory Allocation

Fortran 95 includes two ways to allocate memory dynamically at execution time: allocatable arrays and pointers. Allocatable arrays are arrays whose rank is specified at compilation time, but whose shape is not specified until the program is executed. Pointers are variables that contain the address in memory of another variable where data is actually stored. Pointers can also be used for dynamic memory allocation.

Dynamic allocation has been chosen in the current program to make it flexible, faster and more efficient by using just the amount of memory required in our arrays, saving space, which is release afterwards in a de-allocation statement. This simple

but powerful instruction allows big changes when introducing arrays that will allocate cells within phases with different duration times. See module *starting up* as an example.

Therefore we can go further towards the implementation of a new module within our existing model. This report will discuss the use of CelCyMUS as a generic framework to support a module for an especial cell line: *Schizosacharomyces Pombe.*

3.5 A PROPOSED MODEL FOR *S. pombe*

A model for the description of the *S. pombe* cell cycle is proposed (see figure 1 Appendix A). The model is composed of five phases found in fission yeast (with the G2 phase divided in G2A and G2B phases) with two checkpoints at G1/S and G2B/M phases.

Consumption of glucose and oxygen play an important role in both the checkpoints as implicit controllers of them. Since consumption of glucose is linked to the individual growing of cells (cell size) and the two checkpoints being considered are related to cell size it can be assumed that the rate of up-take of glucose is then an indirect measurement of cell size. Undoubtedly, cell size and protein content per cell increase to a certain point during G1 phase, this enhances glucose consumption since is the main source of energy and mass that is taken from the medium.

The first checkpoint in *S. pombe* cells is G1/S. Once cells have completed mitosis they have to achieve a determined cell size before synthesising DNA, measuring the protein content per cell has proved this. In *S. pombe* cell division (separation of mother cell and daughter) also occurs here; hence the newborn cells appear at the beginning of the S phase. If cells have not achieved the desired cell size they will remain in G1 phase degrading Cdc25 at an elevated rate until they are large enough to leave G1 phase.

The second checkpoint G2B/M has to do with preparation during the G2-phase for mitosis. Cells ensure that repair and synthesis of DNA are completed and that cells are large enough to divide. At metaphase they ensure that all chromosomes are aligned in the right position before sister chromatids segregate to opposite poles of the mitotic spindle. Therefore, the G2/M checkpoint can also be controlled by the rate of uptake of glucose.

A G0 phase has been incorporated where cells remain for a certain period of time when exposed to certain environmental conditions such as starvation or heat shock. Cells in this phase become resistant to heat and chemical treatment. They can be reinserted in the main cycle once they 'sense' conditions in the environment (such as medium, temperature) are normal for them to re-start the mitotic cycle. The events described above will happen if after a certain period of time, the conditions improve. Cells in this 'dormant state' will enter a meiotic cycle where haploid cells of opposite mating type (h^+ and h^-) conjugate to form a diploid which will continue to divide in its own meiotic cycle. It is believed that fission yeasts conjugate in order to 'save nutrients and energy'. In the *S. pombe* model presented, cells can leave the mitotic cycle to join the G0 phase from any phase at any time, such an assumption is supported by Nurse (1993) who discovered the ability this type of cells have to leave the cycle from any phase.

However, if a diploid cell is starved of nutrient it has the option of undergoing a meiotic cycle to produce four haploid spores. The process of sporulation forms a distinct kind of cell division cycle that has similarities and differences with mitotic progression. Therefore, in S. *pombe* conjugation, meiosis and sporulation combine in an emergency response to nutrient limitation.

The model also has a D phase or pre death phase to account for the cells which have left the cycle with no option at all of returning to the cycle.

It is assumed that glucose is taken up during G2A and G2B phases only. Production of CO_2 is also an important parameter (Mitchison and Novak, 1986) being released through out the whole cell cycle with an increment of the rate of CO_2 production

right at the mid-point of the S period at 0.97 of the cycle (Mitchison and Creanor, 1969). Within the *S. pombe* module and as a new feature in the generic framework of CelCyMUS mass transfer is considered. The model is required to represent an aerated system with oxygen being taken up by the cells and CO_2 produced by them. This gives the opportunity of introducing a new module within CelCyMUS, capable of considering mass transfer processes between gas and liquid phases in a bioreactor.

3.6 MASS TRANSFER

In aerobic systems, the oxygen transfer rate from the gas phase to the liquid is often a limiting factor, and the bioreactor has to provide good mixing characteristics to provide good gas-liquid transfer. The consumption or production affects the levels of dissolved oxygen and carbon dioxide respectively and the rate of transfer between phases.

Carbon dioxide diffuses through the cell membrane and is hydrated in the liquid medium by the following reactions

$$CO_2 + H_2O \longleftrightarrow H_2CO_3 \longleftrightarrow H^+ + HCO_3^- \qquad (3.5)$$

The dissociation of bicarbonate to form carbonate ions, is considered negligible at pH 7 (Royce and Thornhill, 1991). The hydratation equilibrium is very slow, whereas the bicarbonate forming equilibrium is almost instantaneous. Hence the conversion between carbon dioxide and bicarbonate ions is described by the overall reaction:

$$CO_2 + H_2O \underset{K_{-1}}{\overset{K1}{\longleftrightarrow}} H^+ + H_2CO_3 \qquad (3.6)$$

Where K_1 and K_{-1} are the rate constants for the indicated reactions. Therefore if a balance for carbon dioxide is written this should include the hydratation in the liquid medium of carbon dioxide to bicarbonate. Oxygen and carbon dioxide transfer in the gas-liquid interface are physical phenomena limited by the transfer in liquid side of

the interface (Perry, 1984). The oxygen transfer rate is expressed usually as a product of the volumetric mass transfer coefficient, $K_La^O{}_2$, and the driving force of oxygen. The equilibrium oxygen concentration, C^*_{O2}, is expressed by the solubility in water at the culture temperature. The carbon dioxide transfer rate can be described in the same way to oxygen transfer rate. The equilibrium concentration C^*_{CO2} is given by:

$$C^*_{CO2} = 10^3 RT \frac{C^G_{CO2}}{H} \tag{3.7}$$

H ($Pa.m^3.mol^{-1}$) is the Henry's law constant, T (K) is the temperature of the gas phase, C^G_{CO2} is the gas carbon dioxide concentration, and R (8.3143510 $Pa\ m^3\ mol^{-1}\ K^{-1}$) is the ideal gas constant. K_La^{O2} and K_La^{CO2} (s^{-1}) are estimated with a mass transfer model (Arranz, 1993; Yagi and Yoshida, 1977) based on a fluid dynamic model which takes into account the bioreactor configuration and the operational conditions. On the other hand, the estimation of oxygen uptake rate and carbon dioxide production were obtained from experimental data (Nurse, 1993).

For the prediction of the oxygen transfer coefficient in stirred tanks, some simplifications are made. First of all, it is assumed that the stirrer supplies the energy dissipated. The friction losses and the reduction of power due to the aeration are assumed negligible. The energy dissipation rate is given by Equation (3.8). The interfacial area is calculated from the equations given by Figueredo and Calderbank (1979) for a system air-water Equation (3.9). The power of the aerated liquids is estimated by the expression proposed by Michel and Miller (1962) (Equation 3.10), with C being a constant value for an agitator type turbine with six blades (Fort *et al.*, 1993). The product of the interfacial area and the mass transfer coefficient allows predicting the K_La^{O2} for stirred tanks semi-theoretically.

The volumetric mass transfer coefficients for oxygen and carbon dioxide involve the same interfacial area, solvent properties and agitation variables. Thus, the K_La^{CO2} is calculated as a function of the K_La^{O2} by using the square root of the diffusivity ratio given in Equations 3.11 and 3.12 (Yagi and Yoshida, 1977; Royce and Thornhill,

1991). Although the liquid diffusivities are a function of both compositions, the values for water are assumed for simplification. With the values for the oxygen uptake-rate and carbon dioxide allow estimating the changes in concentration of oxygen and carbon dioxide in the liquid and gaseous phase during batch fermentation in stirred tank bioreactors.

The mass transfer model in general for this particular case is represented through the following equations:

Energy dissipation velocity

$$\xi = \frac{P_0}{\rho_L V} = \frac{N_p N^3 T^5}{V} \tag{3.8}$$

Where Po is the power supplied by a stirrer in a degasified system (W), ρ_L is liquid density, V is volume (m^3), N_p is the power number and N is the liquid velocity profile parameter (dimensionless).

Interfacial area

$$a = 593\left[\frac{P_S}{V}\right]^{0.25} V_S^{0.75} \tag{3.9}$$

Where Po is the power supplied by a stirrer (W), V_S is the gas slip velocity ($m.s^{-1}$).

Power of aerated liquids

$$P_s = C\left(P_0 N T^3 / Q^{0.56}\right)^{0.45} \tag{3.10}$$

Where Q is the volumetric gas flow rate ($l.s^{-1}$). C is a constant value for an agitator type turbine with six paddles.

Volumetric Oxygen Transfer Coefficient

$$K_L a^{O2} = \frac{2}{\sqrt{\pi}} \sqrt{D_L{}^{O2}} \frac{6\varepsilon}{d_b(1-\varepsilon)} \left(\frac{V_s \rho_L g \varepsilon}{K}\right)^{\frac{1}{2(n+1)}} \tag{3.11}$$

Where D_L^{O2} is the diffusivity of the oxygen in the liquid phase ($m^2.s^{-1}$), ϵ is dimensionless constant for stirred tanks ($\epsilon = 0.070$), g is the gravitational constant ($m.s^{-2}$), d_b is the diameter of bubbles (m) and n is the flow behaviour index (dimensionless)

Volumetric CO_2 Transfer Coefficient

$$K_L a^{CO2} = K_L a^{O2}\left(\frac{D_L^{CO2}}{D_L^{O2}}\right)^{\frac{1}{2}} \tag{3.12}$$

Where K_{La} (s^{-1}) are the volumetric mass transfer coefficients for oxygen and carbon dioxide respectively. Studies carried out on bioreactors processes (Guardia and Calvo, 2000) where mass transfer of oxygen and carbon dioxide where analysed have been implemented in our model through the following equations:

Species	Mass balance equations	
Liquid phase oxygen	$\frac{dC_{O2}^L}{dt} = K_L a^{O2}\left(C_{O2}^* - C_{O2}^L\right) - \gamma_{O2}$	(3.13)
Liquid phase carbon dioxide	$\frac{dC_{CO2}^L}{dt} = \gamma_{CO2} - K_L a^{CO2}\left(C_{CO2}^L - C_{CO2}^*\right) - \gamma_b$	(3.14)
Liquid phase bicarbonate	$\frac{dCb}{dt} = K_1 C_{CO2}^L - K_{-1} C_h C_b = \gamma_b$	(3.15)
Gas phase oxygen	$V_G \frac{dC_{O2}^G}{dt} = Q_0 C_{O2}^{G,0} - Q_1 C_{O2}^{G,1} - K_L a^{O2}(C_{O2}^* - C_{O2}^L)V_L$	(3.16)
Carbon dioxide	$V_G \frac{dC_{CO2}^G}{dt} = Q_0 C_{CO2}^{G,0} - Q_1 C_{O2}^{G,1} - K_L a^{CO2}(C_{CO2}^L - C_{CO2}^*)V_L$	(3.17)

TABLE 3.1

Where γ represents the constant of reactions for the different species in the reactor. Q_0 is the volumetric gas inlet flow rate ($l.s^{-1}$).

A schematic representation of what the mass transfer module looks like when working with CelCyMUS is presented here:

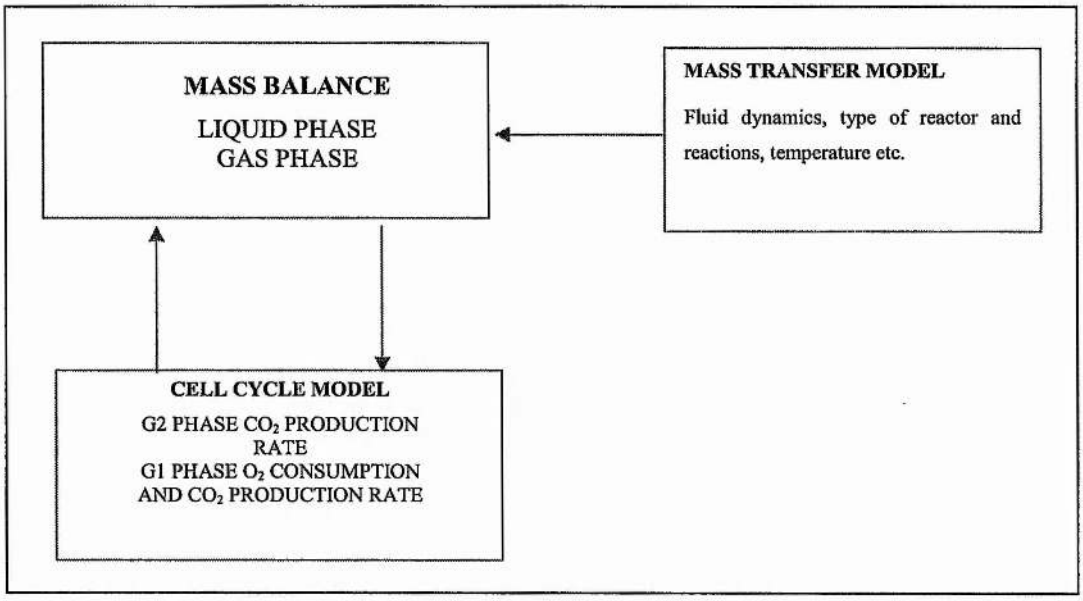

3.7 MAIN FEATURES OF THE MODEL

The main features for a model of the cell cycle of *S. pombe* have been stated above. A generic one-dimensional age population balance model of a fission yeast cell cycle based upon cell age is proposed. The model is a module within the generic frame model of CelCyMUS. It describes changes in age population, interactions of cell population with a multi-component medium and changes in the cytological state.

The *S. pombe* cycle divided in five phases has been presented in the model, where a phase is defined as a 'state' in which all cells obey the same set of transition rules, executing the same internal functions and interacting in the same way with the environment.

Transition is defined as the flow of cells from one phase to another due to changes in the cell age distribution mainly because cells have become older or they have achieved a 'transition rule' events these ones, which are mutually exclusive. As follows a list of all of the main assumptions in the model is outlined there are seven phases – G0, G1, S, G2A, G2B, M and D;

a) the S phase is the DNA synthesis phase and where a new daughter cell is born;
b) the M phase is where mitosis occurs;
c) G1 and G2 are the gap phases between the M and S phases;
d) the G2 phase is divided into two distinct periods, referred to as G2A and G2B phases;
e) the G10 phase accounts for the initial lag period and cells in this phase re-enter the cell cycle via G2A;
f) cells in the D phase stain as though still viable, although irreversibly out of the cell cycle and approaching death;
g) cells progress around the cell cycle in the following order – G2A, G2B, M, G1, S and back to G2A;
h) the G2A, S, M and G10 phases are of fixed duration - 63, 18, 9, 30 min, respectively;
i) the G2B and G1 phases are of variable duration, with maximum durations of 29 and 25min, respectively;
j) glucose is consumed at constant rates for cells throughout the cycle except during G2B phase where it reaches a peak twice as big as the uptake rate in the other phases;
k) CO_2 is produced at a rate which is proportional to the rate of assimilation of glucose and is excreted to the medium in the G1 and G2B phases;
l) Oxygen is assimilated in all of the phases at a rate which is proportional to the oxygen concentration in the medium;
m) the initiation of the S and M phases is controlled by a stochastic transition;
n) the probability of this transition is dependent on the cumulative amount of glucose consumed cells in phases G1 and G2B.
o) the relationship between the probability of this transition and the cumulative glucose content is a quadratic form;
p) once cells enter the D phase, they are trapped in this phase and the death rate of these is in accordance with first order kinetics.
q) During glucose exhaustion, cells which remain in G2B for the whole of its maximum duration will immediately enter D, instead of going into S; and
r) in a glucose free medium, cells which complete mitosis are incapable of initiating the G1 phase and enter the G0 phase. Cells which enter G2B after

glucose exhaustion will be trapped and will enter the D phase after the maximum duration of the G2B phase.

3.7.1 Phase Transition Rules

Each phase has a finite maximum duration and, in all cases, the first transition rule is used to account for this fact.

In this model, cells start in G2A phase and move around the cycle undergoing transitions from G2B through to M then G1 (cells recovering from mitosis) going to S, and finally going back to G2A phase. As stated above, cells must remain in each phase for a predetermined period of time (the maximum duration of the phase) unless they are forced to leave due to a transition rule. In the *S. pombe* case there are some specific transition rules to be considered:

For S, M and G2A phases only the first transition rule that applies (Equations 3.2 and 3.3). In the cases of G1 and G2B this transition is dependent upon the cumulative amount of glucose a cell has consumed since it entered this phase. This is given by:

$$r_{2G1}\left(\tau_{G1}, n_{G1}(t,\tau_{G1}), C_c(t,\tau_{G1}), C(t)\right) = \frac{2n_{G1b(t,\tau_{G1})}}{\left(C_{CGLUC}(t,\tau_{G1}) - S_{MAX}\right)} \frac{\partial C_{CGLUC}(t,\tau_{G1})}{\partial t} \tag{3.20}$$

Where C_{GLUC} is the intra-cellular concentration of glucose (kg cell^{-1}) and S_{MAX} is the maximum cumulative amount of glucose a cell can consume before it must initiate the M phase (kg cell^{-1}).

For the D phase (death) it is assumed that the rate of transition is dependent upon the prevalent CO_2 or Ethanol concentration as follows:

$$r_{2D}\left(\tau_D, n_D(t,\tau_D), C_c(t,\tau_D), C(t)\right) = k_{ETHO} C_{ETHO}{}^{n_x}(t, T_x) \tag{3.21}$$

As it is proved that high concentration of ethanol inhibits mitosis and induces death in *S. pombe*. Where k_{ETHO} is a constant to be determined empirically and C_{ETHO} is the ethanol concentration in the growth medium (kg m^{-3}).

3.7.2 Boundary Conditions

The boundary conditions have to be defined for each phase depending upon the transitions between phases. In the model proposed cells go through the phases S, G2A, G2B, M, and G1 before dividing. It is assumed that cells will duplicate right at the start of the S phase. Cells in the quiescent state (G10) enter the cell cycle in phase G2 (but within the model they could do it from any phase). Cells facing starvation are arrested in G0 phase.

Bearing in mind the assumptions made above the boundary conditions for the model phases are:

G2A Phase

$$n_{G2A}(t,0) = n_S(t, T_S) \qquad \text{If } C_{glucose} > 0 \qquad (3.22)$$

$$n_{G2A}(t,0) = 0 \qquad \text{If } C_{glucose} = 0 \qquad (3.23)$$

G2B Phase

$$n_{G2B}(t,0) = n_{S2A}(t, T_{G2A}) \qquad (3.24)$$

For M Phase:

$$n_M(t,0) = \int_0^{T_{G2B}} \frac{2n_{G2B}(t,\tau_{G2B})}{(C_{GLUC}(t,\tau_{G2B}) - S_{MAX})} \frac{\partial C_{CGUC}(t,\tau_{G2B})}{\partial t} \partial\tau_{G2B} \qquad (3.25)$$

G1 Phase

$$n_{G1}(t,0) = n_M(t,\tau_M) \tag{3.26}$$

For S Phase:

$$n_S(t,0) = 2 * \int_0^{\tau_{G1}} \frac{2n_{G1}(t,\tau_{G1})}{(C_{GLUC}(t,\tau_{G1}) - S_{MAX})} \frac{\partial C_{CGUC}(t,\tau_{G1})}{\partial t} \partial\tau_{G1} + n_{G1}(t,\tau_{G1}) \tag{3.27}$$

For D Phase:

$$n_D(t,0) = n_{G1}(t,T_{G1}) + n_{G2B}(t,\tau_{G2B}) \qquad \text{If } C_{glucose} > 0 \tag{3.28}$$

For G0 Phase:

$$n_{G0}(t,0) = n_{G1}(t,T_{G1}) + n_{G2B}(t,\tau_{G2B}) \qquad \text{If } C_{glucose} = 0 \tag{3.29}$$

3.7.3 Growth Medium

The model describes the consumption of glucose, oxygen and the production of CO_2. It is assumed that glucose is consumed in all of the phases with two big increments in glucose uptake rate for G2B and G1 phases, and the consumption kinetics are zero order. Carbon dioxide (CO_2) is produced in all of the phases (Mitchison, Novak, 1986). A change in the rate of production right at the end of the cycle made CO_2 production a special marker in the cycle of *S. pombe*. The increase in this rate is a pattern in *S. pombe* and different kind of mutants of the same micro-organism (Novak *et al.*, 1998. See figure 2 Appendix A).

With the assumption that increments of glucose uptake rates during G1 and G2B, a material balance gives the rate of change of concentration of glucose in the growth medium as follows:

$$\frac{\partial C_{GLUC}(t)}{dt} = (C_{FGLUC}(t) - C_{GLUC}(t))\frac{F(t)}{V(t)} - R_{GLUC}\left(\int_0^{T_{G2B}} n_{G2B}(t,\tau_{G2B})d\tau + \int_0^{T_{G1}} n_{G1}(t,\tau_{G1})d\tau\right) \qquad (3.30)$$

Where R_{GLUC} is the rate of consumption of glucose, approximately 1.04027×10^{-14} kg.gluc.cells^{-1}.hr^{-1}. (data gathered from Fotuhi, 2000 for batch fermentors). C_{GLUC} is the concentration of glucose in the growth medium (kg m^{-3}), and C_{FGLUT} is the glucose concentration in the feed stream (kg m^{-3}).

Since carbon dioxide is being produced at a constant rate throughout the cycle with a rate of change right at the end of the cycle in S phase. Then it is logical to affirm that the rate of CO_2 production will be constant in all of the phases but S phase. Therefore, the rate of change of concentration of CO_2 in the medium is given by:

$$\frac{dC_{CO_2}(t)}{dt} = R_{CO_2}\left(\int_0^{T_S} n_S(t,\tau_S)d\tau\right) - C_{CO2}(t)\frac{F(t)}{V(T)} \qquad (3.31)$$

Where R_{CO2} is the rate constant for the production of CO_2 from a cell (kg cell^{-1} hr^{-1}) and C_{CO2} is the concentration of CO_2 in the growth media (kg m^{-3}). It is assumed that there is not carbon dioxide in the feed stream at the beginning of the process.

3.8 ESTABLISHING THE MODEL

In order to establish numbers from the model, some parameters have to be fixed, such as real values of glucose and oxygen consumption throughout different phases of the *S. pombe* cell cycle. The knowledge of these parameters gives a better approach to the age population balance, improves the accuracy in cycle timing per single phase and a real view of this particular cycle. The experimental determination of glucose, oxygen and any other nutrients consumption per phase is achieved by synchronising cultures of fission yeast using either chemical blocks (growth arrest) or physical selection. Physical arrest is achieved by centrifugation selecting the smaller cells in a elutriating rotor following Mitchison *et al.* selection method (1965) using lactose and sucrose density gradients, such cells are then taken

to a different flask to initiate a new culture. Chemical blocks stop a specific event necessary for progression around the cycle. Once the entire population reaches this point the block can be removed and the resultant cell population is synchronised. This method includes the use of chemicals such as hydroxyurea and deoxyadenosine, both of which inhibit DNA synthesis in *S. pombe* for a period of time. This process is usually uniform during two to three cycles, time enough to determine the real consumption of glucose in every particular phase of the cycle rather than a general average value per cycle. The sampling and analysis of glucose consumption is done before de-synchronisation.

Cell de-synchronisation happens since cells with larger size will have shorter cycle times and vice-versa despite initiating the cycle at the same phase. It is expected to find changes in the rate of consumption of glucose at different phases. Such changes will be more representative at the checkpoints, since both of them (G1/S, G2B/M) depend on cell size, which enhance glucose, and oxygen as the medium responsible of individual anabolic growing.

Creanor (1992) carried out such experiments, when he studied the consumption of oxygen throughout the whole cell cycle for *S. pombe*. Creanor found two increments in the consumption of oxygen, which ended up being twice as much at the end of every cycle. The first increment in the oxygen uptake rate half way through the cycle (G2B phase) and a second one right at the end of it (G1/S phase). Each change in the rate was an increase of about 50%, with the result that overall the rate doubled each cycle.

Data from synchronised cultures of *S. pombe* where consumption of oxygen, production of CO_2 and other variables were analysed to be used within our model as indicators of a checkpoint and also as parameters in transition rules of the cycle. From Creanor's results, three sets of experiments were selected for analysis.
Their analysis will provide specific information about division and synthesis of DNA. The rate of production follows a linear pattern in synchronous cultures with a rate of change per cycle at the time of cell division, which seems to be more related to S phase.

The inclusion of CO_2 production is perfectly valid since it is a measure of the glycolytic flux and about half the total ATP production. All growth patterns in S. *pombe* yeast show these periodicities and there is not case of an exponential smooth increase. This is true for total dry mass (Mitchison, 1969), cell length (Mitchinson, Nurse 1985), oxygen consumption (Creanor, 1978), total protein (Creanor and Mitchison, 1969), ribosomal RNA (Elliot, 1983a), messenger RNA (Nurse *et al.*, 1978), and DNA (Mitchison and Creanor, 1969). Therefore CO_2 production would be a good parameter to control timing and cell division within the model. In figure 2 Appendix A the cell cycle times for different mutants of *S. pombe* based on CO_2 production are displayed.

Based on these data consumption of oxygen can be linked with the metabolic activity of the cell throughout ATP generation. The glucose consumed in the process is directly proportional to the amount of energy generated in the cycle, P/O ratio and the yield of glucose with respect of ATP production and formation of biomass. It is important to say that is highly unlikely that Y_{ATP} is constant at all growth rates, since it is known that the protein content of *S. pombe* increases significantly with increasing growth rate both under aerobic and anaerobic conditions. Therefore a decrease in Y_{ATP} is expected with increasing growth rate.

3.9 CONCLUDING COMMENTS

In this chapter a model for the *S. pombe* cell has been proposed. The mathematics behind the generic framework of CelCyMUS have been explained and the mathematical modifications needed to introduce the different phases in the cell cycle of *S. pombe* and its transition rules have been presented. The next chapter will elaborate on the development of the *S. pombe* model. The experimental data selected to support the model (Creanor, 1978) and the experiments used to test it (Fotuhi, 2002).

CHAPTER 4

DEVELOPMENT AND TESTING OF THE MODEL IN BATCH AND REPEATED BATCH CULTURES

4.1 INTRODUCTION

The basis and foundations for a new module containing the main features of the cell cycle for *S. pombe* as well as the new Fortran 95 features introduced in CelCyMUS have been presented in Chapter 3. In this chapter, the new code was checked to assure the reproducibility of the data by running the new program against the old version of it. The following chapter then explains how the *S. pombe* module has been developed, the assumptions made within the module, the analysis of experimental data both batch and repeated batch to develop the model and to compare them with predictions of real batch cultures run in the *S. pombe* model.

The *S. pombe* works as a module within the generic framework of CelCyMUS (Cell Cycle Model University of Surrey). The basic principle of the model of *S. pombe* is based on the individual consumption of oxygen per phase and subsequently CO_2 generation (Creanor, 1978), plus the consumption of glucose throughout the cycle (experiments in synchronised cultures) as a first order kinetic parameter (Fotuhi, 2002). The control and knowledge of these three parameters allow the model to establish the transition rules at different checkpoints within the cell cycle. In this chapter it will be demonstrated how the model has included a relationship between oxygen and glucose consumption, as part of the internal reactions in the cell to generate the necessary energy (ATP) to keep the cell cycling. The analysis of post-synchronisation data, error analysis for each one of the parameters and the adaptations made to simulate the behaviour of *S. pombe* in batch fermentors is presented. Experimental data used to corroborate the accuracy of the model were collected by (Fotuhi, 2002). The experimental results gathered from shake flasks, batch and repeated batch reactors were key factors in the development of the model.

4.2 VALIDATION OF THE NEW CODE

Since the code of the framework CelCyMUS has been re-built, two tasks were carried out to validate the new program. The first task was to run the program following the Smith and Martin model (1973), which basically divides the cell cycle in two stages. Some time after mitosis the cells enter a state (stage A, figure 4.1) in which their activities are deterministic, and leading towards replication. At this stage (A) cells are leaving with a constant probability, in our case such probabilities vary between 1%cell.h^{-1} and 7%cell.h^{-1}. The B state includes the conventional S, G2 and M phases as it can be seen in figure 4.1 below.

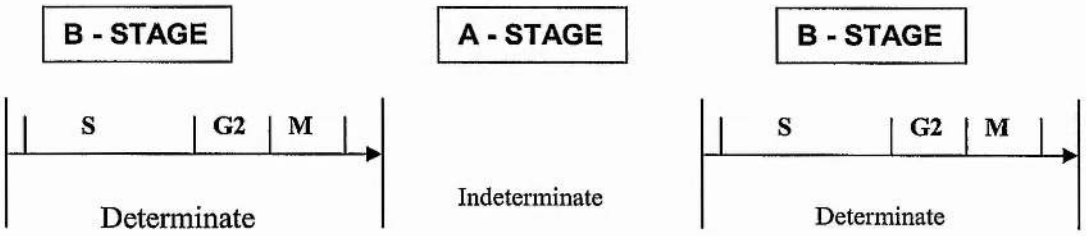

FIGURE 4.1

The Smith and Martin model (general population balance model, Figure 4.2) was applied to simulate synchronised cell culture runs for the mm 321 hybridoma cell line. It was assumed that a synchronised cell culture is released from a double block. Cells are arrested in G2 phase due to the action of chemical blocks (thymidine and hydroxyurea), which inhibit mitosis, and the progress of the cell population through the cell cycle in G2 phase. Glutamine is consumed through out G1A and G1B phases and there is a constant probability transition from G1B to S phase. Neither death phase nor washout was considered in these runs the phases and timing for this cell culture are displayed in Figure 4.2.

The second task was to run the new program against the old version of CelCyMUS once again for a mm321 cell line in a batch reactor, to test how reproducible the data would be. Here the cells are released from a G' phase (where they are evenly distributed) into the G1B phase where they follow a transition probability based in

the cumulative amount of glutamine per cell as a function of time. Consumption of glutamine in phases G1A and G1B, production of antibody to paraquat in phase G1B and S and excretion of ammonia into the medium (phases G1A and G1B) are taken into account. Schematic representation of the cell cycle for the mm321 hybridoma cell line can be seen in figure 3 (Appendix A).

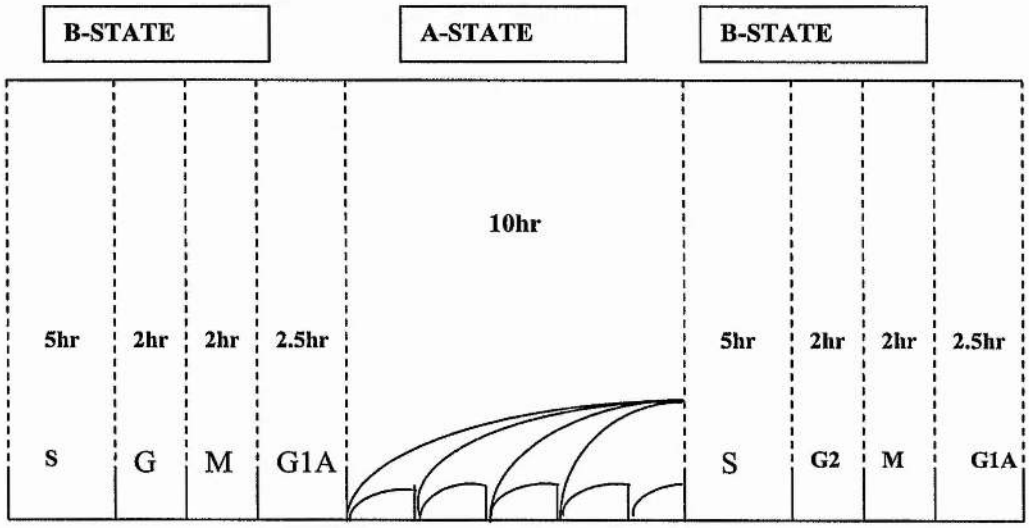

FIGURE 4.2

Having validated the new CelCyMUS code against previous runs on the model for hybridoma mm321 cell line it was then necessary to select experimental data to develop a specific model for *S. pombe*. The main data to be used in the new model had to come from synchronised cultures that allow following of the behaviour of parameters and kinetics in every phase of the cell cycle. The methods and techniques employed to achieve synchronisation of cell cultures, the importance of this procedure, its main advantages and the main researches that used synchronisation techniques in *S. pombe* are now discussed in detail.

4.3 SYNCHRONISATION OF CELL CULTURES

A synchronised culture is a population of cells, in which each cell has the same biological age (same cell cycle phase) carrying out the same activities over a common period of time. Creanor achieved synchrony by using lactose (7.5-30%)

and sucrose gradients (10-40% concentration). Such method works by suspending the cells in the medium (sucrose/lactose) and then centrifuging the solution in a centrifuge tube. Cells with different size and weight will spread in different layers down the tube. The top layer cell is then removed and the degree of synchrony is measured by the cell plate index, which is the percentage of cells in a population showing cell plates. This is roughly equivalent to the measurement of mitotic index in other systems.

Chemical blocking is also a common technique used to confirm the independence of metabolite uptake pattern from DNA synthesis, nuclear division and cell division. Mitomycin C inhibits nuclear division in *S. pombe* (Robinson, 1976) and *S. cerevisiae.* While hydroxyurea and deoxyadenosine (Mitchinson and Creanor, 1969) arrest cells in G1 phase.

4.4 ANALYSIS OF OXYGEN UP-TAKE IN INDUCED SYNCHRONOUS CULTURES WITH CHEMICAL BLOCKS

The addition of deoxyadenosine and hydroxyurea both of which inhibit DNA synthesis in *S. pombe* were carried out by Mitchinson and Creanor (1969), in order to confirm the independence of the oxygen uptake pattern from DNA synthesis, nuclear division and cell division. When added to an exponentially asynchronous culture for 3hr and then extracted by filtration, these inhibitors cause cells to undergo a synchronous division 2hr later, followed by a second semisynchronous division 1.5hr after. In this culture although DNA synthesis, nuclear division and cell division are occurring in a synchronous manner, the rate of oxygen uptake is increasing continuously.

A second type of experiment was carried out by introducing Mitomycin C which inhibits nuclear division in *S. pombe* (Robinson, 1972) and *S. cerevisiae* (Willianson and Scopes, 1962). While hydroxiurea and deoxyadenosine arrest cells in G_1, after nuclear division has occurred but before DNA synthesis, mitomycin C arrests cells in G2. The difference here was that the mitomicyn C was not removed from the cell culture, and the rate of oxygen uptake continues to increase during this period. This

of course suggests that the increase in oxygen uptake is independent of nuclear division, DNA synthesis and cell division.

4.5 ANALYSIS OF THE EXPERIMENTS OF CREANOR *et al.*

Creanor (1978) conducted experiments where the consumption of oxygen throughout the cycle in synchronised cultures was measured. The rate of oxygen uptake was found to increase in a step-wise manner at the beginning of the cycle (G1-S phase) and in the middle of it (G2B phase). The increments doubled the amount of oxygen uptake at the end of each cycle. In an induced synchronous culture where DNA and nuclear division were inhibited, oxygen uptake increased continuously in rate and it did not appear to affect growth. The step-wise behaviour also disappears. Creanor's findings agreed with those of Poole and Lloyd (1973). These cases are similar to those shown for the production of CO_2 in synchronous cultures of *S. pombe* (Creanor 1978) and are another case where a rate change persisted after DNA/cell division block. These changes in uptake during the cycle are therefore support of the "cell size growth" concept or the cells having to achieve a determined size before moving into DNA synthesis or cell division. Increase in cell size is therefore related to the internal accumulation of nutrients (proteins, carbon source) to be used in metabolic processes such as ATP production (energy) and in the repairing and duplication of the genetic information from mother cell to daughter cell.

The average results of three different experiments performed by Creanor et al in synchronised cultures of *S. pombe* were studied and named as Creanor A, B and C (see Table 4.2 and Graphs 1, 2 and 3 Appendix A). Such experiments where synchrony can clearly be seen were carried out for a period of six hours, after this time de-synchronisation takes over and the consumption rate of oxygen per phase becomes less evident because the data obtained are of those of cells with different cell age in different phases. From Creanor's experiments was established that the first two hours of the experiment are an initial lag or G10 phase, which is were cells are released into the medium and they acquaint themselves with their new environment. This is just after being released from synchrony. This G0 phase will

also be used for those cells that for some reason (to be explained later) do not successfully complete mitosis and leave the cycle permanently to join a quiescent phase. Initially, the data obtained from Creanor experiments were from logarithmic graphs presented in his paper. These graphs were then digitally scanned and actual data from oxygen consumption rates was extracted. Once the data were available this was translated into a decimal scale form by using a normal linear regression from the logarithmic scale.

Phase	Time(min)	Time (hr)	O2Rate	O2Rate non-log (ul.cell-1.min-1)
	51.80	0.86	0.620	4.171
	63.02	1.05	0.610	4.077
	75.97	1.27	0.728	5.347
	88.92	1.48	0.783	6.062
	102.73	1.71	0.848	7.046
	115.68	1.93	0.949	8.886
Mphase	129.50	2.16	0.972	9.372
Cell Plate Index Peak	135.60	2.26	0.966	9.247
G1Phase	144.17	2.40	0.972	9.372
G1Phase	157.12	2.62	1.070	11.748
G1/Sphase	169.21	2.82	1.159	14.432
End Sphase	178.62	2.98	1.202	15.907
G2A Phase	182.16	3.04	1.216	16.461
G2A Phase	195.11	3.25	1.256	18.035
G2A Phase	205.47	3.42	1.276	18.899
G2A Phase	216.69	3.61	1.308	20.301
G2BPhase	227.91	3.80	1.463	29.031
G2BPhase	241.73	4.03	1.572	37.355
G2BPhase	255.54	4.26	1.624	42.034
G2BPhase	267.63	4.46	1.624	42.034
G2BPhase	277.99	4.63	1.846	70.126
Cell Plate Index Peak	280.80	4.68	1.802	63.387
	289.21	4.82	1.921	83.444
	303.02	5.05	1.891	77.772

Phases	Time(hr)	Time(min)
M/G1Phase	2.26	135.6
G1/Sphase	2.67	160.2
S/G2Phase	2.977	178.62
G2/Mphase	4.53	271.8
M/G1Phase	4.68	280.8

TABLE 4.1

From the six hour period since the start of the synchrony until the beginning of de-synchronisation (5-6hr) just the intermediate part (3-5hr) was analysed. The criterion for this selection was that during the first two 2hr of synchronisation the cells were recovering from the induced synchrony (either throughout glucose gradients and/or

chemical blocks) and adjusting to the new medium. Such a period can be considered as a lag phase and is usually about half an hour (30min) long. At three hours the synchrony is most noticeable (were most cells are cycling together) even though synchrony is not perfect, since not all of cells would be in the same phase by now. Creanor measured the cell plate index of the cells, which is similar to the measurement of mitotic index. About 60% of the cells reached this peak (when seen under the microscope) about two hours into the experiment and a clear partition (an unequivocal sign of cells about to undergo cytokinesis) can be seen at this moment (M phase). The *S. pombe* model simulates the behaviour of cells when released from synchrony at the beginning of the G2A phase, about 45min later. This indication was common for the three experiments (Creanor A, B and C) where about two hours into the experiment cells would show the highest percentage of cells in synchrony (60%). This is the reason why the data in between 2.82 hr and 5.05 hr were selected as initial data to run the model (see Table 4.5). In fact the least square error in this part of the model is just about 3.09 compared with the 26.26 total from the whole graph covering the synchronisation experiment.

Even though the *S. pombe* model predicts de-synchronisation the initial fitting of the model to experimental data was made strictly on the basis of perfect synchronisation, in order to find the right values of oxygen consumption and CO_2 production in the different phases of the cell cycle. Therefore the last two hours of the experiments marking the beginning of the de-synchronisation in full scale were not considered as data for a perfect synchronisation experiment.

4.6 CARBON DIOXIDE PRODUCTION (MITCHINSON AND NOVAK EXPERIMENTS)

Changes in the rate of production of carbon dioxide was studied by Novak and Mitchison (1986) and appears once per cycle at the time of cell division being a predominant pattern right at the end of the cycle. The actual increase of CO_2 production occurs during the S phase, which is when the cells are splitting up. Carbon dioxide has been shown to have a big influence in the cell cycle of *S. pombe* (Novak 1998). Novak examined the effect of CO_2 removal finding that this

shortened the G2 phase of the cell cycle and arrested the cells in G1 phase in minimal medium. The slow down of anapleurotic CO_2 fixation might be responsible for this effect, as aspartatic acid could abolish the G1 block. The shortening of G2 phase in the wild type cells was observed in every medium irrespective of whether the growth rate was changed or not. Therefore it was proposed that CO_2 would inhibit mitosis in fission yeast explaining the proportionality between growth rate and cell size at mitosis.

In faster growing and dividing cells the CO_2 production rate is larger than in slow growing cells. The larger CO_2 production lead to a higher CO_2 concentration in the cell and the intracellular CO2 concentration is proportional to the specific growth rate. Thus the growth rate of cells could be measured through the intracellular CO_2 concentration. Since CO_2 inhibits mitosis, the faster growing cells might divide their nuclei only at a larger size. Mitchinson's experiments confirmed the findings from Creanor (1978) regarding the relationship between cell size and metabolic activity in the cell throughout the cycle. Based in the information gathered from these experiments it is now possible to establish a model for the *S. pombe* cell and its phases.

4.7 PHASES IN *S. pombe* AND THEIR DURATION

In the conventional cell cycle four phases are known, the so-called gap phases (due to the duration in time is determined for the length of S and M phases) G1 and G2, the S phase and M phase or mitosis. The S phase is where cell synthesise DNA making sure the genetic information is transferred from mother cell to daughter cell and M phase or mitosis where cells are basically giving birth to a new cell. As discussed in the previous chapter, the cycle for *S. pombe* has five phases instead. The G2 phase is divided in G2A phase and G2B phase. G2A phase is the phase where cells will be recovering from cytokinesis, since in *S. pombe* cells split right at the end of the S phase opposite to what most cells do (cytokinesis at the end of mitosis). The G2B phase is where cells prepare to enter mitosis, which makes them increase the consumption of metabolites in order to start mitosis. Such division of the G2 phase is supported by the fact that consumption of oxygen after cell division

stabilises for a period of time before reaching a new peak that is generally twice as big as the average consumption in the rest of the cell cycle (see Tables 4.1 and 4.2). The ratios calculated in Table 4.2 show the relationship between rates of oxygen uptake. Production of CO_2 (Mitchinson and Novak 1998) and consumption of glucose display similar patterns at this stage through the cycle.

	Phases Included	**Time (min)**	**Average Oxygen Uptake rate ($ul.cell^{-1}.min^{-1}$)**	**Ratio G2A/(M+G1+S)**	**Ratio. G2B/ (M+G1+S+G2A)**
Creanor A	M+G1+S	52	**$1.8729x10^{-6}$**	**0.9568**	**2.1669**
	G2A	38.07	**$1.79205 x10^{-6}$**		
	G2B	61.29	**$4.01466 x10^{-6}$**		
Creanor B	M+G1+S	52	**$2.19176 x10^{-6}$**	**1.1104**	**2.4765**
	G2A	42.05	**$2.43362 x10^{-6}$**		
	G2B	64.15	**$5.57762 x10^{-6}$**		
Creanor C	M+G1+S	50.7	**$1.63292 x10^{-6}$**	**0.82835**	**1.665379**
	G2A	25.04	**$1.35263 x10^{-6}$**		
	G2B	75.97	**$2.48604 x10^{-6}$**		

TABLE 4.2

As it can be seen from Graphs 1,2 and 3 (Appendix A), M, G1 and S phases have a combined duration of approximately 52min (data presented in Table 4.2) G2A is about 40 min long except for Creanor C where G2A is quite short (25min) compared with Creanor A and B. The ratio from G2A with regards of M+G1+S phases is close to 1. Therefore the consumption of oxygen in these phases is almost constant. However, that is not the case for G2B phase where the ratio of oxygen consumption compared with the rest of the phases in the cycle is twice as big (2.1 on average). The G2B phase has a length of 63min on average (Creanor A and B) except once again for Creanor C. These measurements indicate a far better synchrony in Creanor A and B than in Creanor C. This fact guided us to the conclusion that for practical purposes Creanor A and B should be used as the experiments to use to extract the values for oxygen consumption rate.

4.8 PARAMETERS CONSIDERED AND THEIR RELATIONSHIP

There are three main features to be followed in the *S. pombe* cycle for the purposes of this model. They are: oxygen consumption, carbon dioxide production and

glucose consumption as a representation of the amount of energy (ATP) spent in a cell throughout the cycle in assimilatory and dissimilatory processes. About 33% of the glucose is spent in dissimilatory processes or processes related to energy production, synthesis of proteins and other metabolites and movement. The 67% left is used in assimilatory processes or reactions related to growth of cells regarding individual cell size. Glucose is transformed into energy by means of the ATP production and consumption. In order to do so, glucose would have to go through different metabolic pathways that will happen depending on the circumstances, they are; glycolysis, respiration from adding EMP reaction (Embden-Meyerhof-Parnas pathway) with TCA reaction (tricarboxylic acid cycle).

The general reaction involving all intermediate reactions for the glycolytic pathway is:

$$C_6H_{12}O_6 + 2Pi + 2ADP \rightarrow 2C_2H_5OH + 2CO_2 + 2ATP + H_2O \qquad (4.1)$$

Where Pi represents piruvate.

4.8.1 The Energy Balance Sheet for Glucose Oxidation

For each molecule of pyruvate oxidised to completion, 12 molecules of ATP are formed in the four NAD-linked steps. 2 molecules of ATP are formed during the flavin-linked oxidation of succinate and 1 molecule of ATP is formed by the substrate level phosphorylation at the expense of succinyl CoA, to make a total of 15ATPs formed per molecule of pyruvate oxidized. We can therefore write an equation for the complete oxidation of pyruvate by mitochondria, including the coupled phosphorylations:

$$\text{Pyruvate} + 2\frac{1}{2}O_2 + 15Pi + 15ADP \rightarrow 3CO_2 + 15ATP + 17H_2O \qquad (4.2)$$

It is now possible to write a set of equations for the complete aerobic oxidation of glucose to CO_2 and water and the conservation of free energy as ATP. For the glycolytic sequence to pyruvate we have the reaction:

$$C_6H_{12}O_6 + 2Pi + 2ADP + 2NAD^+ \rightarrow 2Pyruvate + 2NADH + 2H^+ + 2ATP + 2H_2O \quad (4.3)$$

and for the tricarboxylic acid cycle:

$$2Pyruvate + 5O_2 + 30Pi + 30ADP \rightarrow 6CO_2 + 30ATP + 34H_2O \quad (4.4)$$

To these we must add the equation for the oxidation of the two molecules of extra-mitochondrial NADH formed in the glycolytic conversion of glucose to pyruvate. Oxidation of extra-mitochondrial NADH may generate either two or three molecules of ATP per pair of electron, depending upon how the electrons from extra-mitochondrial NADH enter the mitochondria. If it is assumed that two molecules of ATP are formed in this process, we have:

$$2NADH + 2H^+ + O_2 + 4P_i + 4ADP \rightarrow 2NAD^+ + 4ATP + 6H_2O \quad (4.5)$$

The sum of Equations 4.6, 4.7 and 4.8 is therefore:

$$C_6H_{12}O_6 + 6O_2 + 36Pi + 36ADP \rightarrow 6CO_2 + 36ATP + 42H_2O \quad (4.6)$$

The second reaction to be considered is the general reaction for the ATP yield from glucose in a respiring cell. This reaction results from adding EMP reaction (Embden-Meyerhof-Parnas pathway) with two times TCA reaction (tricarboxylic acid cycle) with ten times the equation for the oxidation of all NADH + H^+ generated in the EMP (two) and TCA reactions, and twice Eq. 1.2 ($FADH_2$ oxidation) giving:

$$C_6H_{12}O_6 + 38Pi + 38ADP \rightarrow 6CO_2 + 38ATP + 44H_2O \quad (4.7)$$

Since ATP hydrolysis has a standard free-energy change of –7.3-kcal/mol glucose, the free energy of the reaction is approximately:

$$\Delta G^{\circ} \equiv (38 molATP / mo\lg lu\cos e) * (-7.3 kcal / mol) \approx -277 kcal / mo\lg lu\cos e$$

This is 19 times the energy that the cell captured during glycolysis. As in glycolysis, energy retention is very efficient: Energy captured efficiency = 277/686 = 40%. If this figure is corrected for the non-standard concentrations within the cell a rather astounding efficiency estimate of greater than 70% results. Most of the remaining energy is dissipated as heat, which must be removed in some fashion to keep the temperature in the physiologically suitable range.

4.8.2 Energy Requirement for Biomass Formation: Y_{ATP}

In the classical studies has been found that the biomass yield was related to the energy yield in the dissimilation. This led to the introduction of the term Y_{ATP} (g cell per mol ATP formed). This Y_{ATP} was calculated from product formation in anaerobic (batch) cultures and thus was an experimental value. As it was shown later that the observed Y_{ATP} maybe affected by maintenance, notably in the case of bacterial growth, a second term, Y_{ATP}^{MAX} (Stouthamer & Bettenhaussen, 1976) was introduced, which is Y_{ATP} corrected for growth independent maintenance energy. For yeast no large differences in between Y_{ATP} and Y_{ATP}^{MAX} are observed (Harder and Dijkhuizen, 1982).

4.8.3 Parameter Values to Be Implemented

The parameters and the relationship between them have been explained. Using experimental data from synchronised cell cultures for the rate of consumption of oxygen (RCOXY) in *S. pombe,* the rate of production of carbon dioxide (RCO2) and glucose consumption have been justified. It is possible to follow the stoichiometry of the reactions where these metabolites are being produced or consumed to find out the production of ATP throughout the cell cycle in the same form as it was calculated from experiments, or simply by calculating P/O ratios throughout the

cycle. Therefore calculating the amount of ATP produced at different stages in the cycle is also a reality. The initial values for the chosen parameters are shown in Table 4.3:

PARAMETER	S	G2A	G2B	M	G1
RCOXY	1.5169 uL.cell^{-1}min^{-1}	1.7921 uL.cell^{-1}min^{-1}	6.125x10^{-14} **(mol.cell^{-1}.min^{-1})**	1.86183uL.cell^{-1}min^{-1}	5.66x10^{-14} **(mol.cell^{-1}.min^{-1})**
RCO2	---	---	6.655x10^{-14} **(mol.cell^{-1}.min^{-1})**	---	---
RCLUCOS	---	---	1.0403x10^{-14} KgGluc.cell-1.hr^{-1}	---	---
SMAX	---	---	4.5982x10^{-11} (molO2.cell^{-1})	---	1.05371x10^{-11} (molO2.cell^{-1})
GLUCLIMIT	1.73x10^{-14} g glucose.ml^{-1}	1.73x10^{-14} g glucose.ml^{-1}	1.73x10^{-14}g glucose.ml^{-1}	1.73x10^{-14} g glucose.ml^{-1}	1.73x10^{-14} g glucose.ml^{-1}

TABLE 4.3

4.9 INITIAL CONDITIONS AND S_{MAX} VALUES

The cell cycle phase duration and the number of probability distributions associated with each phase are presented in Table 4.4:

	G2A	G2B	M	G1	S	G0
Phase Duration (min)	40	62	9	25	18	125
Number of Transition Rules (G)	1	2	1	2	1	1

TABLE 4.4

The duration of the phases were calculated from the synchronisation experiments that Creanor carried out in *S. pombe* for oxygen consumption and has been explained above. The number of probability transitions was also allocated based on the oxygen consumption ratios presented in Table 4.2 where it can be seen that the uptake rate of oxygen peaks in G2B and G1 (see Creanor analysis). Data for the

initial number of cells in synchronised experiments were not given in Creanor's experiments but were inferred by running the model assuming perfect synchronisation ($5x10^6$ cells starting at G2A). The next step was fitting the data obtained (in terms of oxygen consumption) to the experimental values given by Creanor, see Table 4.5:

Time (hr.)	Experimental Value. Oxygen consumption ($mol.cell^{-1}.min^{-1}$)	Model Value. Oxygen consumption ($mol.cell^{-1}.min^{-1}$)	LSQE
0.86	4.17	13.64	5.15
1.05	4.08	13.64	5.50
1.27	5.35	13.70	2.44
1.48	6.06	14.16	1.78
1.71	7.05	15.52	1.45
1.93	8.89	17.40	0.92
2.16	9.37	19.44	1.15
2.26	9.25	20.44	1.47
2.40	9.37	21.93	1.80
2.62	11.75	26.18	1.51
2.82	14.43	26.74	0.73
2.98	15.91	27.61	0.54
3.04	16.46	27.75	0.47
3.25	18.04	28.45	0.33
3.42	18.90	29.37	0.31
3.61	20.30	30.94	0.27
3.80	29.03	32.93	0.02
4.03	37.35	36.37	0.00
4.26	42.03	40.57	0.00
4.46	42.03	44.27	0.00
4.63	70.13	47.19	0.11
4.68	63.39	48.04	0.06
4.82	83.44	50.33	0.16
5.05	77.77	54.25	0.09
TOTAL SUM OF LSQE (Highlighted data)			3.09

TABLE 4.5

Initially the number of cells calculated by the model was considerably different from the one obtained in the experiments. This is due to the fact that at the beginning there were no death rules included (to account for the number of cells dying or leaving the cycle) in the model, instead adjusting the proliferation factor PF (fraction of cells that make it throughout cytokinesis or average number of daughter cells per cell) the number of cells was fitted. The method employed to fit these data was the least square error.

Once a reasonable fitting from the synchronised experiments had been obtained (total summa of square errors being equal to 3.09) the introduction of death rules, and transition probabilities breaking the synchrony were the steps forward towards the simulation of batch experiments. Such experimental data were taken from Fotuhi (2002) experiments on batch and repeated batch cultures of *S. pombe.*

4.10 FOTUHI EXPERIMENTS

Fotuhi (2002) conducted research in order to develop an automated repeated batch propagation system and used this system to validate theoretical findings from other researchers who had previously worked in *S. pombe.* Fotuhi identified the best batch and repeated batch-operating conditions for this system. The growth kinetics of *S.pombe* in this study were investigated and characterised experimentally against the Monod model. Experiments in flask, batch and repeated batch cultures were carried out. As follows a compilation of the batch experiments carried out by Fotuhi that were used for this dissertation purposes is presented here.

Batch Culture	Age	Glucose Level (%)	Inoculum Size
Shake Flask	24hr	2	8.9
Bioreactor	24hr	2	1.2
Bioreactor	24hr	2	8.8
Bioreactor	24hr	2	19.2

TABLE 4.6

Fotuhi also used the batch experiments to find out the effect of oxygen transfer on growth by varying the concentration and flow of oxygen in two separate batch experiments with the same initial concentration of glucose (Table 4.7). Despite the fact that during the batch experiments the outlet flow of oxygen and the oxygen dissolved were not measured, the result of these experiments was conclusive regarding growth in cell population. The results showed that those cell cultures with higher oxygen transfer rate achieved maximum cell concentration and higher

specific growth rate. These experiments and the analysis of death cells in other batch experiments were important in finding and understanding the rate at which cells die and the minimum values of glucose and oxygen that are necessary for the cells to cycle at normal conditions.

Parameter	Batch Experiment A	Batch Experiment B
Inoculum (cells/ml)	1.2×10^6	1.7×10^6
Oxygen Flow rate	0.5 L/min	2 L/min
X_{MAX} (cells/ml)	18.5×10^6	73.7×10^6
Time at X_{MAX} (hr)	70	26

TABLE 4.7

The repeated batch experiments that will be analysed in Chapter 5 were all based on three sets of operating conditions using a harvest fraction (HF) of 90%, a dilution cycle time (DCT) of 18hr, HF of 80% and DCT of 12hr The data obtained by Fotuhi corroborated the importance of the relationship between HF/DCT combinations and, in part, validate the theoretical findings of Faraday (1994) and Araujo's research on model based observer controller (MBO) in 1998. A compilation of the repeated batch experiments carried out by Fotuhi and used in this dissertation is presented here (Table 4.8).

Repeated Batch Culture in	HF	DCT	Re-suspension number	Initial cell concentration (Million cells/ ml)
Bioreactor	90%	18hr	9	19.8
Bioreactor	90%	18hr	20	12.2
Bioreactor	80%	18hr	20	21
Bioreactor	80%	18hr	8	17.5
Bioreactor	80%	12hr	20	22
Bioreactor	80%	12hr	18	20

TABLE 4.8

4.10.1 Adjusting the Model to Fotuhi's Data

The first challenge faced by the new model was to simulate the behaviour of batch cultures of *S. pombe*. Such runs should fit Fotuhi's experiments. In order to do so there were certain new parameters that had to be introduced, such as oxygen uptake kinetics, carbon dioxide consumption kinetics, glucose consumption rate and finally the introduction of a death rule for the *S. pombe* model.

Results showing the values for glucose consumption from Fotuhi compared with data from the *S. pombe* model are presented in both batch and repeated batch experiments. Batch experiments had in common an 18hr DCT and an average time to initiate next batch experiment (charge and discharge) of 6-12min. The analysis of this experiment allowed for the inclusion of a lag phase and a death phase presented as follows.

4.11 DEATH RULE, D PHASE

To account for the number of cells dying in every batch a constant percentage of death cells per hour was included. This percentage was triggered by reaching critical levels of oxygen dissolve (according to mass transfer module) and a minimum value of glucose concentration per cell in the bioreactor. Cells die in a bioreactor either because they present a genetic failure, having failed to successfully duplicate their DNA sequence or because they get old. Cells also die due to collisions with the paddles of the stirrer in the bioreactor and stretching when a formation of foam collapses, very common in animal cells. The shape, geometry and roughness of the material the paddles are made of are factors to be considered. Collisions with the walls of the reactor are also a common cause of cell death. All of these factors put together (oxygen flow rate, speed of the stirrer, paddles geometry and material) remain constant in every experiment and they are responsible for cell death in general, representing a constant percentage of the cell population. These cells drop out of the cycle, and accounted for in a D phase or death phase placed in the model. The only factor that will change depending of the conditions of the experiment is the glucose concentration. The minimum amount or critical value of glucose will be

reached sooner in experiments with a higher initial cells number hence a larger population to deplete the medium they are being fed. However it was proven that the minimum amount of glucose per cell was the same in all cases. This issue will be discussed in Chapter 5.

4.12 LAG PERIOD IN BATCH AND REPEATED BATCH EXPERIMENTS

From Fotuhi's experiments it was noticeable that at the start of every batch and repeated batch experiment there was a delay for a period of about half an hour at the time before the cells would start cycling and carrying out normal activities in the reactors. This period of time is associated for some researchers with the time the cells need to adjust to the new medium. In the case of batch cultures, cells have usually being taken from a shake flask where they have been cultivated and then re-suspended in a batch reactor with new medium to start the batch.

In order to justify this period of time a lag phase was introduced, in other words cells do not start cycling immediately, cells drop into the cycle from a G0 phase or lag phase. This G0 phase is 30 minutes long and is represented within the model as an array with an evenly distributed number of cells throughout it. Then for a period of 30min cells will be introduced into the cycle in equal numbers after known equal periods of time.

4.13 REPEATED BATCH EXPERIMENTS (FOTUHI, 2002)

The basic principle for repeated batch experiments is to grow a batch culture for a fixed period of time (DCT), after which a known fraction of the cells in the reactor is harvested (HF). The remaining fraction in the reactor will be then the initial amount to start a new batch that will be fed with fresh medium. This process is then repeated several times (cycles number or re-suspension number). The operating parameters DCT and HF are kept constant throughout all cycles. Fotuhi (2002) carried out this type of experiments looking for the best values for DCT and HF that will generate the best yield and the most homogeneous behaviour in a repeated batch experiment.

4.14 SENSITIVITY ANALYSIS FOR THE *S. pombe* MODEL

In order to analyse the influence the main parameters have on the model, a sensitivity study was carried out. The sensitivity analysis was done by comparing the results from the model with batch runs carried out by Fotuhi 2002 in batch reactors with an initial cell number of $5x10^6$ million cells, a glucose concentration of 2% and over a period of time of 24hr The analysis was conducted by varying one parameter at the time while keeping all the others constant. Then a summa of the least square errors compared with the parameters values for which the model had reached a minimum is calculated.

The parameters were varied 5% above and below the initial number set up for those parameters in the model. The criterion used to choose the parameters were based on the impact these parameters would have on the population balance of the model and the variation they would introduce in the model regarding the experimental values. Therefore oxygen consumption was a valid parameter since the model had been adjusted based on experimental values gathered by Creanor (1978) as explained before in this chapter. Other metabolic parameters such as carbon dioxide production, glucose consumption and ATP generation were dependent upon oxygen consumption due to the stochiometric factors. The results of changing these parameters would be in agreement with the results obtained by changing oxygen consumption in the experiments and the model. Therefore oxygen consumption was the only metabolic parameter consider for this study. Furthermore, the importance of modifying the oxygen consumption at the G1/S and the G2B/M checkpoints is linked to the regulation of the probability transitions (S_{MAX}) and the amount of cells that will 'transit' to the following stage of the cycle once they have completed the necessary tasks (achieving cell size or DNA synthesis). It was also considered that the variations in oxygen consumption for this analysis would have to be small (especially below the original value) since our purpose is to simulate an aerobic system and small values of oxygen consumption would lead to a different process and a different metabolic pathway than the one studied here.

The initial number of cells used to fit Fotuhi's data was obtained by running the model over a long period of time to obtain a very well distributed population of cells around the cycle extracting the number of cells in every phase after this time. The idea of changing the initial number of cells in every phase was to visualise the importance of cell population and its distribution around the cycle. The initial number of cells in different phases was then affected. The impact they would have in the outcomes of the model would be reflected in the number of cells arriving at the checkpoints, the number of cells at the end of every cycle, and subsequently the overall amount of cells for every batch. Therefore changing the values at every phase at the time should give us a reference point about the importance of cell distribution in the cell cycle and the importance of individual phases within the cycle. Changing the cell population numbers in different phases seems to be a very sensitive parameter. The response to these variations will be discussed in the Chapter 5.

	Φ		% Error in Oxygen consumption (Creanor)	
	+ AND -		+ AND -	
Oxygen consumption rate (+/-) 5% AT G2B-M	5.934	5.933	0.0169	0.000
Oxygen consumption rate (+/-) 10% AT G2B-M	5.937	5.935	0.0674	0.0337
Oxygen consumption rate (+/-) 5% AT G1-S	5.96	5.982	0.455	0.826
Oxygen consumption rate (+/-) 10% AT G1-S	6.062	6.101	2.174	2.832
Cells starting in G2A phase (+/-) 5%	5.990	6.296	0.961	6.118
Cells starting in G2B phase (+/-) 5%	8.700	7.883	46.637	32.867
Cells starting in M phase (+/-) 5%	16.340	13.760	175.409	131.920
Cells starting in G1 phase (+/-) 5%	21.390	17.650	260.526	197.489
Cells starting in S phase (+/-) 5%	11.230	10.660	89.280	79.673

TABLE 4.9

4.15 CONCLUDING COMMENTS

Throughout this chapter validation of the new code used in CelCyMUS and the inclusion of experimental data to justify the assumptions taken in the *S. pombe* model have been presented. Data regarding the validation of the new code (Fortran 95) was presented by simulating the Smith and Martin model and by reproducing data from the mm321 hybridome cell line previously obtained by Faraday (1994). The results of these tests are discussed in Chapter 5.

Once the model was tested against the old version, this research moved into developing a model for the organism of interest *S. pombe*. Analysis of the synchronisation methods (vital for data collection) was presented in detail. Within the synchronisation experiments, those involving *S. pombe* and the consumption of oxygen in particular (Creanor, 1978) were selected and thoroughly studied due to the quality of data, the fact they were specifically for *S. pombe* and the importance of such parameter (oxygen consumption) in testing the newly introduced mass transfer module in the CelCyMUS framework. The mass transfer module accounts for oxygen (and any other metabolite and their reactions) dissolved in the liquid and gas phases of the reactor at any given time. Results from the mass transfer module explained in Chapter 3 and introduce in Chapter 4 will be discussed in Chapter 5. With the new tools fitted in the CelCyMUS framework and the gathered data from *S. pombe*, final details such as the inclusion of a death phase (D phase) accounting for cell deaths and washout (in the case of repeated batch) and a lag phase were also included. The next step was the to test the newly developed *S. pombe* model in a real system and for those purposes this dissertation adjusted the model to reproduced data generated within the research group at Surrey University by Fotuhi (2002). The data generated by Fotuhi in batch and repeated batch reactors allowed this research to test the model against real systems. Finally a sensitivity analysis in the *S. pombe* module on the parameters chosen to regulate the movement of cells between phases of the cell cycle and the importance of initial number of cells and cells distribution was carried out. The outcome of this analysis is discussed in Chapter 5 and expanded in Chapter 6 in future work as it opens up this research into new conclusions about this particular model.

CHAPTER 5

DISCUSSION OF RESULTS

5.1 INTRODUCTION

The following chapter compares the results obtained from the model for the *S. pombe* cell cycle with those reported in literature. Firstly the results regarding the reproducibility of the revised framework of CelCyMUS in Fortran 95 are compared with those from the model previously developed by Kirby and Faraday (1994) for the mm321 hybridoma. Once the reproducibility of CelCyMUS was checked a comparison was made between data generated for the new module for *S. pombe* and experimental batch and repeated batch runs from Fotuhi (2002). These data were fitted and found to be in good agreement. Discussion and comments regarding the repeated batch experiments are also presented and compared with lab data. Finally analysis on the sensitivity study carried out on the model parameters is presented here.

5.2 TESTING THE ALGORITHM

The results obtained in the CelCyMUS updated version of Fortran 95 have been compared with those gathered from a previous Fortran 77 version where the CelCyMUS model had been used to describe the behaviour of a mouse - mouse mm321 hybridoma cell line. The advantage of the new version is that it can be included in a PC rather than running the program in a supercomputer due to the new Fortran 95 utilities, which made it faster (faster compilation times), more flexible and code portable. The amount of memory required to run the program is just the quantity needed. Dynamic allocation of arrays also allows us to run the program for different conditions and cycle times, which could be very useful when simulating mutants.

The runs carried out for the new versions of the model correspond to population balances of the mm321 cell line with four conventional phases (S, G2 M and G1), with the G1 phase divided in two parts (G1a and G1b), with a constant and variable probability transition (Smith and Martin 1973) see Graphs 1 and 1B (Appendix B), cells leaving G1b phase and moving into S phase. Consumption of glutamine at G1 phase is considered taking into account hydrolysis of glutamine (η_h=-8.917x10^{-7} mg.ml^{-1}.hr^{-1}). Production of Immunoglobulin G antibody to paraquat and consumption of glutamine during G1B and S phases of the cell cycle were also reproduced and can be seen in Graphs 2 and 3 (Appendix B).

Resolution or the ability of looking in detail at every single phase of the cell cycle is one of the main advantages of CelCyMUS. This can be appreciated in graphs 4 to 8 of the Appendix B where a complete sequence for a synchronised cell culture going through every single phase of the cell cycle starting in G2 phase is observed. In these graphs the total number of cells in every phase is plotted against reactor time.

The results for the second task where obtained from an mm321 hybridoma cell line simulating a single run in a batch reactor. These data were compared with those obtained from the old version of the model. Here the probability transition is dependent on the cumulative amount of glutamine a cell has consumed since entering this phase. This transition rule applies only for G1B phase as stated in the equation below (Faraday, Hayter and Kirkby 2001):

$$\Gamma_{2GIB}(\tau_{GIB}, n_{GIB}(t,\tau_{GIB}), Cc(t,\tau_{GIB}), C(t)) = \frac{2n_{GIB(t,\tau GIB)}}{C_{CGLUT}(t,\tau_{GIB}) - S_{MAX}} \frac{\partial C_{CGLUT}(t,\tau_{GIB})}{\partial t} \qquad (5.1)$$

Where C_{CGLUT} is the intra-cellular concentration of glutamine (kgcell^{-1}) and S_{MAX} the maximum cumulative amount of glutamine a cell can consume before it must initiate S phase (Kgcell^{-1}). For the D phase, it is assumed that the rate of transition is dependent upon the prevalent ammonia concentration as follows (Faraday, Hayter and Kirkby, 2001):

$$\Gamma_{2D}(\tau_D, n_D(t,\tau_D), C(t)) = \kappa_{AMM} C_{AMM}^{1.5} n_D(t,\tau_D) \qquad (5.2)$$

Where κ_{AMM} is a constant determined empirically and C_{AMM} the concentration in the growth medium ($kg.m^{-3}$).

Graph 9 (Appendix B) shows cells in $G1_0$ phase. Cells remaining in this phase are introduced into the cycle in phase G1B. This is a continuous process of 'feeding cells' ($1x10^6$ cells) into G1B phase, which last for 14hr.

The number of cells decreasing as a function of time in this phase (G10) can be readily appreciated. Cells start consuming glutamine immediately after entering G1B phase (Graph 10 Appendix B). Once they have achieved an S_{max} (maximum concentration of glutamine per cell) following the probability transition mentioned in Equation 5.1 they leave the phase going to the S phase where they transit normally as the only transition rule is age (cells getting older, ageing) see Graph 11 of (Appendix B). Graph 12 shows cells transiting through the G2 phase. During phase M a normal flow of cells is seen as expected with duplication in the number of cells as a consequence of Mitosis and cell division right at the end of the phase (Graph 13). Cells in G1A phase are recovering from mitosis and start accumulating glutamine (from the medium, Graph 14, Appendix B). The consumption of glutamine from the medium and the production of Antibody are carried out in phase G1A and G1B, the data obtained from the new version for both cases compare with the old one are shown in Graphs 14 and 10 (Appendix B).

5.3 DISCUSSION OF DATA REPRODUCIBILITY OF UPDATED VERSION

The results obtained from the updated generic framework of CelCyMUS are comparable with those of the previous version. The predicted cell cycle distribution from the mm 321-hybridoma cell line shows the results obtained for the previous version of the program. Such graphs (Graphs 1 to 8, Appendix B) were plotted for constant and variable probability transitions following the Smith and Martin model. Cells being released to start the cycle in G2 phase and executing transition from G1b to S phase, assuming that the growth of cells occurs in a well mixed batch bioreactor and in an infinite period of time with no death phase.

Predictions of the cell age population for every phase where the de-synchronisation process can be appreciated and the flow of cells during the G1B/S cell can clearly be seen is presented in Graphs 4, and 8 (Appendix B). These figures represent the ability CelCyMUS has of giving 'resolution' in the results, being capable of locating the total number of cells in each phase of the cell cycle at any time. Once again these graphs are the result of simulations predicting the behaviour of the mm321 cell line (1×10^6 cells starting in G2 Phase) following a constant probability transition (0.03 cell/min) according to the Smith and Martin model.

For the second part of the runs (Graphs 9 to 15 Appendix B) a batch system is simulated for a mm321 cell line culture following a specific transition rule during G1B phase based on the cumulative concentration of glutamine. The graphs from the new CelCyMUS version overlap the ones from the old model showing reproducibility in the data.

5.4 THE MASS TRANSFER MODULE RESULTS AND THEIR ANALYSIS

A mass transfer module accounting for the interactions of oxygen and carbon dioxide in the gas and liquid phase has been introduced as explained in Chapters 3 and 4. The model considers the reaction of carbon dioxide into bicarbonate due to generation of CO_2 and the consumption of oxygen by cells in batch and repeated batch bioreactors. The introduction of this module was necessary not just to reproduce data from Creanor's experiments on oxygen consumption in synchronized *S. pombe* cells throughout the cycle but also to equip CelCyMUS with a new tool to account for interactions between gas and liquid phases in batch and repeated batch bioreactors. The final outcome of this module was the fitting of parameters such as RCOXY and RCO2 in simulation of batch and repeated batch experiments.

The behaviour of oxygen consumption in batch and repeated batch cycles can now be predicted for desynchronised cells as shown in Graphs 1 and 2 from the appendix C. As it can be seen here Graph 1 displays the results for oxygen consumption in synchronised cultures once the parameters have been fitted to the experimental data. It is worth mentioning here that the area fitted for our model purposes corresponds

to the periods between 2.5 and 4.5hr, such assumption was based on the fact that the first 2hr synchronised growing is affected by a lag phase of about 45min and after 4.5hr cells start desynchronising rapidly.

Carbon dioxide production can also be predicted the pattern followed by CO_2 in synchronised cultures shows a single increment per cycle rather than the two per cycle seen in oxygen consumption. This can be explained by assuming that most of the oxygen transformed into carbon dioxide comes mainly from respiration from the *S. pombe* cell related to assimilatory processes (production of biomass) that account for cell size growth. The consumption of oxygen increases when the cell transits throughout G2B phase due to the acceleration in the uptake rates of other metabolites such as glucose, proteins and the generation of energy in the form of ATP, all of these factors together accounting for elongation of the cell before undergoing mitosis. The second point where an increment in the production of CO_2 was expected is the G1-S transition. Here despite the fact that there is an increment in the consumption of oxygen the period over which it occurs is very short (9min) when compared with the increment in the G2B-M transition (40min). Also the reactions that take place generating carbon dioxide do not occur instantaneously, causing the increment in CO_2 to be carried over into the next phase (S) where cells are undergoing cytokinesis reducing metabolic activity to a minimum. In conclusion a second increment in the production of carbon dioxide in the cell is not easily visualised. Right at to this point the cell has been considered as one individual cell and the rate at which carbon dioxide is being produced was considered to be for one cell only, from this point (S phase) onwards the rate of carbon dioxide production will be halved since a new daughter cell is born and cell population is duplicating.

Carbon dioxide plays an important role in the timing of cell cycle events in *S.pombe*. Novak *et al.* (1986) observed the shortening of G2 phase in the wild type of cells by switching off CO_2 and introducing nitrogen into the system removing CO_2 and blaming the slow down of anapleurotic fixation as responsible for this effect. Carbon dioxide inhibits mitosis in *S. pombe* and has an effect on the growth rate and cell size before mitosis. The mass transfer module included in the *S. pombe* model could also allow further testing in this type of experiments.

5.5 THE INTRODUCTION OF GLUCOSE CONSUMPTION IN THE MODEL AND COMPARISON WITH EXPERIMENTAL DATA

Consumption of glucose necessary for growth processes related to cell size has been linked via oxygen consumption and based on studies carried out by Milbrdat and Hofer (1987) on the transport of metabolites from the medium across the membrane cell. They estimated the maximum transport velocity for D-glucose as V_T=90nmol.min^{-1}.mg^{-1}. As explained before (Chapter 4) the G2B/M transition is a consequence of the consumption of glucose. The values calculated when fitting the model with glucose uptake rates were of the order of 2-3 times those estimated in literature under slightly different conditions. This difference as the value used in the model comes from experimental data in desynchronised cultures. Analysing concentration of glucose from the medium, critical value rates of glucose were found from Fotuhi's experiments that are responsible in part for the rate of cell death in the cycle. Below this limit cells would leave the cycle to go into $G1_0$ phase where they will reduce their metabolic activity to a minimum, stop cell division and remain thus for a certain period of time until conditions change.

5.5.1 Analysis of Death Rule and Death Phase

Two critical values of glucose were found by analysing all of the final concentrations and final values of cell number in 8 batch experiments with 17.5x10^6 million cells/ml, HF=80% and DCT=18hr. The first critical value was calculated as the average of several batches in a repeated batch experiment with a value of 1.78x10^{-12} g glucose/ml per cell (see Table 5.1). Cells that reached this state are accounted for in the model with a constant rate of 2% and are taken out right at the end of G1 phase. Cells in bioreactors that reach this low level of glucose in the medium will start to join a G0 where they will remain before commencing a meiotic cell cycle. If the glucose levels continue to drop until values around 1.73x10^{-14} g glucose/ml a percentage of cells in the reactor will automatically die. Cell death is also affected by the common factors for cell death in a reactor such as friction with the paddles, bioreactor walls, and those cells which become fixed in the M phase due to genetic damage unable to go through cytokinesis and finally die.

	Initial Cell Number x 10^6 cell/ml	Final cell Number x 10^6 cell/ml	Initial & Final glucose Concentrations (g.glucose/ml)		Critical Glucose rate (g.glucose/ cell ml x 10^{-12})
BATCH 1	17.5	104	16.50	2.80	2.69
BATCH2	29.3	146	17.19	1.89	1.29
BATCH3	35	134	17.14	3.12	2.33
BATCH4	39	138	16.66	1.83	1.32
BATCH5	42	133	16.60	2.12	1.59
BATCH6	48.5	132	16.22	2.50	1.89
BATCH7	46	138	15.89	1.88	1.36
BATCH8	44	139	16.12	2.44	1.75

TABLE 5.1

5.6 BATCH DATA COMPARISON AND ANALYSIS

Experimental data gathered from Fotuhi were reproduced from simulations of experiments with different initial cell numbers (inoculum size), however glucose concentration was kept constant throughout the experiments. The experiments for 1.2, 8.8, and 19.2x10^6 cells have been named A, B and C respectively (Table 5.2).

Initial cells Number x 10^6		Glucose Concentration (%)	DCT (Dilution Cycle Times in hr)
Exp. A	1.2	2	24
Exp. B	8.8	2	24
Exp. C	19.2	2	24

TABLE 5.2

Graphs 3-8 from Appendix C show the simulation for cell population in batch reactors for periods of time of approximately 24hr. It can be seen that the trend generated for the model data overlaps the experimental results with great accuracy.

The assumption of two checkpoints generating de-synchronisation and a gap phase at the beginning of each experiment seem to have good effect in the final prediction for cell number. It is worth remembering that for modelling purposes the model was fitted with an initial number of cells estimated after having run the model for an initially synchronised culture of *S. pombe* during a period of 20hr. After such time a more homogeneous distribution of desynchronised cells across the different phases was obtained and used as an initial cell number (see Table 5.3).

	CellsSPhase	CellsG2APhase	CellsG2BPhase	CellsMPhase	CellsG1Phase
Cell Distribution (%)	18.97	35.33	30.02	5.41	10.31

TABLE 5.3

This model run was carried out since data for the cell population distribution throughout the cell cycle were not available. The inoculum sizes where chosen by Fotuhi (2002) when trying to find the best conditions for cell growth. These experiments demonstrated that when having the same age of inoculum, maximum cell concentration and growth rate rise by increasing initial glucose concentration.

In accordance with experimental data, when keeping constant the concentration of glucose and increasing initial cell number, glucose will deplete faster accompanied by an increase in the final number of cells. It was also expected that a slight increase in the value of (μ) growth constant (at constant glucose concentration) would be seen due to the effect of inoculum size. In fact Fotuhi's experiments reveal that cell concentration and specific growth rate increase when increasing initial conditions; cell number and glucose concentration. The model was able to reproduce these data and also to simulate the behaviour of cell populations at different values of glucose concentration (2 and 1% glucose).

Values for glucose consumption show a well-defined pattern in the model following experimental data. Furthermore the rates of consumption of glucose throughout Fotuhi's batch experiments were analysed and compared with the glucose uptake rates calculated from Creanor's experiments. The glucose values calculated in the model where obtained indirectly via oxygen consumption (O_2) and carbon dioxide

(CO_2) production as an indicator of energy generation related processes in the cell cycle. Once the glucose uptake rate per phase of the cell cycle was known, this was used to reproduce the behaviour of desynchronised batch cultures from Fotuhi's experiments.

The comparison between the experimental glucose consumption rates and the predicted glucose consumption rates from the model is shown in Appendix C (Graphs 9-11). In every single case the shapes of the curves were in agreement with the experimental patterns taken from batch cultures. However differences in the actual value of consumption rate where noticeable. Graph 9 displays the results for batch experiments in a culture with 1.2 $x10^6$ cells inoculum and 2% glucose (Exp, A). Here whilst the shapes of the graphs were similar, the actual peaks (highest values in glucose consumption rate) differ from each other despite being in the same order of magnitude ($4.40x10^{-6}$ for batch experiments and $3.96x10^{-6}$ g.gluc.cell^{-1}.min^{-1} for the model).

Graph 10 describes a bi-modal behaviour in the experimental glucose consumption rate for a batch culture with 8.8 $x10^6$ cells inoculum and 2% glucose (Exp. B), the two peaks with glucose uptake rate values of $1.12x10^{-6}$ and $5.9x10^{-7}$ g.gluc.cell^{-1}.min^{-1} being placed at 10 and 20hr, respectively. The simulation predicted for the model also displays both peaks this time being placed at 5 and 20hr with a noticeable gap with respect to the time of appearance for the first peak at 10hr. The value of the glucose consumption rate here is very similar about $1.02x10^{-6}$ g.gluc.cell^{-1}.min^{-1} for each peak. It is also worth pointing out that whilst for the model the two highest values of glucose consumption rate appear to be the same, in the experimental case the values of glucose consumption rate in the first peak (5hr) is almost reduced to half of the initial value in the second peak.

Graph 11 displays the results for a batch culture with an inoculum size of 19.2 $x10^6$ cells and a glucose 2% concentration and compares (Exp. C) glucose consumption rates both from the model and experimental data. A mono-modal type of shape is obtained this time; here the glucose consumption rate from the model starts at a higher value than the experimental rate peaking at the same time (7hr) but with a

lower value ($9.35x10^{-7}$ g.gluc.cell^{-1}.min^{-1} compared to $1.18x10^{-6}$ g.gluc.cell^{-1}.min^{-1}). It can also be seen that for all three experiments the initial glucose consumption rate calculated from the model is higher than the experimental rate. It then peaks at lower values throughout the experiment but both coincide at the time glucose is depleted. These differences in results are due to the initial number of cells in the cultures and their distribution in the different phases of the cell cycle. The fact that for number of cell in each phase of the cell cycle were not available meant that an initial number of cells had to be assumed (see Table 5.2) hence some of the differences with the experimental data. However, since the glucose values of consumption rate were estimated from metabolic and stoichiometric analysis from synchronised cultures this can be a platform to infer and predict upon other variables from the cell cycle.

In fact the variables plotted in the graphs were the result of indirect measurements obtained from oxygen consumption data estimated from Creanor experiments (1978) in synchronised cultures. These data allow accurate metabolic predictions to be made for (oxygen consumption, glucose consumption and ATP production, carbon dioxide generation) in each phase of the cell cycle. The P/O ratio was estimated for every single phase in the cycle and values of ATP production can be reproduced for the model. The behaviour of ATP production in the cycle can also be simulated despite the fact that there were no experimental data to compare with, glucose consumption and cells number from the model fitted the lab data making them good initial parameters to link other related metabolic variables from the cycle, thus allowing other variables to be studied throughout the cycle with a good degree of accuracy. The metabolic and biochemical processes that justified this assumption were previously explained in Chapter 3 (energy balance).

5.7 REPEATED BATCH SIMULATIONS

Experimental results of aerobic repeated batch cultivation in bioreactors were obtained by Fotuhi (2002). In his study two experiments were performed at 90% HF and 18hr DCT, two other at 80% HF and 18hr DCT and two more carried out at 80% and 12hr DCT. These experiments performed consecutively up to 22 times by using an automatic and novel feeding system developed by Fotuhi. The *S. pombe*

model then simulated the experimental data obtained here. In order to keep a logical order the simulations carried out for the *S. pombe* module were based on the Fotuhi (2002) experiments for repeated batch.

Fotuhi ran several experiments looking for values of harvest fraction, dilution cycle times and initial cell number that would produce the best values of biomass production per cycle. In order to find the impact of HF and DCT in repeated batch cultures, experiments were carried out at constant HF and different DCT, Fotuhi (2002) also performed another set of experiments with constant DCT varying HF. The effect of changing the HF while keeping DCT constant showed that when increasing HF the final cells number in a repeated batch reactor throughout a number of cycles will decrease. On the other hand final concentrations of glucose increased while increasing HF. However the yield for both experiments turn out to be similar. The changes in cells number and glucose concentration throughout the cycles were successfully achieved by *S. pombe*. The model values represent a good accurate real fit from the experimental data.

The second set of experiments kept HF constant while changing DCT. These runs showed that when decreasing DCT the final number of cells increased as did biomass production per cycle when using more glucose. The *S. pombe* model follows the experimental patterns throughout. An advantage from the model is the accuracy when predicting values from intermediate batches or cycles.

5.7.1 Analysis of Harvest Fraction in Experimental Data

It is necessary to point out that the experimental values of HF fraction in the entire repeated batch experiments did not correspond to the expected initial cell number and the glucose concentration at the start of every new batch. A comparison between the reported value from Fotuhi and the corrected values taking into account the real HF in repeated batch experiments is presented in Table 5.4.

Repeated Batch Experiment with $1.65x10^6$ initial cell number, HF= 80%, DCT=18hr								
Batch number	Initial and Final cell number/ml $x10^6$		Initial and Final Glucose concentration (g/ml)		Expected glucose conc. and % error		Expected cell number$x10^6$ and %error	
1	1.65	16.38	15.70	4.37	-	-	-	-
2	2.77	20.08	15.88	4.50	16.87	5.89	3.28	15.45
3	5.79	25.1	15.65	2.28	16.90	7.40	4.02	-44.17
4	5.23	33.13	15.54	2.01	16.46	5.57	5.02	-4.18
5	7.63	49.35	15.47	2.38	16.40	5.68	6.63	-15.15

TABLE 5.4

Here it is clear that at the start of a new batch after taking out the harvest fraction and introducing fresh medium the reported values do not correspond to what it should have been under controlled conditions. The errors introduced in the concentration of glucose at the start of a new batch are evident. The experimental values of glucose are below the estimated values after adding the new medium. The experimental values of initial cell number in every batch also differ from the estimated by the correct HF.

Repeated Batch Experiment with $12.2x10^6$ initial cell number, HF=80%, DCT=18hr								
Batch number	Initial and Final cell number/ml $x10^6$		Initial and Final Glucose concentration (g/ml)		Expected glucose conc. and % error		Expected cell number $x10^6$ and % error	
1	12.20	89.30	18.41	3.6	-	-	-	-
2	20.21	92.20	18.79	3.1	16.72	12.38	17.86	-12.54
3	17.30	100.7	18.49	2.35	16.62	11.25	18.44	16.18
4	26.60	120	18.32	0.43	16.47	11.23	20.14	-32.07
5	26.70	122.7	18.73	0.46	16.09	16.44	24.00	-11.25
6	29.30	134.35	18.03	0.47	16.09	12.04	24.54	-19.40

TABLE 5.5

Another example of the differences introduced in the HF fraction appears illustrated in Table 5.5 where from a set of 22 repeated batches the first 7 batches are considered to illustrate the error. As it can be seen the error introduced by the HF is in average 12.67% for the glucose concentration and 16.29% for the cell numbers.

The expected values for cell number and glucose presented in Tables 5.4 and 5.5 were the values calculated for the model did not match the initial number of cells neither glucose concentration introduced experimentally for the next batch. To solve the problem the values of numbers of cells harvested and the new value of glucose concentration at the beginning of every batch had to be introduced as a separate file in the program. Based on the actual number of cells at the beginning of every batch the real value for HF was then recalculated and fed back to the program in order to estimate a more accurate initial number of cells for the next batch. It is probable that these fluctuations in the experimental values reported by Fotuhi (2002) of HF between separate batches, were the consequence of malfunctioning in the electronic systems that controlled the pumping out of the harvested fraction introducing fresh medium.

5.7.2 Comparison between Repeated Batch Experiments and Model Simulations

The comparison between the simulations for repeated batch experiments and the *S. pombe* model are presented in Appendix C Graphs 12 to 17. Graphs 12 and 13 compare the results for a repeated batch experiment with an initial cell number about 17.5×10^6 cells/ml, HF=80% and a DCT=18hr for cell number and glucose concentration respectively. It can be seen that in the first batch the final number of cells calculated by the model is slightly higher than the one reported experimentally, most probably due to the initial distribution of cells assumed by the model. From the second batch onwards the model tends to match the cell number obtained experimentally.

The discrepancies between the initial number of cells in the model and the reported experimentally are expected since this is a very difficult parameter to control. The

final number of cells after harvesting every batch is almost a random figure (10-20% deviation in most cases) around the desire value since the cells are spread all over the reactor and harvesting a percentage of the cells does not guarantee an exact number of cells left for the next batch. The model however works with exact estimated number of cells after harvesting assuming that the percentage left to start the new cycle is an exact percentage.

Despite the model taking exact number of cells at the start of a new batch, the results for final number of cells are very close to the experimental data and even closer when considering the final values of glucose concentration (Graph 13, Appendix C).

The fact that the final number of cells and the final glucose concentration estimated by the model were very similar to the reported data leads to the conclusion that there is in fact a critical value of glucose concentration were the cells switch off their metabolic activity before being arrested in a G0 phase where they remain until conditions improve otherwise they leave the mitotic cycle to start meiosis. In the case of repeated batch the conditions are critical enough to arrest cells in a G0 phase but never to go into meiosis. This also explains the existence of a lag phase at the beginning of every batch were cells are re-suspended in new medium. Cells in G0 phase will re-start cycling once they have sensed that conditions (nutrients concentration, temperature etc.) are normal for them to start again. This lag phase (about half an hour) is clearly seen in most of the repeated batch experiments presented here. There are critical values of glucose concentration which produce an increase death rate since cells undergoing mitosis, or synthesising DNA will not have the required amount of nutrients to carry out these activities.

Graphs 14 and 15 compare the simulations from the model with experimental data for repeated batch experiments with an initial number of cells 21×10^6 cells/ml, HF=80% and a DCT=18hr for cell number and glucose concentration respectively. The results from the model in this particular experiment are the closest of the three experiments presented here. Only in the last five batches of this experiment do the simulated results vary from the experimental. This is most probably due to the fact that the initial cell number also changes and as seen from the sensitivity analysis

presented in Chapter 4 initial cell distribution has a big effect in the final outcome of the model. In Graph 15 the comparison for glucose concentration also displays very close approximation from the model to experimental data. However most of the experimental final values of glucose concentration are below the ones estimated for the model. Once again cell distribution might be responsible for this, since cells can deplete glucose faster in some phases of the cycle (G2B and G1) than others.

Graphs 16 and 17 compare the simulations from the model with experimental data for repeated batch experiments with an initial number of cells $12.2x10^6$ cells/ml, HF=80% and a DCT=18hr for cell number and glucose concentration respectively. The results for this simulation are the less accurate from the three experiments simulated. Here the final cells number calculated by the model in every batch is lower than the one reported experimentally. It is also noticeable that final values of glucose concentration estimated by the model are higher than the ones in experimental data. It is clear here that the critical value of glucose is reached faster in the model than the one in the bioreactor, stopping cell division, decreasing the final number of cells at the end of the batch and leaving final values of glucose concentration in the model higher than the ones shown in data from the bioreactor. All this indicates that the assumed value in the model of glucose consumption does not match the one seen in the bioreactor for this experiment. It is unlikely that cell distribution has an effect in the results since the patterns for glucose concentration in the experiment constantly differ from the ones in the model.

5.8 DISCUSSION ON THE SENSITIVITY ANALYSIS

From the sensitivity analysis presented in Chapter 4 can be seen that parameters that have an influence in metabolic behaviour such as oxygen (and all the other metabolically linked to it) have little effect on the final outcome of the model when compared with the cell distribution around the cycle. Increasing the consumption rates of oxygen that regulates the transition between phases has a minor effect when compared with the cell number at the start of every phase. The closer to the check points (G2B/M and G1/S phases) the bigger the impact in the final cell distribution that is expected since checkpoints determine the flow of cells around the cycle. The

biggest impact is clearly in the S phase with a 197.49% error. This is mainly due to cytokinesis occurring in this phase. The duplication in the number of cells at this stage has a big effect in the cycle. Increasing or decreasing the number of cells in any percentage at this phase has a direct implication in how successful cells are giving birth to a new daughter cell and the consumption or production of any metabolites in the cycle. G2A is clearly a recovery period after cytokinesis with only a 6.12 % margin error. G2B has a higher impact but this is dissipated by the length of this phase (almost 70%) of the cell cycle. M and G1 phases are of very short duration in the cycle, but the fact that they are part of both checkpoints (G2B/M and G1/S) makes them more important. Their short duration as phases that control the transition of cell between different stages of the cycle makes them more important. The sensitivity analysis suggests that varying cell number at the G1/S checkpoint is the most critical part of the *S. pombe* model.

5.9 CONCLUDING COMMENTS

In this chapter the discussion of results presented in Chapter 4 has been studied. First a demonstration of the reliability of the new code by reproducing data from the mm321 hybridoma cell line was made clear. Then simulations from the mass transfer module were displayed and the importance of this new module within the generic framework of CelCyMUS explained. Comparisons between batch runs simulated for the model and experimental data were analysed. These simulations of batch runs were also studied to follow the pattern of glucose consumption rates in different experiments. The behaviour of the glucose consumption rate introduced in the *S. pombe* model followed the one given in the experimental data.

Discrepancies between expected values of HF and the ones used in the repeated batch bioreactors were detected. The assumptions taken in the model to cope with this difference has also been included. A thorough comparison between the model results and those for three different results from batch experiments concluding on the importance of cell distribution and the impact checkpoints have in the cycle has been examined. Finally comments on the sensitivity analysis presented in Chapter 4 elucidate the importance of cell distribution and initial number of cells in different

phases of the cell cycle. G1/S appears to be the most critical part in the model regarding cell distribution; the effect of the probability transition over its short period of time makes it very critical in the cycle.

CHAPTER 6

CONCLUSIONS AND RECOMMENDATIONS

6.1 INTRODUCTION

A cell cycle model for the fission yeast *S. pombe* has been described in a model which accounts for the different cell cycle phases and the probability transition between phases (G2B/M, G1/S). A G0 phase is also present, where cells remain when environmentally threatened, switching to meiosis under severe conditions of starvation and a death phase. A value for the consumption of glucose per phase through out the cycle has been estimated.

CelCyMUS, the generic framework model has been updated by introducing powerful new features of Fortran 95, making of the model a 'platform' with facilities to support specific modules containing mathematical models for particular types of cells. In this context the research can be summarised in four points here:

1) The results obtained from the updated generic framework of CelCyMUS, are comparable with those of the previous version.
2) A new mass transfer module has been incorporated in the CelCyMUS framework, which describes the interactions in bioreactors between the gas and liquid phases in the medium.
3) The new *S. pombe* model proposed which describes cell cycle phases, transition between phases, death phase, and a pre-meiotic G0 phase. This model is the first and only physiological model that exists for *S. pombe.* It also accounts for consumption and production of different metabolites.
4) The model is able to simulate work previously carried out by Fotuhi (2002) on batch and repeated batch bioreactors for *S. pombe.*

In this chapter the steps needed to improve and complete the model will be established as well as the future work towards the implementation of MBO control in a real system for bioreactors batch in S. *pombe.*

6.2 THE GENERIC FRAMEWORK

With regards to CelCyMUS, this research has focused on introducing the new Fortran95 tools. The generic framework has now a stronger, portable and flexible code as a result of the dynamic allocation of memory, implementation of modules and the derive types described in the theory chapter. Changes in the mathematical framework were not needed in this module apart from the introduction of a Runge Kutta 4^{th} order method when solving the mass transfer module, which accounts for dissolved oxygen and carbon dioxide exchanges in bioreactors for the gas and liquid phases. This will be of especial use in the *S. pombe* model since O_2 production and CO_2 consumption play particular roles as markers of cell division in the fission yeast, enhancing the opportunity to establish a controller in the *S. pombe* cycle. Data and graphs presented in the report were in accordance with those simulated in the model for the mm321 hybridoma cell line in the CelCyMUS model under the same conditions.

Once the model was complete, further testing was done in order to simulate the behaviour of batch and repeated batch cultures. Fitting values for rate of consumption of oxygen, rates of production of carbon dioxide and linking other metabolites such as glucose and ATP were part of the process. The fitting came from experimental data by Creanor (1992) who measured the consumption of oxygen in synchronised cultures of *S. pombe*. Once these values were fitted for batch experiments, the results of the simulations showed a good degree of accuracy. Thereafter the prediction of experimental results for repeated batch experiments was equally good this time the fitting was based on experimental runs made by Fotuhi (2002) in batch and repeated batch bioreactors.

Differences were detected between experimental values of HF reported by Fotuhi and expected data of HF for every batch in repeated batch experiments. Throughout the experiments the values of HF fluctuated for every batch in repeated batch runs when it should have been kept constant, this was apparently due to errors in the amount of biomass being flushed out of the system after every batch and the amount of fresh medium used for the next run. To solve this problem the model was fed

with the actual value of HF for every single batch in any given number of cycles, allowing the model to work with real data instead of the aimed value of HF. This correction allowed for a more accurate response from the model however one of the recommendations of this thesis would be to review the device used when reloading the bioreactor for a new batch run.

6.3 THE MATHEMATICAL MODEL FOR *S. pombe*

A mathematical model for the *S. pombe* strain has been proposed its main features are explained below:

1. The division of G2 phase is derived from observations made by other researchers who have determined that there is a period of time after cytokinesis where cells recover before accumulating nutrients from the medium and achieving a desired cell size to start synthesising DNA (Faraday, Kirkby, 2001). The actual transition occurs at the checkpoint G2B/M. As an increase in the consumption of glucose starts at the beginning of G2B (being a cumulative function), where once cells have assimilated certain level of glucose (enhancing a cell size length), they will execute the transition.

2. G2B/M transition is dependent on the consumption of glucose as the main source of energy for the cells to actually reach the size threshold (Novak 1998, Nurse 1985).

3. At the metaphase checkpoint, which occurs before initiating anaphase (the separation of sister chromatids to the poles of the mitotic spindle) the cell checks that all chromosomes are properly aligned with each kinetochore attached. This checkpoint is not considered. The argument to omit this checkpoint is that it does not have direct influence in the population balances and is more a regulatory genetic control rather than a physiological one.

4. Cells can exit the cell cycle at both check points to go and remains in a G0 phase where they become resistant to heat and chemical treatment, this is usually as a

consequence periods of starvation. Cells will go to this stage depending on minimum values of glucose concentration or critical values of glucose set up within the program. This critical value of glucose was found from analysis of experiments in batch and repeated batch bioreactors carried out by Fotuhi. The experiments clearly show that at a certain point when cells reach the critical value they stop dividing and remain in the cycle before leaving to a G0 phase where they will remain almost inactive. At this point cells remain at a very low metabolic level and if the starvation conditions persist after a long period of time they will leave the mitotic cycle to go in a meiotic cycle. They will revert to the main cycle when the concentration of glucose reaches an acceptable level for cells to go back into the main cycle. Entrance to the cycle will occur at those points where glucose consumption increases; in the G2B and G1 phases.

5. In practice if starvation persists, cells would sporulate starting a meiotic cycle typical of sexual cells, since this meiotic cycle has another behaviour and is presented just under extreme circumstances, is not considered within the model. Instead the G0 phase has been introduced as explained in the point before.

6. The rate of production of CO_2 increases right at the end of mitosis and during S phase. This feature allows the use of carbon dioxide as a marker for the end of the cycle and a hypothetical value for a probability transition from G1/S. The implementation of a transition considering CO_2 production is valid as a marker of the septation process. It has been proved that this change in the production rate is at the start of the S phase, based on the assumption that glucose will be taken up in G1B. Increments in CO_2 production are used as markers for the cell cycle time of different *S. pombe* mutants whose cell cycle times are specified in table 1 from Appendix D.

7. The model accounts for cell population age distribution with the specific timing for wild type cells (WT cells). Specific values for rate of oxygen and glucose consumption, production of CO_2 and generation of ATP are presented here. The values mentioned for rate of consumption of glucose are average values from experimental batch cultures through out a period of 24 hours.

8. The model can accomplish the simulation of mutants *S. pombe* cells since the framework of the program can be adjusted to different cycle times for the different phases. All that is required for simulation of these cells is the new times for the cell cycle phases to be determined (see Table 1.0) and these data can be fitted to the parameters for RCOXY and RCO2 in the cycle.

A graphical representation of the *S. pombe* model suggested appears in figure 1 with the timing, transitions, and consumption of nutrients at discrete phases and production of metabolites through out the cycle.

The running conditions of the program at the moment are presented as follows:

a) Cells being released from G10 phase to start the cycle in G2A phase.

b) Executing transition from G2B to M phase and G1b to S phase.

c) Fixed period of times for the phases of the cycle.

d) Probability transitions vary depending upon the value of cumulative glucose in the cycle for the G2B/M phase transition and oxygen consumption for the G1/S checkpoint.

e) The mass transfer module regulates and controls the amount of oxygen dissolved in the medium and calculates the rate of oxygen consumed for the cells in a bioreactor at all times

f) It is assumed that growth of cells occurs in a well-mixed batch bioreactor and death occurring as a consequence of low levels of glucose in the medium during extremely long periods of time.

6.4 NOVEL FEATURES INTRODUCED BY *S. pombe* MODEL

The model proposed for *S. pombe* is the first physiological model developed for this particular type of yeast. The model enhances metabolic interactions of the cell throughout different phases in the cycle allowing for simulations of batch and repeated batch cultures in any given period of time. Existing models for *S. pombe* concentrated on the genetics of the micro-organism and the kinetics of all the different proteins responsible for transition between phases and cell growth. The model proved to be very accurate in following behaviour of specific genes but was too specific for our purposes. It concentrated on protein kinetics of the products of certain genes and specific rates of production metabolites acting as markers at certain stages of the cell cycle, leaving out the physiological processes within the cell cycle. This type of approach specialises in certain points of the cell cycle but fails to predict general behaviour in batch and repeated batch cultures; it is more a micro approach to understanding the cell cycle from a genetic point of view rather than a physiological one.

The model has also identified a critical value of glucose concentration in the medium for batch reactors below which *S. pombe* switches from a mitotic cycle to a quiescent phase where cells remain, waiting for conditions in the medium to improve. If conditions persist they will conjugate into diploid cells and then sporulate before starting a meiotic cycle where they can remain for months or even years, this as a defence mechanism. Such ability to leave the cycle when threaten for internal and/or external conditions is also seen in other type of cells such as cancer cells. *S. pombe* can leave the cycle from any phase but for purposes of this model they leave from any of the transition points, G2B/M and G1/S. This value of critical glucose concentration was found when analysing Fotuhi's results in both batch and repeated batch experiments.

The mass transfer module incorporated in CelCyMUS will be useful for any other type of cell to be simulated in this framework. The interactions between metabolites in the liquid phase and gas phase such as oxygen and carbon dioxide can be studied.

Considerations about the geometry of the stirrer and the amount of energy input to the system by stirring will also have a direct influence in the amounts of material dissolved in the medium due to changes in the K_{la}, and the amount of cells that die as a consequence of injury loss (impacts with the paddles and bioreactor walls). These effects are considered as explained in Chapter 4 and make part of the assumptions in the calculation of a death rate of cells in batch reactors.

The capability this model has of following cells in different phases of the cycle at any given time form part of the resolution inherited from CelCyMUS. This tool is very useful when studying transition points (G2B/M and G1/S) since it allows us to pin point the changes in rates of consumption and/or production of metabolites responsible for physiological changes in the cell. It is also useful to single out cells in a particular phase at all times, allowing understanding of population balances. Resolution enhances simulations of both synchronised and de-synchronised cell culture. For the particular case of *S. pombe* data from repeated batch can be reproduced and analysed per batch and per any given time within the batch. This features virtual sampling of the cell culture at any desired time in every cycle, which would very time consuming and expensive when being carried out in a lab.

The model can be used to find the best values of glucose concentration, HF and DCT necessary to improve the yield in a batch culture. *S. pombe* simulates runs for repeated batch cultures of different DCT and for any given number of cycles. Normally runs of 20 cycles with DCT of 18hr can be reproduced in less than 3 minutes, so that by implementing optimisation routines the *S. pombe* model can find the best conditions to obtain the best possible yield in terms of growth and/or production metabolites. This again will allow for reduction in experimental times and cost.

The *S. pombe* model can also calculate the energetic demands in the cycle based on ATP production and glucose consumption in the cell cycle. Such demands will vary accordingly with the concentration of carbon source available (glucose in this case) as the primary source of energy, the type of cell (wild/mutant), growth rate and type of process fermentative or respiratory as in this model. An energy balance (see

Chapter 3) helps in evaluating the best concentration of nutrients in the medium to achieve the best possible yield, the minimum amount of oxygen both in the gas and liquid phase necessary to complete the breaking down of glucose into ATP.

6.5 M.B.O CONTROLLER

With the model fitted, the future work of the project will be on line control. This stage is about implementing a model-based observer (MBO) controller in a real batch system for the growing of *S. pombe* yeast.

Modelling provides a means for estimating process information on-line in a permanent way. Therefore, it may be used as an alternative to the monitoring of key process variables. However, the use of such an approach for control purposes can only be successful if the models employed are a good representation of the process. The MBO technique has been tested by Araujo (1998) using a copy of the mathematical model produced to correct the behaviour of a model, which executes a feedback loop on the outcome of the real system being controlled. The model replica will then adjust parameters within the first copy of the model improving it to make it closer to real behaviour of the system. The principle of model-based observer (MBO) control is illustrated in Figure 1 Appendix D. Two distinct feedback loops can be identified: the process loop in blue and the model loop in green. These loops are interconnected as indicated in red; disturbances to the system are shown in brown. In the process loop, the process controller manipulates process parameters according to the difference between a set point and a process output (the set point error). The process is thus altered so that its output is driven towards the set point. In the model loop, the model adaptor modifies model parameters dependent upon the difference between the 'desired' value of the model output and its actual value (real output of the system). The purpose of the model adaptor is to modify parameters in the model so that its output is driven towards the 'desired' value. Such parameters could be the inlet flow to the system, the rate of consumption of glucose in the particular case of *S. pombe*, or even temperature as an external factor that might induce sporulation under extreme conditions.

The interaction between the process and model loops allows information from the model to be used by the process controller and the model to be updated on the basis of actual process behaviour. The disturbances to both process and model may be considered to be the same and, thus, process and model outputs should be the same if the model is a good representation of the process. The model infers some process information, which is now available on-line but still expensive and difficult to obtain (Gawthrop and Ponton, 1991); in this case, the model is said to act as an observer.

As can be seen in Figure 1 Appendix D, the process parameter thus manipulated is employed as input not only to the process, but also to the model. The model is updated by comparing the model output to the process output, which is the 'desired' value; thus, process/model mismatches can be identified and corrected by the model adaptor.

6.6 OTHER COMMENTS

The complete *S. pombe* model has the necessary tools to determine the consumption of glucose, oxygen, ATP production, and CO_2 generation per phase at the *S. pombe* cycle. This has been achieved by analysing data from cells whose DNA synthesis has been blocked chemically and released afterwards to determine glucose consumption in a synchronised culture. The rate of production of CO_2 and oxygen consumption has been included, operating as 'markers' at the end of the cell cycle division, making this model the first physiological model for *S. pombe*. The *S. pombe* model has also been adjusted to simulate cell population behaviour, batch and repeated batch bioreactors experiments.

The model performance is very satisfactory to the point that can be used to spot abnormalities or to detect irregularities in the bioreactors system as was the case with the values of HF reported in Fotuhi's experiments.

The future work of this project will be orientated towards implementing an MBO controller technique in a real system with a batch bioreactor for a culture of *S. pombe*. This aim is possible since previous results for an MBO control system

(Araujo 1998) implemented for the mm321 hybridoma cell line working with a copy of the program have been successful.

6.7 FUTURE WORK AND RECOMMENDATIONS

The future work regarding MBO controllers and some recommendations to further develop not only the generic framework CelCyMUS but also the *S. pombe* model are introduced as follows:

- Adjusting and running the program implementing MBO model control for *S. pombe*. The next steps of the research will be orientated towards the on-line control of batch and repeated batch bioreactors. The on-line control of different parameters in the model will help to study other aspects of the research such as optimisation of yield in biomass production or metabolites in particular and cells culture that exhibit chaotic behaviour in their kinetics.

- The mass transfer model here installed could also allow further testing in different type of experiments such as inhibition of mitosis by carbon dioxide suppression. The study of these and other features such as different nutritional carbon sources can also be predicted as long as the parameters of consumption and/or production of the different metabolites are known.
- To adjust the MBO controller to a real system (controlling a Bio-reactor) growing *S. pombe* and therefore to determine the effectiveness and usefulness of the controller by comparing its performance and comparing it against existing control on-line systems in bioreactors.

6.7.1 Recommendations on the Model Containing Intracellular Pools of Stored Energy

Cells continue to pass round the cell cycle even in the presence of low levels of glucose and other metabolites essential for cell growth. This phenomenon was observed in several experiments by Fotuhi (2002).

The critical levels of glucose concentration found in this research which were responsible for cell death in batch reactors still apply when analysing the latest findings. However, it is also evident that cells do store energy and can continue to grow before leaving the mitotic cycle, hence the low rate of cell death (2% after reaching critical levels of glucose concentration). Energy for driving the cell cycle must therefore come from other intracellular pools of metabolites. Many different explanations can be found to this phenomenon; the use of other hydrocarbon sources present in the medium as a way to generate energy, the ability cells have to adapt to extreme conditions by reducing metabolic activity to minimum levels or by operating other metabolic pathways. Further research into finding the mechanisms that allow cells to store the energy levels necessaries to continue cycling should be implemented. In order to carry out the study of internal intracellular pools of metabolites this dissertation proposes the introduction of markers (isotopes) to track down the routes of consumption of glucose (and other carbon sources) in media with low levels of carbohydrates. Labelling metabolites will allow for a better understanding of when these intracellular pools are activated and how they work. It is possible that at this point (low levels of carbon source in the medium) the cells adopt different metabolic pathways in order to save energy and maximise its use.

6.7.2 Recommendations on Exploring Chaotic Growth Kinetics

Once the model was completed two runs on repeated batch experiments with an initial number of cells of 17.5×10^6 million cells/ml, 80% HF, 18hr DCT and 100 cycles (Graphs 1-4 appendix D) and another simulating a reactor with 20×10^6 cells 80% HF, 18hr DCT and 200 cycles (Graphs 5-9 Appendix D) were executed by the model. The purpose of this exercise was to try to find chaotic behaviour in repeated batch cultures. The results did not show chaotic behaviour in the growth kinetics of repeated batch experiments under the conditions and parameters established for the model. However it is worth to mention here that the *S. pombe* model can be induced into chaotic behaviour according to the sensitivity analysis presented in Chapter 4 and discussed in Chapter 5. The sensitivity analysis shows that for the parameters chosen in the model, variations in the initial number of cells in G1 and S phase have a very large impact upon the results of the model and cell population (up to 197%

error) when deviating +/- 5% from the initial cell number. Following these results it is clear that by altering cell number in a phase of the cycle or by changing the length of the phases in the cycle, chaotic behaviour could be observed. It was then considered worthwhile to run a sensitivity analysis by altering the length of the cell cycle phases and their initial cell numbers. As part of the future work this dissertation proposes to run repeated batch experiments looking for chaotic behaviour in cell cultures of *S. pombe*. Such chaotic behaviour maybe induced by manipulating the amount of cells harvested from the system (HF), and by altering the duration of phases in the cycle as demonstrated by Mitchinson when altering the concentration of CO_2 produced the elongation and shortening of the G2 phase due to an anapleurotic effect. Achieving the shortening or elongation of the phases should trigger chaotic behaviour according to the sensitivity analysis especially during G2B/M and G1/S phases.

6.7.3 Recommendations on Running Experiments with Mutants

Since a complete set of data are available on the different mutants of *S. pombe* (see Table 1 Appendix D) and a flexible model has been developed for the wild type of cells, executing the program for mutants should in theory be just as successful. The cell cycle times for different type of synchronised cultures of *S. pombe* mutants are available and the exact times at which increments in the rate of production of CO_2 are also known, therefore the implementation of these data within the model could be simply done as a file with specific characteristics of the cell that could be used by the program user. CO_2 could be used as the marker for metabolic events within the cycle (cytokinesis) and the handling of the timing in the cell cycle phases of the mutants can be done by means of dynamic allocation in the program. The reason to simulate data with mutant cells is simply because it allows us to study in more detail especial conditions that otherwise would be difficult to study with wild type cells, such as the influence of cells size in the checkpoints when growing wee mutants.

6.7.4 Recommendations on Different Carbon Sources and Glucose Concentrations

An area that needs to be improved in the program is the extension of the model to simulate different concentrations of glucose in the medium and the use of other carbon sources by this particular type of cell. Most of the experiments simulated here were 2% glucose concentration and only one was done for a slightly different level of glucose (1% glucose, Graphs 10 and 11 Appendix D). Furthermore care is needed when making changes in glucose concentrations in the medium since metabolic pathways of *S. pombe* will change depending upon glucose concentration and they will vary all the way from respiration at low levels of glucose and highly aerated systems to fermentation processes with high concentrations of glucose. Phenomena such as the Crabtree effect and the Paster effect need to be addressed if radical changes of glucose concentration are introduced in the model.

The experiment run in the model at 1% (Graph 11 Appendix D) glucose was simulated successfully, by changing the parameters in the system, however further changes would need to be made in order to simulate different glucose concentrations. The inclusion of yield and growth (μ) as parameters to improve estimates at different levels of carbon source could be of help since they change regarding the concentrations and type of carbon source in the medium.

6.7.5 Recommendations on Periodic Feeding

Periodic time sequences in feeding strategies influence variations in cell growth more easily than a repeated batch or continuous reactor would. Moreover, a periodic feeding process offers the flexibility of changing parameters in an experiment such as the length of the cycle and the length of the feed period, parameters that can be varied with the same residence time. The influence of these parameters on the biomass behaviour in a bioreactor, and then on the performance of yeast cultures deserves more investigation.

Arzumanov (2001) worked on the growing of *S. pombe* yeast. The goal of his research was to apply periodic feeding in bioreactors in order to study the dynamics of biomass and glucose at different frequency of periodicities. From Arzumanov's results was interesting to see the different patterns of glucose consumption and biomass production when exposed to periodic perturbations of 4, 7 and 8hr In these experiments cell concentration was reproducible whereas residual glucose concentration was dependent on the level of culture adaptation to glucose-limited conditions.

The simulation of periodic feeding is definitively an alternative within the model, periodic feeding can be simulated by introducing different types of feed functions (step, pulse etc.). A better understanding will be obtained when a module is introduced that accounts for transport phenomena from the external medium, through the cell wall and into the cytoplasm. Transport phenomena will be of importance since during periodic feeding the conditions and concentrations of the carbon source vary from time to time. For instance in an on-off experimental run in a batch reactor the cells in the medium will quickly be switching between a medium with a high source of carbon to a medium with minimum concentrations of carbon and the transport of nutrients from the medium to the cell will change from simple diffusion in the presence of high concentrations of the carbon source to active transport by the use of proteins carriers generated by specialised RNA.

6.7.6 Recommendations on the Application of the Model to the Enzymes Involved in the Cell Cycle

Tyson, Novak *et al* (1998) have developed a complete set of equations to describe the certain cell cycle kinetics of the proteins produced by genes in the *S. pombe* yeast and their behaviour at different stages of the cycle. A parallel module following the kinetic equations given by Novak's model can easily be implemented here. The diversity of data and molecular details from different researchers (Tyson *et al.* 1998, Novak *et al.* 1998, Nurse *et al.* 1985 etc.) has made possible the construction of more realistic mathematical models of the cell cycle. In these

molecular models, biochemical reactions have been translated into systems of non-linear equations (ODEs). By numerical simulation, the solution of these ODEs, could be compared to the physiological behaviour of living cells. Within this context CelCyMUS and the *S. pombe* model are the perfect complement since the physiological behaviour and the influence of shortening and elongation of phases in the cycle can be studied here.

Including the behaviour of the relevant kinases into the cell cycle model will help to display the interactions between these enzymes and other proteins generated by different genes and the final physiological consequences of their actions. For instance it is known that the cell cycle in *S. pombe* is driven by fluctuations in the activity of M-phase promoting factor (MPF or Cdc13/Cdc2) which is a heterodimer of a catalytic subunit (Cdc2 protein kinase) the actual execution of events in *S. pombe* yeast requires that MPF activity oscillates between low (S and G2 phases) and high (M phase) levels. The production of these proteins could therefore be linked to the increments in the uptake rates of consumption for oxygen and glucose and any other metabolic activity considered in the model.

6.8 CONCLUDING COMMENTS

This dissertation has proven to be successful when achieving the objectives initially proposed for this research. The *S. pombe* model is now fitted within the generic framework of CelCyMUS, recommendations on future work regarding CelCyMUS and fine tuning of the model regarding introduction of intracellular pools of energy, genetics, MBO controllers and application of the model in periodic feeding have also been suggested in this chapter.

REFERENCES

Abu-Absi, Zamamiri A., Kacmar J., Balough S.J. and F. Srienc, Automated flow cytometry for acquisition of time-dependent population data. *Cytometry* **51** (2003), pp. 87–96.

Agger, T., Nielsen J., Genetically structured modelling of protein production in filamentous fungi. *Biotechnol Bioeng* **66** (1999), pp. 164–170

Araujo, S., The Application of Model-based Observer Control to Bioreactors. PhD Thesis, Chemical & Process Engineering, School of Engineering, University of Surrey, UK (1998).

Aristidou, A.A., San K.Y. and Bennett G.N., Metabolic flux analysis of *Escherichia coli* expressing the *Bacillus subtilis* acetolactate synthase in batch and continuous cultures. *Biotechnol Bioeng* **63** (1999), pp. 737–749.

Arranz, M.A., Transferencia de materia en columnas de burbujeo: clasicas y con recirculation. Tesis doctoral, Universidad de Alcala, Spain (1993)

Arzumanov, T., Slater, G., Kirkby, N., Underwood, B., Faraday, D., Periodic feeding of *Schizosaccharomyces pombe* in continuous culture. Chemical & Process Engineering, School of Engineering, University of Surrey, UK (2003).

Ataai, M.M., Shuler M.L., Simulation of CFSTR through development of a mathematical model for anaerobic growth of *Escherichia coli* cell population. *Biotechnol. Bioeng.* **27** (1985), pp. 1051–1055.

Bailey, J.E., Mathematical modeling and analysis in biochemical engineering: past accomplishments and future opportunities. *Biotechnol Prog* **14** (1998), pp. 8–20.

Bailey, J.E., Toward a science of metabolic engineering. *Science* **252** (1991), pp. 1668–1675.

Bakker, B.M., Westerhoff H.V., How yeast cells synchronize their glycolytic oscillations: a perturbation analytic treatment. *Biophys. J.* **78** (2000), pp. 1087–1093.

Bhalla, U.S., Iyengar R., Emergent properties of networks of biological signalling pathways. *Science* **283** (1999), pp. 381–387.

Birol, G., Undey C., Parulekar S.J. and Cinar A., A morphologically structured model for penicillin production. *Biotechnol. Bioeng.* **77** (2002), pp. 538–552.

Birol, G., Zamamiri A.M. and M.A. Hjortso, Frequency analysis of autonomously oscillating yeast cultures. *Process Biochem.* **35** (2000), pp. 1085–1091.

Bulsari, A., and Saxén, H., Using feed-forward neural networks for estimation of microbial concentration in a simulated biochemical process. Biosensors and Bioelectronics, Volume 9, Issue 2, 1994, Pages 105-109.

Çalik, G., Takaç S. and Özdamar T.H., Metabolic flux analysis for serine alkaline protease fermentation by *Bacillus licheniformis* in a defined medium: effects of the oxygen transfer rate. *Biotechnol Bioeng* **64** (1999), pp. 151–167.

Christensen, B., and Nielsen J., Isotopomer analysis using GC-MS. *Metab Eng* **1** (1999), pp. 282–290.

Christensen, B., and Nielsen J., Metabolic network analysis: a powerful tool in metabolic engineering. *Adv Biochem Eng Biotechnol* **66** (1999), pp. 209–231.

Cooney, M.J., Goh L.T., Lee P.L.and Johns M.R., Structured model-based analysis and control of the hyaluronic acid fermentation by *Streptococcus zooepidemicus*: physiological implications of glucose and complex-nitrogen-limited growth. *Biotechnol Prog* **15** (1999), pp. 898–910.

Creanor, J. (1978a). Carbon dioxide evolution during the cell cycle of the fission yeast Schizosaccharomyces *pombe* . *Journal of Cell Science* **33**, pp. 385-397.

Creanor, J., (1978b). Oxygen uptake during the cell cycle of the fission Yeast *Schizosaccharomyces pombe. Journal of Cell Science* **58**, pp. 263 – 285.

Dano, S., Sorensen P. and Hynne G.F., Sustained oscillations in living cells. *Nature* **402** (1999), pp. 320–322.

Daoutidis, P., and Henson M.A., Dynamics and control of cell populations in continuous bioreactors. *AIChE Symp. Ser.* **326** (2002), pp. 274–289.

De Graaf, A.A., Striegel K., Wittig R.M., Laufer B., Schmitz G., Wiechert W., Sprenger G.A. and Sahm H., Metabolic state of *Zymomonas mobilis* in glucose-, fructose- and xylose-fed continuous cultures as analysed by ^{13}C- and ^{31}P-NMR spectroscopy. *Arch Microbiol* **171** (1999), pp. 371–385.

Domach, M.M. and Shuler M.L., A finite representation model for an asynchronous culture *of E. coli. Biotechnol. Bioeng.* **26** (1984), pp. 877–884.

Duboc, P. and von Stockar U., Modeling of oscillating cultivations of *Saccharomyces cerevisiae*: identification of population structure and expansion kinetics based on on-line measurements. *Chem. Eng. Sci.* **55** (2000), pp. 149–160.

Elliot, S.G., Co-ordination of growth with cell division: Regulation of synthesis during the cell cycle of the fission yeast *Schizosaccharomyces pombe.* Molec.gen.Genet.**192** (1983), pp. 204 – 211.

Faraday, D. B. F., Hayter P. and Kirkby N. F., A mathematical model of the cell cycle of a hybridoma cell line, *Biochemical Engineering Journal,* Volume 7, Issue 1, January 2001, pp. 49-68

Faraday, D.B.F., The Mathematical Modelling of The Cell Cycle of a Hybridoma Cell Line. PhD Thesis, Chemical & Process Engineering, School of Engineering University of Surrey, UK. (1994)

Ferenci, T. (1999) 'Growth of bacterial cultures' 50 years on: Towards an uncertainty principle instead of constants in bacterial growth kinetics. Research microbiology. **150** (1999), pp. 431 – 438.

Figueredo, L.M., Calderbank. P.H., The scale-up of aerated mixing vessels for specified oxygen dissolution rates. *Chem. Eng. Sci.* **34** (1979), pp. 1333-1338.

Follstad, B.D., Balcarcel R.R., Stephanopoulos G. and Wang D.I.C., Metabolic flux analysis of hybridoma continuous culture steady state multiplicity. *Biotechnol Bioeng* **63** (1999), pp. 675–683.

Forsburg L., The beast Yeast?.TIG Vol 15No9 (1999), pp. 340 – 344.

Fotuhi, H., Investigation of Repeated Batch Propagation Strategy. PhD Thesis, Chemical & Process Engineering, School of Engineering, University of Surrey,UK (2002).

Frank, P. M., and Köppen-Seliger B., New developments using AI in fault diagnosis. Engineering Applications of Artificial Intelligence, Volume 10, Issue 1, February 1997, Pages 3-14
Fredrickson, A., and Mantzaris N.V., A new set of population balance equations for microbial and cell populations. *Chem. Eng. Sci.* **57** (2002), pp. 2265–2278.

Friedrickson A., Friedrich S., Hatzis C., Multistaged corpuscular models of microbial growth: Monte Carlo Simulations. Bio systems **36** (1995), pp. 19 – 35.

Frykman, S. and Srienc F., Cell cycle dependent protein secretion by *Saccharomyces cerevisiae. Biotechnol. Bioeng.* **76** (2001), pp. 259–268.

Futcher, B., Cell cycle synchronization. *Methods Cell Sci.* **21** (1999), pp. 79–86.

G. Bastin, G. and Dochain, D., Where mathematics and microbiology meet. Process Measurement and Control, Vol. 1: On-line Estimation and Adaptive Control of Bioreactors, Manchester Biotechnology Centre, UMIST. ISBN 0444884300,1990.

Ganusov, V.V., Bril'kov A.V. and Pechurkin N.S., Mathematical modeling of population dynamics of unstable plasmid-bearing bacterial strains under continuous cultivation in a chemostat. *Biophysics* **45** (2000), pp. 881–887.

Gershenfeld, N.A., The Nature of Mathematical Modeling. Cambridge University Press, Cambridge (1999).

Ginovart, Lopez D. and Valls J., INDSIM, an individual-based discrete simulation model to study bacterial cultures. *J. Theor. Biol.* **214** (2002), pp. 305–319.

Goel, A., Lee J., Domach M.M. and Ataai M.M., Metabolic fluxes, pools, and enzyme measurements suggest a tighter coupling of energetics and biosynthetic reactions associated with reduced pyruvate kinase flux. *Biotechnol Bioeng* **64** (1999), pp. 129–134.

Gomm J. J., Browne P. J., Coope R. C., Liu Q. Y., Buluwela L. and Coombes R. C. Isolation of Pure Populations of Epithelial and Myoepithelial Cells from the Normal Human Mammary Gland Using Immunomagnetic Separation with Dynabeads. Analytical Biochemistry, Volume 226, Issue 1, March 1995, Pages 91-99

Guardia, M.J., Garcia Calvo, E., Kinetic model for *Escherichia coli* growth in different operational conditions, *Appl. Microbiol. Biotechnol. Submitted* (2000).

Gujer, W., Microscopic versus macroscopic biomass models in activated sludge processes. *Water Sci. Technol.* **45** (2002), pp. 1–11.

Gygi, S.P., Rochon Y., Franza B.R. and Aebersold R., Correlation between protein and mRNA abundance in yeast. *Mol Cell Biol* **19** (1999), pp. 1720–1730.

Harder, W., Dijkhuizen, L., Strategies of mixed substrate utilization in microorganisms. Philos. *Trans. R. Soc. Lond. B. Biol. Sci.* **297** (1982), pp. 459-480

Hatzimanikatis, V., and Lee K.H., Dynamical analysis of gene networks requires both mRNA and protein expression information. *Metab Eng* **1** (1999), pp. 275–281

Hatzimanikatis, V., Choe L.H. and Lee K.H., Proteomics: theoretical and experimental considerations. *Biotechnol Prog* **15** (1999), pp. 312–318.

Hatzimanikatis, V., Emmerling M., Sauer U. and Bailey J.E., Application of mathematical tools for metabolic design of microbial ethanol production. *Biotechnol Bioeng* **58** (1998), pp. 154–161.

Hatzimanikatis, V., Floudas C.A. and Bailey J.E., Analysis and design of metabolic reaction networks via mixed-integer linear optimization. *AIChE J* **42** (1996), pp. 1277–1292.

Hatzimanikatis, V., Lee K.H. and Bailey J.E., A mathematical description of regulation of the G1-S transition of the mammalian cell cycle. *Biotechnol Bioeng* **65** (1999), pp. 631–637.

Hatzis, C., Srienc F. and Fredrickson A.G., Multistaged corpuscular models of microbial growth: Monte Carlo simulations. *Biosystems* **36** (1995), pp. 19–35.

Hayles, J., Nurse P., Genetics of the fission Yeast Schizosaccharomyces *pombe.* Annual review genetics **26** (1992), pp. 373-402.

Henson, M.A., Dynamic modeling and control of yeast cell populations in continuous biochemical reactors. *Comput. Chem. Eng.* **27** (2003), pp. 1185–1199.

Henson, M.A., Muller D. and Reuss M., Cell population modeling of yeast glycolytic oscillations. *Biochem. J.* **368** (2002), pp. 433–446.

Hjortso, M.A. and Nielsen J., Population balance models of autonomous microbial oscillations. *J. Biotechnol.* **42** (1995), pp. 255–269.

Hofer, M., Aerobic and Anaerobic Uptake of Sugars in S. pombe. Journal of general microbiology (1897), 133, pp.2163-2172

Hua, Q., Yang C. and Shimizu K., Metabolic flux analysis for efficient pyruvate fermentation using vitamin-auxotrophic yeast of *Torulopsis glabrata. J Biosci Bioeng* **87** (1999), pp. 206–213.

Hynee, F., De Monte S., d'Ovidio F., Sorensen P.G. and Westerhoff H., Synchronization of glycolytic oscillations in a yeast cell population. *Faraday Discuss* **120** (2001), pp. 261–276.

Hynne, G.F., Dano S. and Sorenson P.G., Full-scale model of glycolysis in *Saccharomyces cerevisiae. Biophys. Chem.* **94** (2001), pp. 121–163.

Joshi, N. V., Murugan, P. and Rhinehart R. R., Experimental Comparison Of Control Strategies, Control Engineering Practice, Volume 5, Issue 7, July 1997, Pages885-896

Katoh, T., Yuguchi D., Yoshii H., Shi H. and Shimizu K., Dynamics and modeling on fermentative production of poly (β-hydroxybutyric acid) from sugars via lactate by a mixed culture of *Lactobacillus delbrueckii* and *Alcaligenes eutrophus. J Biotechnol* **67** (1999), pp. 113–134.

Kurtz, J., Control of Oscillating Microbial Cultures Described by Population Balance Models. Ind. Eng. Chem. Res. **37** (1998), 4059 – 4070.

Leaf, T.A. and Srienc F., Metabolic modeling of polyhydroxybutyrate biosynthesis. *Biotechnol Bioeng* **57** (1998), pp. 557–570.

Lee, P.L., Yen J., Yang L. and Liao J.C., Incorporating qualitative knowledge in enzyme kinetic models using fuzzy logic. *Biotechnol Bioeng* **62** (1999), pp. 722–729.

Lloyd, D., Poole, R.K. and Edwards, S.W. The cell division cycle: temporal

organisation and control of cellular growth and reproduction (1st edition), Academic Press, London, UK (1982)

Lübbert A., and Simutis R., Using measurement data in bioprocess modelling and control. Trends in Biotechnology, Volume 12, Issue 8, August 1994, Pages 304-311

Mantzaris, N.V., Daoutidis P. and Srienc F., Numerical solution of multi-variable cell population balance models: I. Finite difference methods. *Comput. Chem. Eng.* **25** (2001), pp. 1411–1440.

Mantzaris, N.V., Daoutidis P. and Srienc F., Numerical solution of multi-variable cell population balance models: II. Spectral methods. *Comput. Chem. Eng.* **25** (2001), pp. 1441–1462.

Mantzaris, N.V., Daoutidis P. and Srienc F., Numerical solution of multi-variable cell population balance models: III. Finite element methods. *Comput. Chem. Eng.* **25** (2001), pp. 1463–1481.

Mantzaris, N.V., Liou J.-J., Daoutidis P. and Srienc F., Numerical solution of a mass structured cell population balance model in an environment of changing substrate concentration. *J. Biotechnol.* **71** (1999), pp. 157–174.

Mantzaris, N.V., Srienc F. and Daoutidis P., Nonlinear productivity control using a multi-staged cell population balance model. *Chem. Eng. Sci.* **57** (2002), pp. 1–14.

Marx, A., De Graaf A.A., Wiechert W., Eggeling L. and Sahm H., Determination of the fluxes in the central metabolism of *Corynebacterium glutamicum* by nuclear magnetic resonance spectroscopy combined with metabolic balancing. *Biotechnol Bioeng* **49** (1996), pp. 111–129.

Matsoukas T., and Smith M., Constant-number Monte Carlo simulation of population balances. *Chemical Engineering Science* **53** (1996), pp. 1777 – 1786.

Mete, M., Altnta, Betül Krdar, Z. Isen Önsan and Kutlu Ö. Ülgen. Cybernetic modelling of growth and ethanol production in a recombinant *Saccharomyces cerevisiae* strain secreting a bifunctional fusion protein .Department of Chemical Engineering, Boaziçi University, 80815 Bebek, Istanbul, Turkey. Process Biochemistry Volume 37, Issue 12, July 2002, Pages 1439-1445.

Mhaskar, P., Hjortso M.A. and Henson M.A., Cell population modeling and parameter estimation for continuous cultures of *Saccharomyces cerevisiae*. *Biotechnol. Prog.* **18** (2002), pp. 1010–1026.

Michel, B.J., Miller, S.A., Power requirements of gas-liquid agitated systems, *AIChE. J.* **8** (1962), pp. 262-267.

Mitchison, J..M. and Creanor, J., Further measurements of DNA synthesis and

enzyme potential during the cell cycle of *Schizosaccharomyces pombe.* Expl. Cell Res. **69** (1969), pp. 244 – 247.

Mitchison, J.M. & Cummins, Changes in the acid-soluble pool during the cell cycle of *Schizosaccharomyces pombe.* Expl. Cell Res. **35** (1964), pp. 394 – 401.

Mitchison, J.M. & Nurse P., Growth in cell length in the fission yeast *Schizosaccharomyces pombe.* J.Cell.Science. **75** (1985), pp. 357 – 376.

Montague, G. A., Morris, A. J. and Tham, M. T. Enhancing bioprocess operability with generic software sensors. Journal of Biotechnology, Volume 25, Issues 1-2, August 1992, Pages 183-201

Montague, G., and Morris, J., Neural-network contributions in biotechnology. Trends in Biotechnology, Volume 12, Issue 8, August 1994, Pages 312-324

Montague, G., Tham, M., and Lant, P., Estimating the immeasurable without mechanistic models. Trends in Biotechnology, Volume 8, 1990, Pages 82-83

Munz, P.W., Kohli H., Leupold, U., Genetics Overview. Molecular Biology of fission Yeast. New York: Academic (1989), pp. 1-30.

Nielsen, J and Jørgensen H.S., A kinetic model for the penicillin biosynthetic pathway in *Penicillium chrysogenum. Control Eng Practice* **4** (1996), pp. 765–771.

Nielsen, J., Villadsen J, Bioreaction engineering principles. New York: Plenum Press (1994).

Nishimura, Y. and Bailey J.E., Bacterial population dynamics in batch and continuous-flow microbial reactors. *AIChE J.* **27** (1981), pp. 73–81.

Novak, B., Attila Csikasz-Nagy, Bela Gyorffy, Chen K., Tyson John, Mathematical model of the fission yeast cell cycle with checkpoint controls at the G1/S, G2/M and metaphase/Anaphase Transitions. *Journal of Biophysical Chemistry* **72** (1998), pp. 185-200.

Novak, B., Mitchinson J.M., 'Change in the rate of CO_2 production in synchronous cultures of the fission yeast Schizosaccharomyces pombe: A periodic cell cycle event that persist after the DNA-division cycle has been blocked. *Journal of cell science* **86** (1986), 191-206.

Novak, B., Mitchison, J., Sveiczer, A., The size control of fission Yeast revisited. *Journal of Cell Science* **109** (1986), pp. 2947 – 2957.

Nurse, P., Wen W., Broek D., Yeast Cells can enter a Quiescent State Through G1,S,G2, or M phase of the cell cycle. *J. of Cancer Research* **53** (1993), pp. 1867-1870.

O'Connell M., Walworth N., Carr A., The G2-phase DNA-damage checkpoint. Trends in Cell Biology **10** (2000), pp. 296 – 303.

Peper, Grimbergen C.A, Spaan J.A.E, Souren J.E.M. and van Wijk R., A mathematical model of the hsp70 regulation in the cell. *Int J Hyperthermia* **14** (1998), pp. 97–124.

Perry, R.H., Chemical Engineering Handbook, 6th., McGraw-Hill, New York (1984)

Pissara, P.N., Nielsen J. and Bazin M.J., Pathway kinetics and metabolic control analysis of a high-yielding strain of *Penicillium chrysogenum* during fed batch cultivations. *Biotechnol Bioeng* **51** (1996), pp. 168–176.

Ponton J. W., and Gawthrop P. J., Systematic construction of dynamic models for phase equilibrium processes, Computers & Chemical Engineering, Volume 15, Issue 12, December 1991, Pages 803-808

Postlethwaite. B.E., Building a model-based fuzzy controller. Fuzzy Sets and Systems, Volume 79, Issue 1, 8 April 1996, Pages 3-13.

Pramanik, J., Trelstad P.L., Schuler A.J., Jenkins D. and Keasling J.D., Development and validation of a flux-based stoichiometric model for enhanced biological phosphorus removal metabolism. *Wat Res* **33** (1999), pp. 462–476.

Ramkrishna, D., *Population Balances: Theory and Applications to Particulate Processes in Engineering.* New York: Academic Press (2000).

Ramkrishna, D., Varner J., Mathematical models of metabolic pathways. Current opinion in Biotechnology **10** (1999), pp. 146 – 150.

Rieseberg, M., Kaspar C., Reardon K.F. and Scheper T., Flow cytometry in biotechnology. *Appl. Microbiol. Biotechnol.* **56** (2001), pp. 350–360.

Rizzi, M., Baltes M., Theobald U. and Reuss M., *In vivo* analysis of metabolic dynamics in *Saccharomyces cerevisiae*: II. mathematical model. *Biotechnol Bioeng* **55** (1997), pp. 592–608.

Robinson, J.H., Smith, J.A., Totty, N.F., Riddle, P.N. Transition probability and the hormonal and density dependent regulation of cell proliferation. *Nature* **248** (1976), pp. 704-707

Royce, P., Thornhill, N.F., Estimation of dissolved carbon dioxide concentrations in aerobic fermentations. *AIChE J.* **37** (1991), pp. 1680-1686

Schilling, C.H., Edwards J.S and Palsson B.O., Toward metabolic phenomics: analysis of genomic data using flux balances. *Biotechnol Prog* **15** (1999), pp.

288–295

Schilling, C.H., Schuster S., Palsson B.O. and R. Heinrich, Metabolic pathway analysis: basic concepts and scientific applications in the post-genomic era. *Biotechnol Prog* **15** (1999), pp. 296–303

Schmidt, K., Carlsen M., Nielsen J. and Villadsen J., Modeling isotopomer distributions in biochemical networks using isotopomer mapping matrices. *Biotechnol Bioeng* **55** (1997), pp. 831–840.

Schmidt, K., Nielsen J. and Villadsen J., Quantitative analysis of metabolic fluxes in *Escherichia coli*, using two-dimensional NMR spectroscopy and complete isotopomer models. *J Biotechnol* **71** (1999), pp. 175–190.

Schuster, S., Dankekar T. and Fell D.A., Detection of elementary flux modes in biochemical networks: a promising tool for pathway analysis and metabolic engineering. *Trends Biotechnol* **17** (1999), pp. 53–60.

Shi, H., Nikawa J. and Shimizu K., Effect of modifying metabolic network on poly-3-hydroxybutyrate biosynthesis in recombinant *Escherichia coli*. *J Biosci Bioeng* **87** (1999), pp. 666–677.

Shuler, M.L., Single-cell models: promise and limitations. *J. Biotechnol.* **71** (1999), pp. 225–228.

Sipiczki M., Taxonomy and physiogenesis. Molecular Biology of Fission Yeast. New York : Academic (1989), pp 431-52.

Smith, J.A., Martin, L., Do cells cycle? *Proc. Natl. Acad. Sci. U.S.A* **70(4)** (1973), pp. 1263-1267

Southamer, A.H., Bettenhausen, C., Utilization of energy for growth and maintenance in continuous and batch cultures of microorganisms: a reevaluation of the method for the determination of the ATP production by measuring molar growth yields. *Biochim. Biophys. Acta.* **301** (1976), pp 53-70

Srienc, F., Friedrickson A., Liou J., Solutions of Population Balance Models Based on a Successive Generations Approach. *Chemical Engineering Science.* Vol 52, No 9 (1996), pp. 1529 – 1540.

Srienc, F., Cytometric data as the basis for rigorous models of cell population dynamics. *J. Biotechnol.* **71** (1999), pp. 233–238.

Srienc, F., Mantzaris, N. et al., Numerical Solution of a mass Structured cell population balance model in an environment of changing substrate concentration. *Journal of Biotechnology* **71** (1998), pp.157 – 174.

Stephanopoulos, G., Metabolic fluxes and metabolic engineering. *Metab Eng* **1**

(1999), pp. 1–11.

Szyperski, T., ^{13}C-NMR, MS and metabolic flux balancing in biotechnology research. *Q Rev Biophys* **31** (1998), pp. 41–106

Theilgaard, H., and Nielsen J., Metabolic control analysis of the penicillin biosynthetic pathway: the influence of the LLD-ACV : bisACV ratio on the flux control. *Anton Leeuw Int J G* **75** (1999), pp. 145–154.

Tholudur, A., Ramirez W.F. and McMillan J.D., Mathematical modeling and optimization of cellulase protein production using *Trichoderma reesei* RL-P37. *Biotechnol Bioeng* **66** (1999), pp. 1–16.

Tsuchiya, H.M., Fredrickson A.G. and Aris R., Dynamics of microbial cell populations. *Adv. Chem. Eng.* **6** (1966), pp. 125–206.

Tyson, J., Models of cell cycle control in Eukaryotes. *Journal of Biotechnology* **71** (1998), pp. 239 – 244.

Uchiyama, K., Morimoto M., Yokoyama Y. and Shioya S., Cell cycle dependency of rice α-amylase production in a recombinant yeast. *Biotechnol. Bioeng.* **54** (1997), pp. 262–271.

Vallino, J.J., and Stephanopoulos G., Flux determination in cellular bioreaction networks: applications to lysine fermentations. In: S.K. Sikdar, M. Bier and P. Todd Editors, *Frontiers in Bioprocessing* CRC Press, Boca Raton (1990), pp. 205–219.

Van Can, H.J.L., te Braake H.A.B., Bijman A., Hellinga C., Luyben K.C.A.M. and Heijnen J.J., An efficient model development strategy for bioprocesses based on neural networks in macroscopic balances: part II. *Biotechnol Bioeng* **62** (1999), pp. 666–680.

Van Can, H.J.L., te Braake H.A.B., Bijman A., Hellinga C., Luyben K.C.A.M. and Heijnen J.J.,An efficient model development strategy for bioprocesses based on neural networks in macroscopic balances. *Biotechnol Bioeng* **54** (1997), pp. 549–566.

Van Riel, N.A.W., Giuseppin M.L.F., TerSchure E.G. and Verrips T., A structured, minimal parameter model of the central nitrogen metabolism in *Saccharomyces cerevisiae*: the prediction of the behaviour of mutants. *J Theor Biol* **191** (1998), pp. 397–414.

Varma, A., and Palsson B.O., Metabolic flux balancing: basic concepts, scientific and practical use. *Bio/Technology* **12** (1994), pp. 994–998.

Varner, J., and Ramkrishna D., Metabolic engineering from a cybernetic perspective. 1. Theoretical preliminaries. *Biotechnol Prog* **15** (1999), pp. 407–425.

Varner, J., and Ramkrishna D., Metabolic engineering from a cybernetic

perspective. 2. Qualitative investigation of nodal architectures and their response to genetic perturbation. *Biotechnol Prog* **15** (1999), pp. 426–438.

Varner, J., and Ramkrishna D., Metabolic engineering from a cybernetic perspective: aspartate family of amino acids. *Metabol Eng* **1** (1999), pp. 88–116.

Vaseghi, S., Baumeister A., Rizzi M. and Reuss M., *In vivo* dynamics of the pentose phosphate pathway in *Saccharomyces cerevisiae*. *Metab Eng* **1** (1999), pp. 128–140

Verbruggen H.B., Van Can H.J.L., Fuzzy modeling of enzymatic penicillin-G conversion. *Eng Applic Artif Intell* **12** (1999), pp. 79–92.

Villadsen, J., On the use of population balances. *J. Biotechnol.* **71** (1999), pp. 251–253.

Wang, J., Ellwood K., Lehman A., Carey M.F. and She Z.S., A mathematical model for synergistic eukaryotic gene activation. *J Mol Biol* **286** (1999), pp. 315–325 A nice example of a detailed mechanistic description of eukaryotic gene expression.

Ward, J.P., King J.R., Koerber A.J., Williams P., Croft J.M. and Sockett R.E., Mathematical modeling of quorum sensing in bacteria. *IMA J. Math Appl. Med. Biol.* **18** (2001), pp. 263–292.

Wegener R., Nusslin F., A Novel Radiobiological Cell Cycle Model. Department of medical physics, Radiological University Clinic, Hoppe Seyler-Str. 3 – 7206 Tubingen Germany (2000).

Wiechert, W. and De Graaf A.A., Bidirectional reaction steps in metabolic networks: I. modeling and simulation of carbon isotope labeling experiments. *Biotechnol Bioeng* **55** (1997), pp. 101–117.

Wiechert, W., Siefke C., De Graaf A.A. and Marx A., Bidirectional reaction steps in metabolic networks: II. Flux estimation and statistical analysis. *Biotechnol Bioeng* **55** (1997), pp. 118–135.

Wolf, J., and Heinrich R., Effect of cellular interaction on glycolytic oscillations in yeast: a theoretical investigation. *Biochem. J.* **345** (2000), pp. 321–334.

Wolf, J., Passarge J., Somsen O.J.G., Snoep J.L., Heinrich R. and Westerhoff H.V., Transduction of intracellular and intercellular dynamics in yeast glycolytic oscillations. *Biophys. J.* **78** (2000), pp. 1145–1153.
Wong, P., Gladney S. and Keasling J.D., Mathematical model for the *lac* operon: inducer exclusion, catabolite repression, and diauxic growth on glucose and lactose. *Biotechnol Prog* **13** (1997), pp. 132–143.

Yagi, H., Yoshida, F., Gas absorption by newtonian and non-newtonian fluids in

sparged agitated vessels. *Ind. Chem. Process. Dev.* **14** (1977), pp. 488-493.

Yang, Y.T., Bennett G.N. and San K.Y., Effect of inactivation of *nuo* and *ackA-pta* on redistribution of metabolic fluxes in *Escherichia coli*. *Biotechnol Bioeng* **65** (1999), pp. 291–297.

Yarnold J., Molecular aspects of cellular responses to radiotherapy. Radiotherapy and Oncology **44** (1997), pp. 1-7.

Yin, K.K., Yang H., Daoutidis P. and Yin G.G., Simulation of population dynamics using continuous-time finite-state Markov chains. *Comput. Chem. Eng.* **27** (2001), pp. 235–249.

Zafiri, C., Kornaros M. and Lyberatos G., Kinetic modelling of biological phosphorus removal with a pure culture of *Acinetobacter* sp. under aerobic, anaerobic and transient operating conditions. *Wat Res* **33** (1999), pp. 2769–2788.

Zamamiri, A.M., Birol G. and Hjortso M.A., Multiple steady states and hysteresis in continuous, oscillating cultures of budding yeast. *Biotechnol. Bioeng.* **75** (2001), pp. 305–312.

Zamamiri, A.M., Zhang Y., Henson M.A and Hjortso M.A., Dynamics analysis of an age distribution model of oscillating yeast cultures. *Chem. Eng. Sci.* **57** (2002), pp. 2168–2181.

Zhang, Y., Henson M.A. and Kevrekidis Y.G., Nonlinear model reduction for dynamic analysis of cell population models. *Chem. Eng. Sci.* **58** (2003), pp. 429–445.

Zhang, Y., Zamamiri A.M., Henson M.A. and Hjortso M.A., Cell population models for bifurcation analysis and nonlinear control of continuous yeast bioreactors. *J. Process Contr.* **12** (2002), pp. 721–734.

Zhu, G.Y., Zamamiri A.M, Henson M.A. and Hjortso M.A., Model predictive control of continuous yeast bioreactors using cell population models. *Chem. Eng. Sci.* **55** (2000), pp. 6155–6167.

Zorzetto, L. F. M., and Wilson, J. A. Monitoring bioprocesses using hybrid models and an extended Kalman filter. Computers & Chemical Engineering, Volume 20, Supplement1, 1996, Pages S689-S694

APPENDIX A

FIGURE 2 CYCLE TIMES BASED ON CO_2 PRODUCTION.

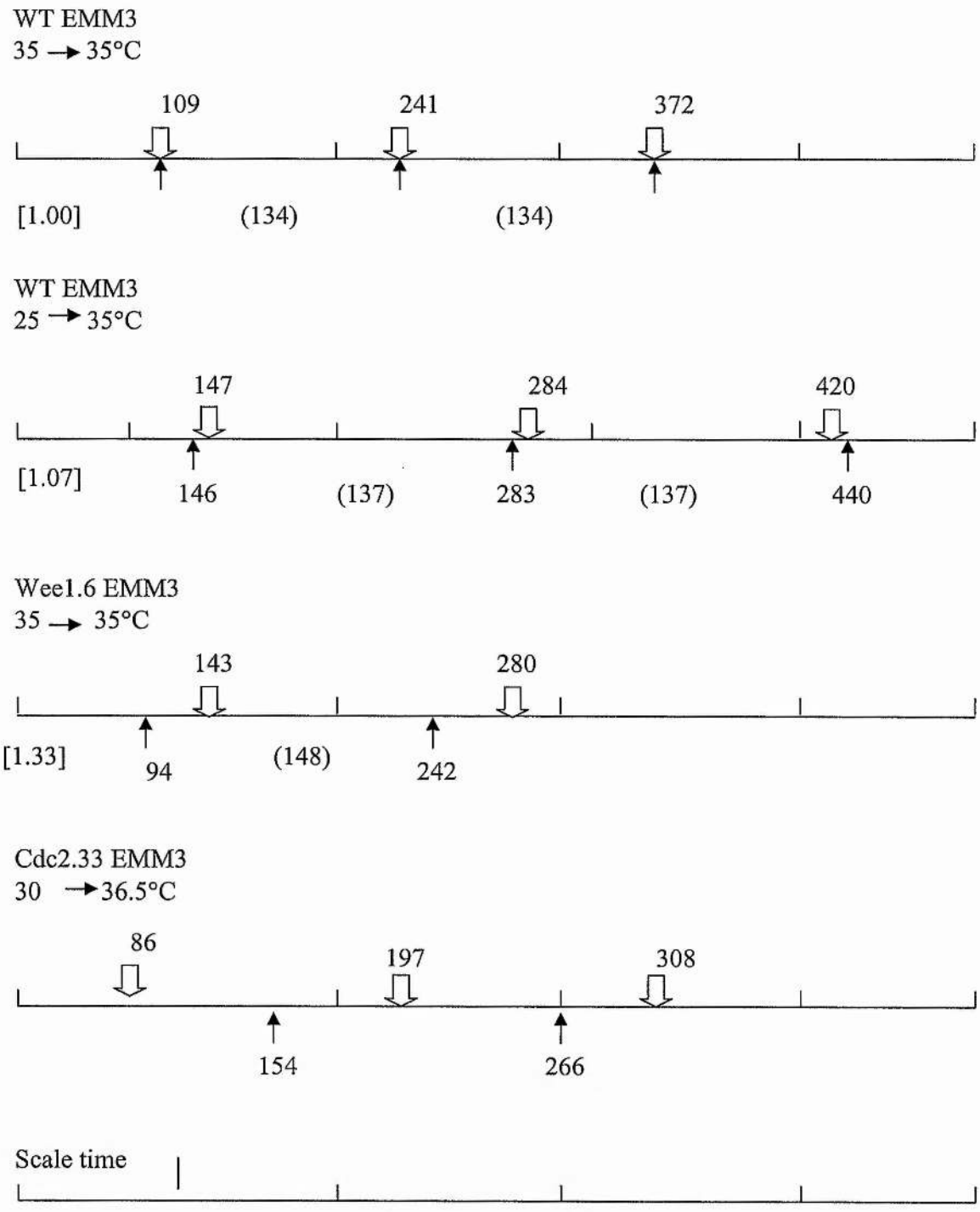

Cell cycle maps. Each upper arrow shows the time at a rate change point in CO_2 production in a synchronous culture estimated from the mid point of the step in acceleration. The lower arrows give the means of the mid points of the steps in cell numbers. The value in brackets represents the fraction of the cycle time at which rate of change of CO_2 production is happening. The value in parenthesis is the cell cycle time for the particular mutant of *S.pombe.*

FIGURE 3. CELL CYCLE OF MM321 HYBRIDOME CELL LINE

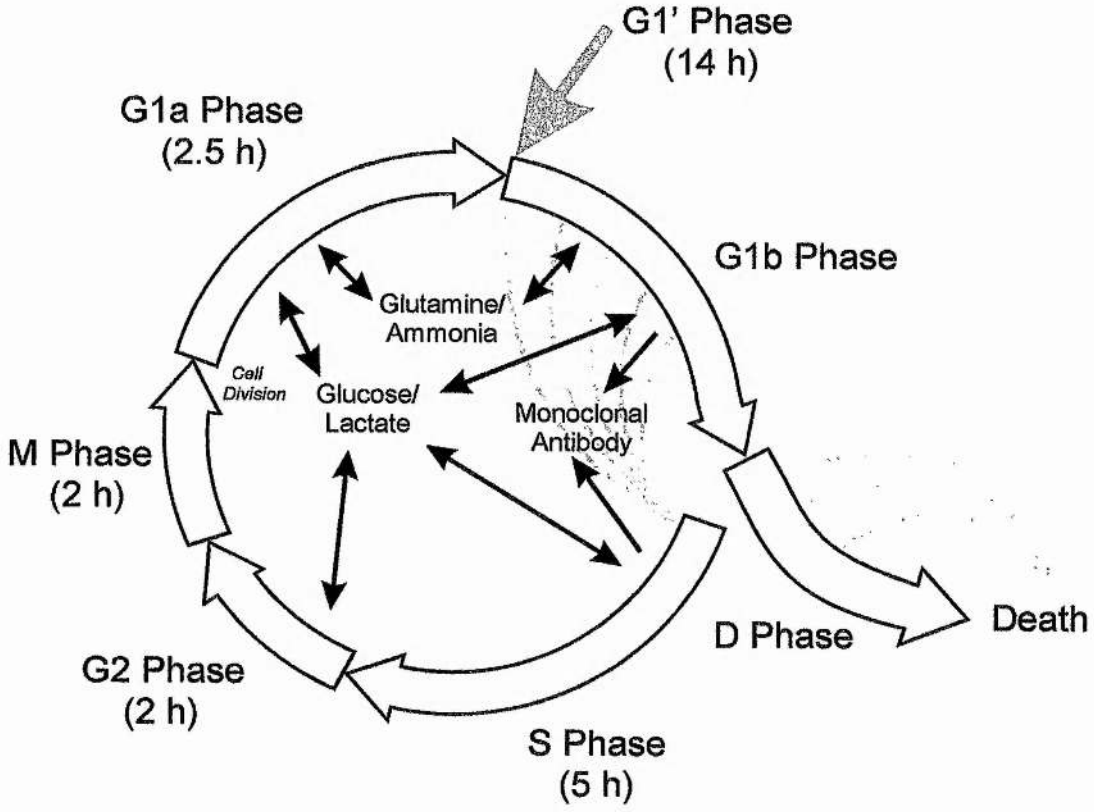

Schematic of the specific model employed as an observer for the application of the MBO control strategy (Faraday, 1994 - adapted).

FIGURE 1. CELL CYCLE *S. pombe* PROPOSED

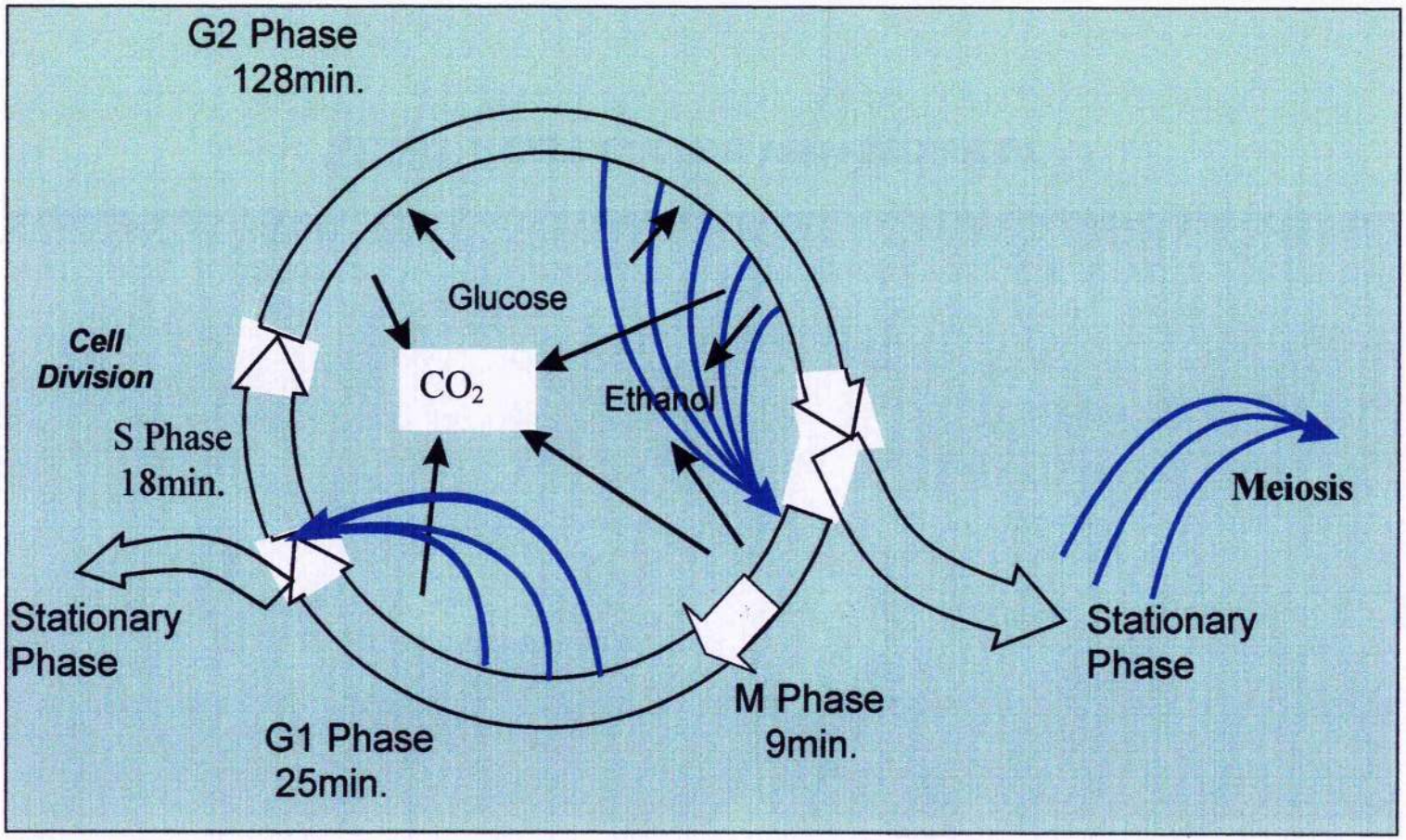

CREANOR EXPERIMENTS

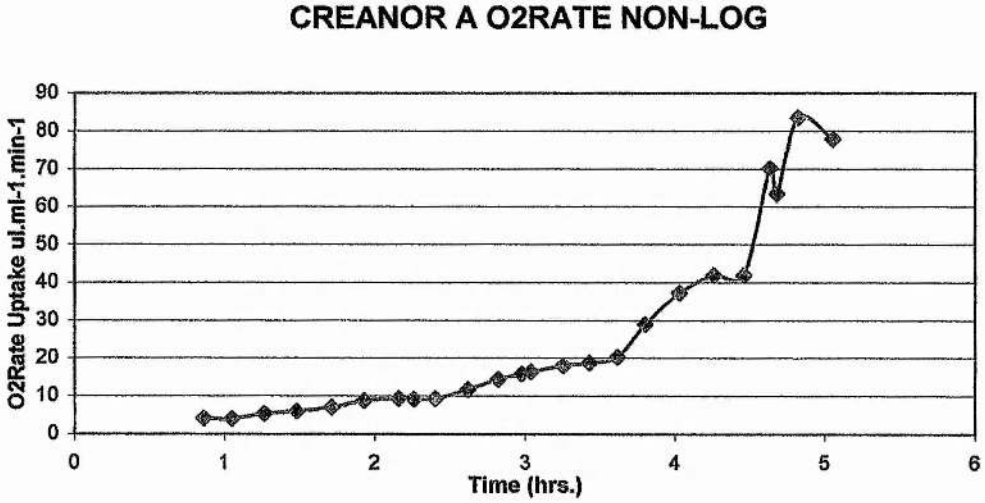

GRAPH 1
Creanor Experiments in oxygen consumption throughout the cell cycle of *S. pombe.* Creanor A

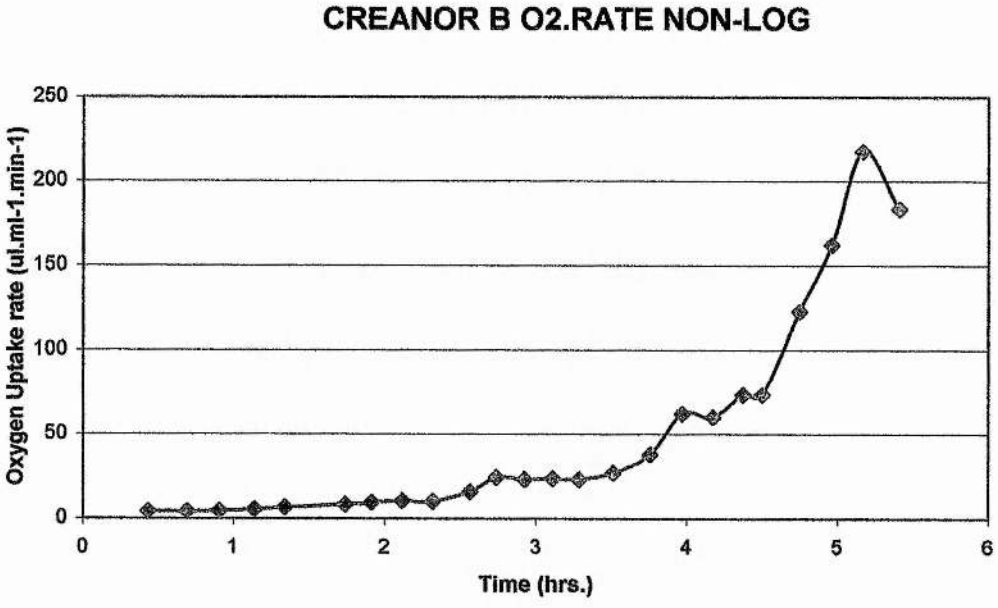

GRAPH 2
Oxygen consumption throughout the cell cycle of *S. pombe.* Creanor B

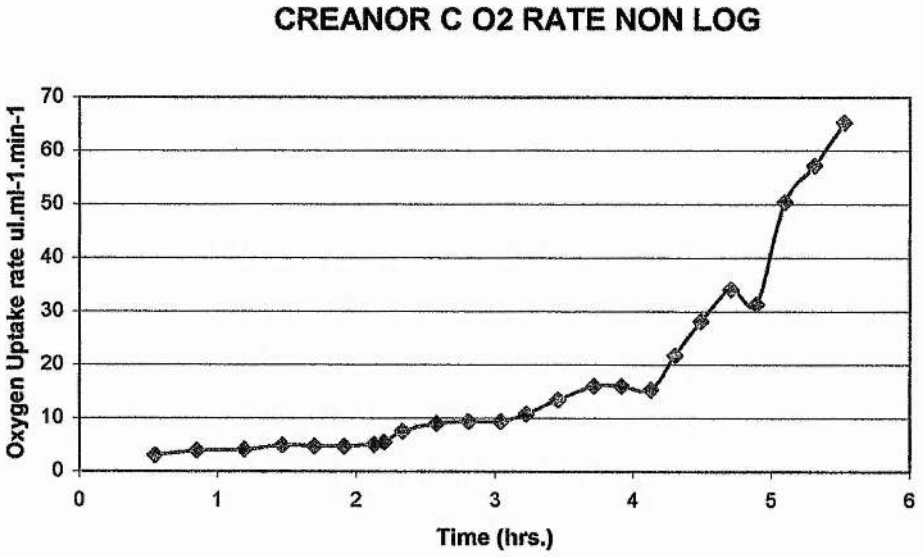

GRAPH 3

Oxygen consumption throughout the cell cycle of *S. pombe*. Creanor B

APPENDIX B

GRAPH 1

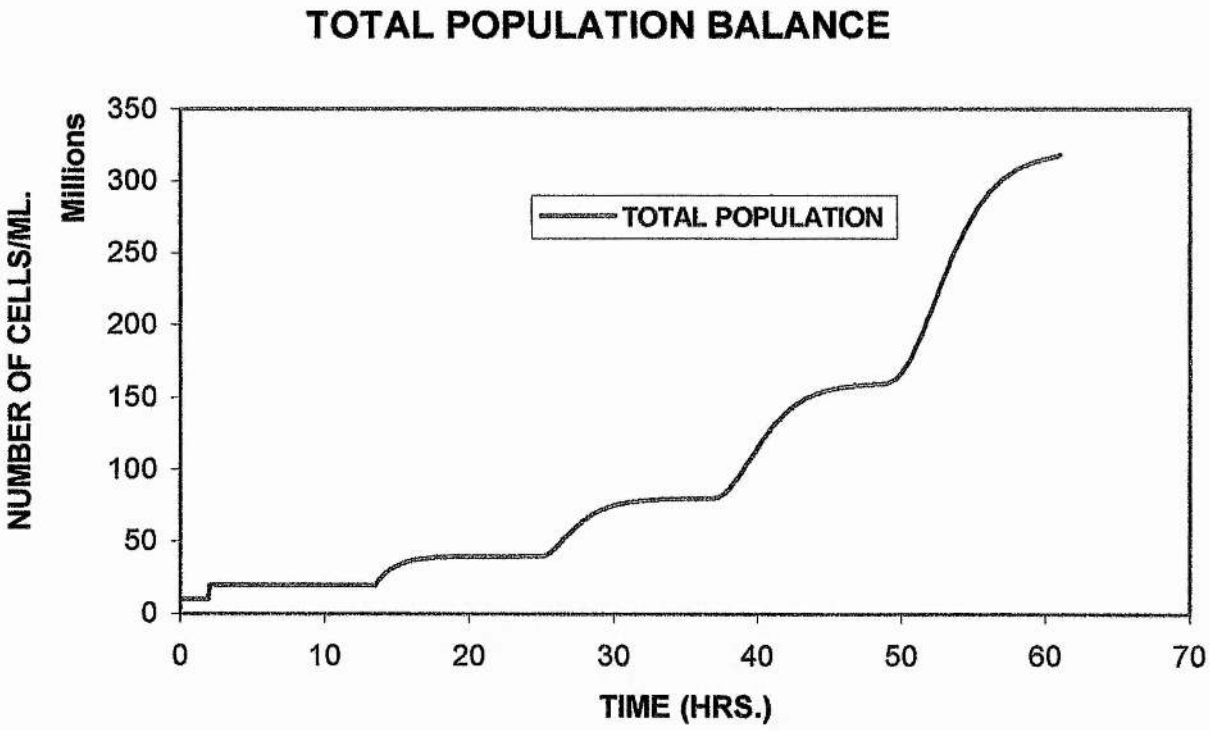

Number of mm321 Cells through out the Cycle

Cell population Balance for a synchronised cell culture following Smith and Martin Model with constant probability transition,: 0.03cells per min. 10 million cells starting to cycle in G2 phase.

Graph 1B : POPULATION BALANCES FOR DIFFERENT mm321 CELL LINE

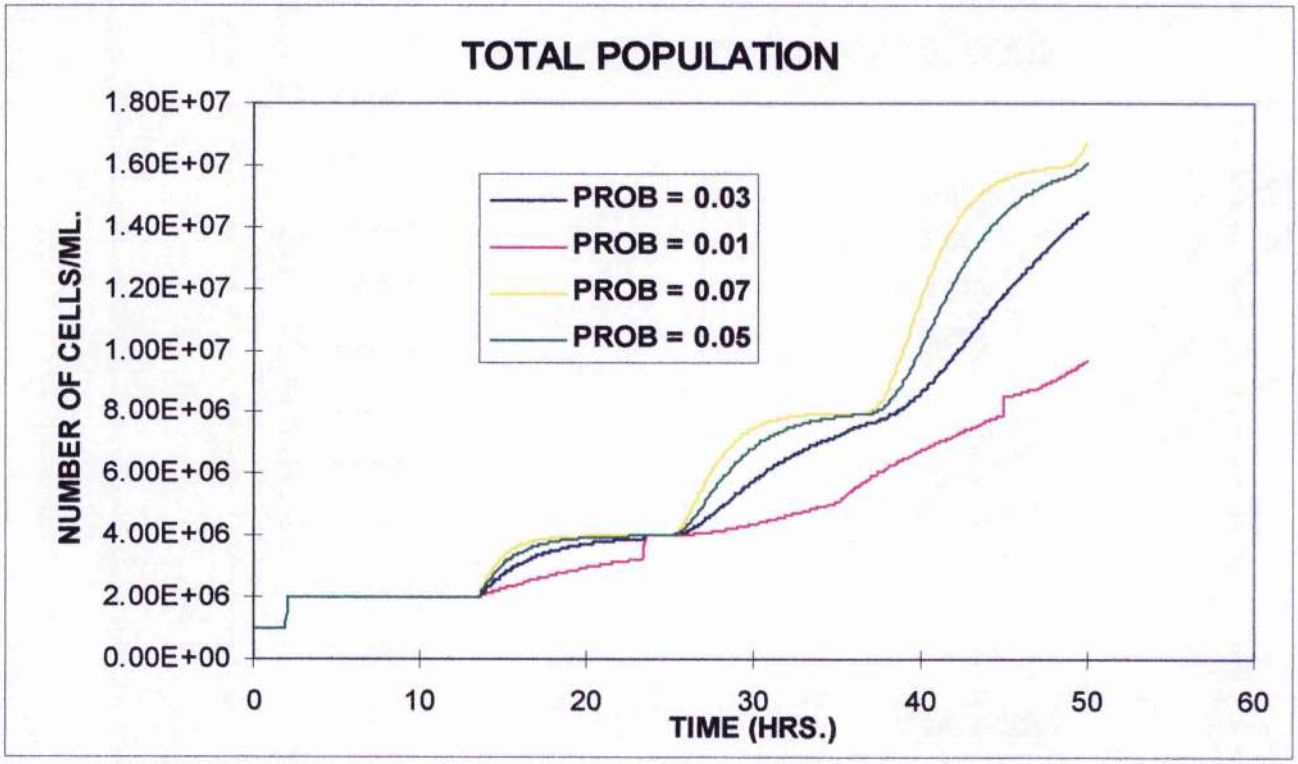

Different Probability Transitions in a synchronised culture following Smith and Martin model. 1million cells start ing to cycle in G2phase

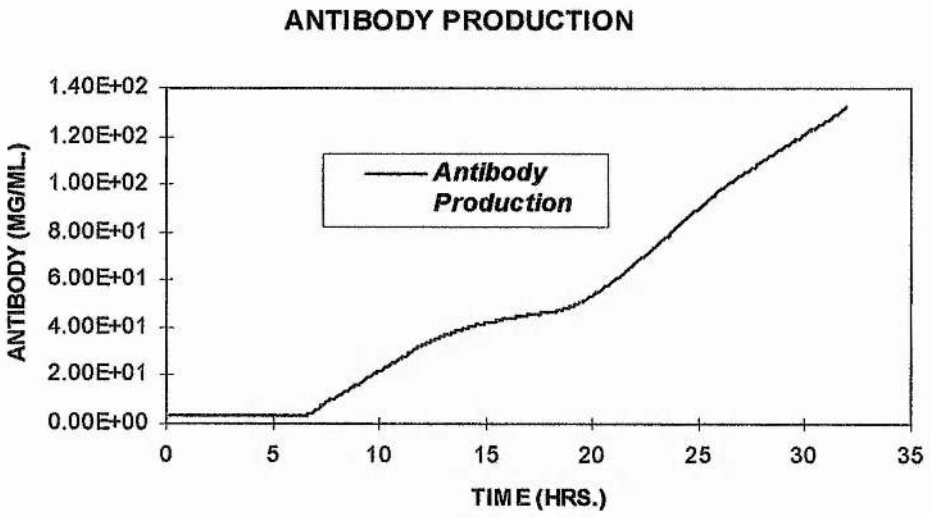

GRAPH 2

Antibody Production in mm321 Cell line

Antibody production in a Synchronised Culture. 1million cells starting to cycle in G2 phase. Contant probability transition following the Smith and Martin model

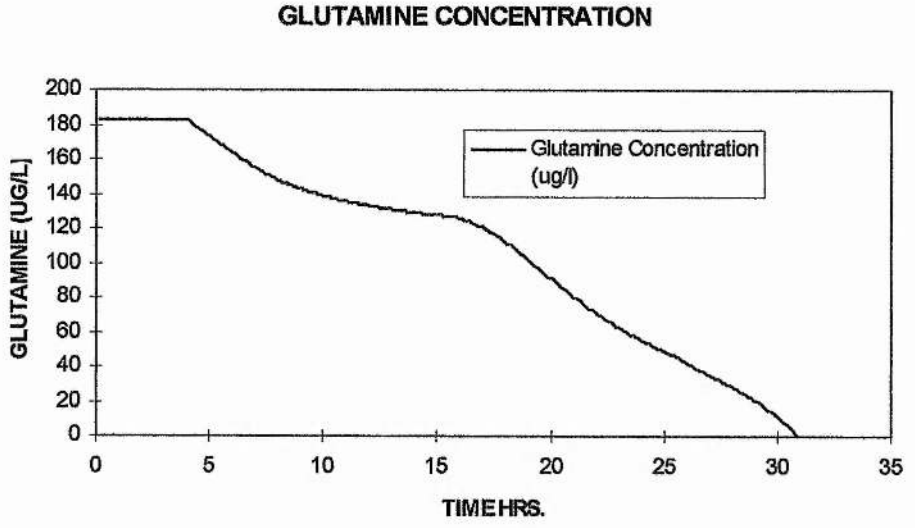

GRAPH 3

Consumption of Glutamine Through out the Cycle

Glutamine consumption in a mm321 cell line consuming Glutamine in G1A and G1B phases with a constant probability distribution (0.02 cell/min).

GRAPH 4
NUMBER OF CELLS IN PHASE S

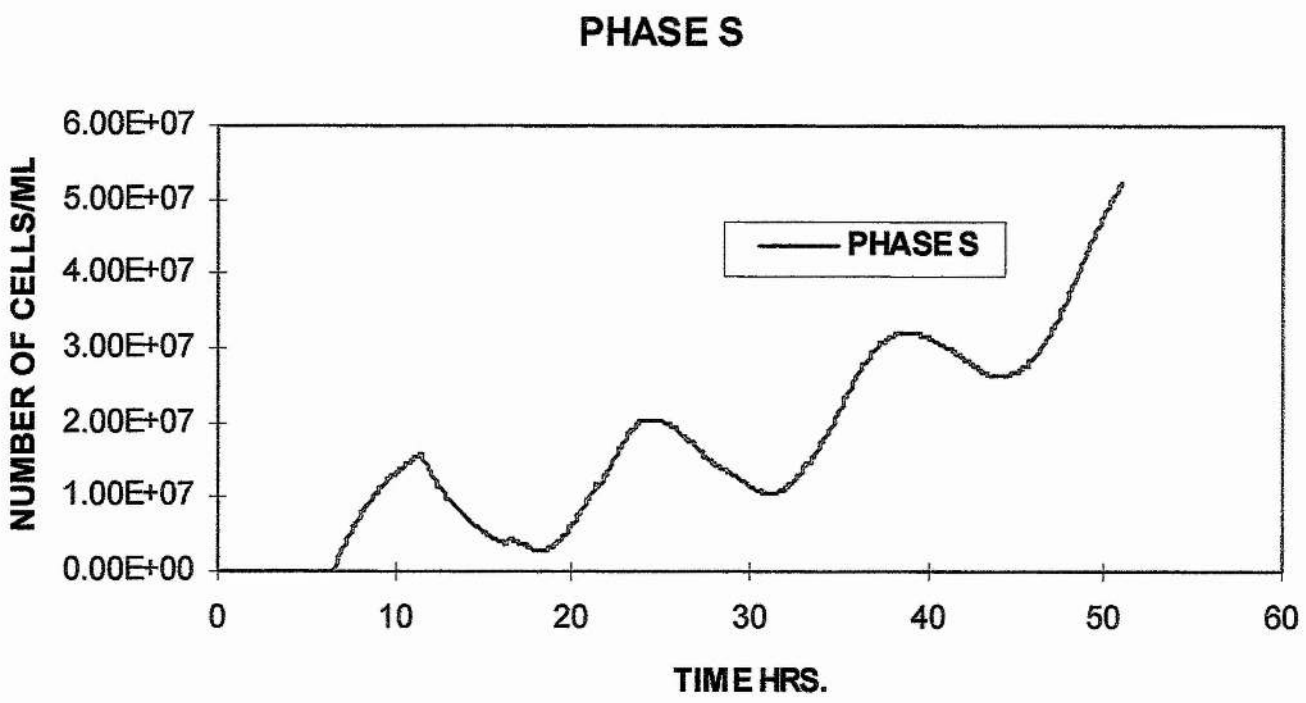

GRAPH 5
NUMBER OF CELLS PHASE G2

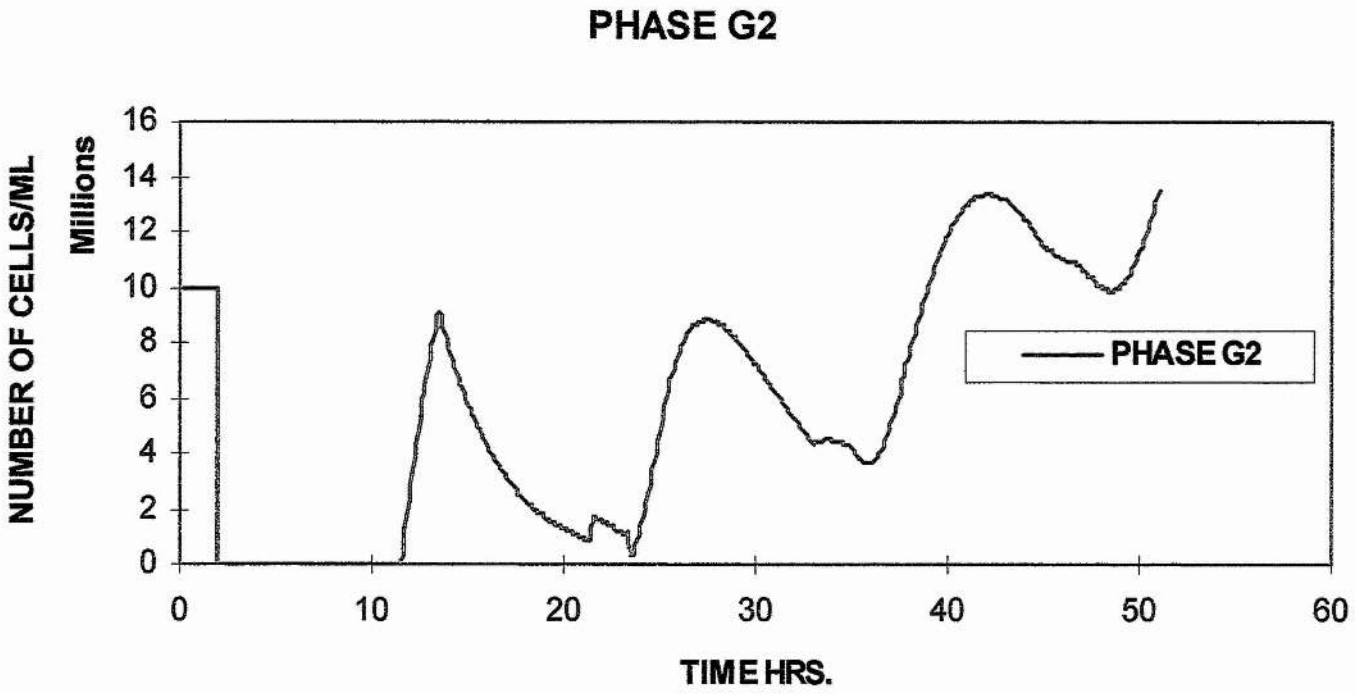

GRAPH 6
NUMBER OF CELLS PHASE M

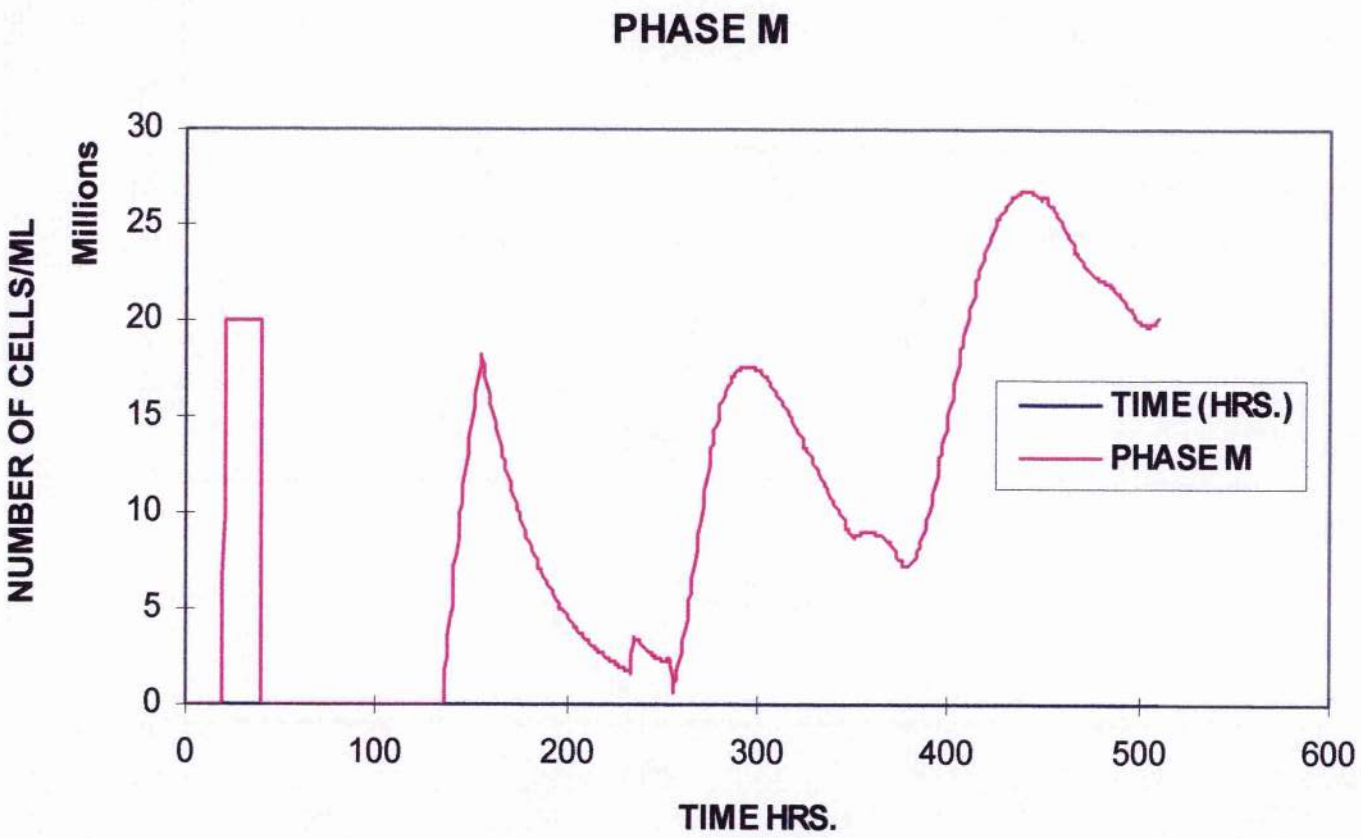

GRAPH 7
NUMBER OF CELLS G1A

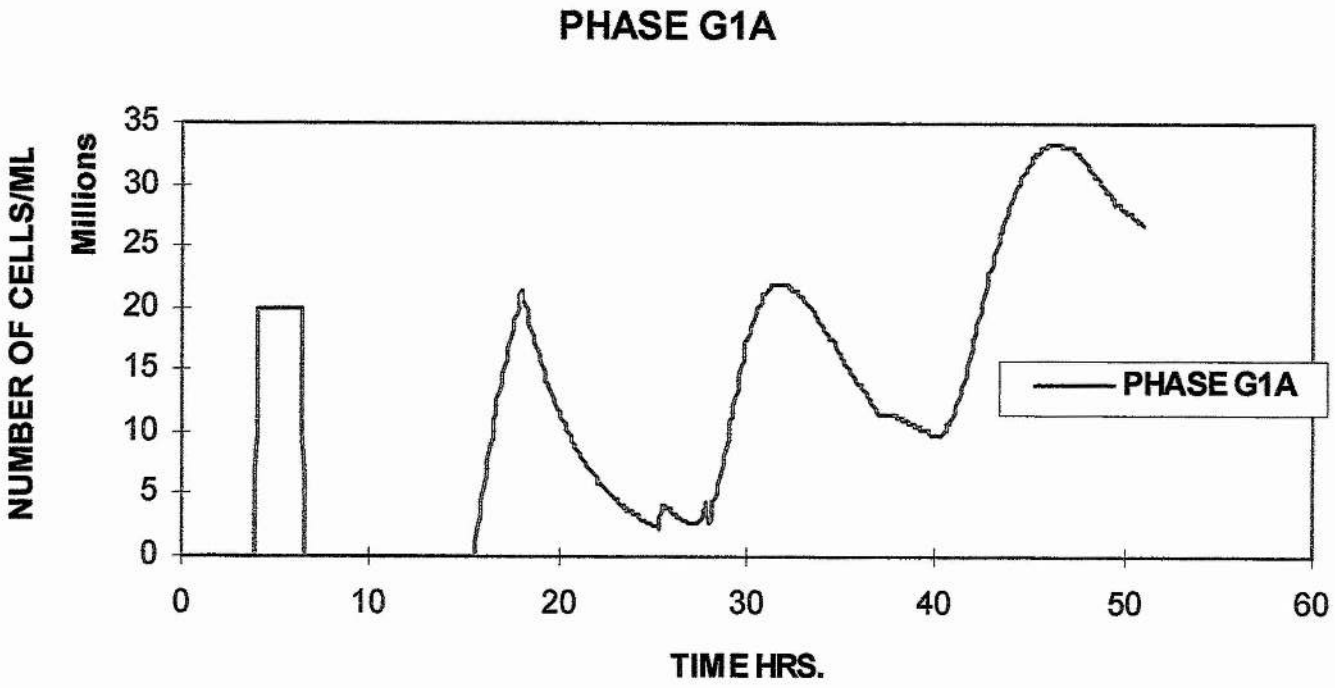

GRAPH 8
NUMBER OF CELLS PHASE G1B (TRANSITION)

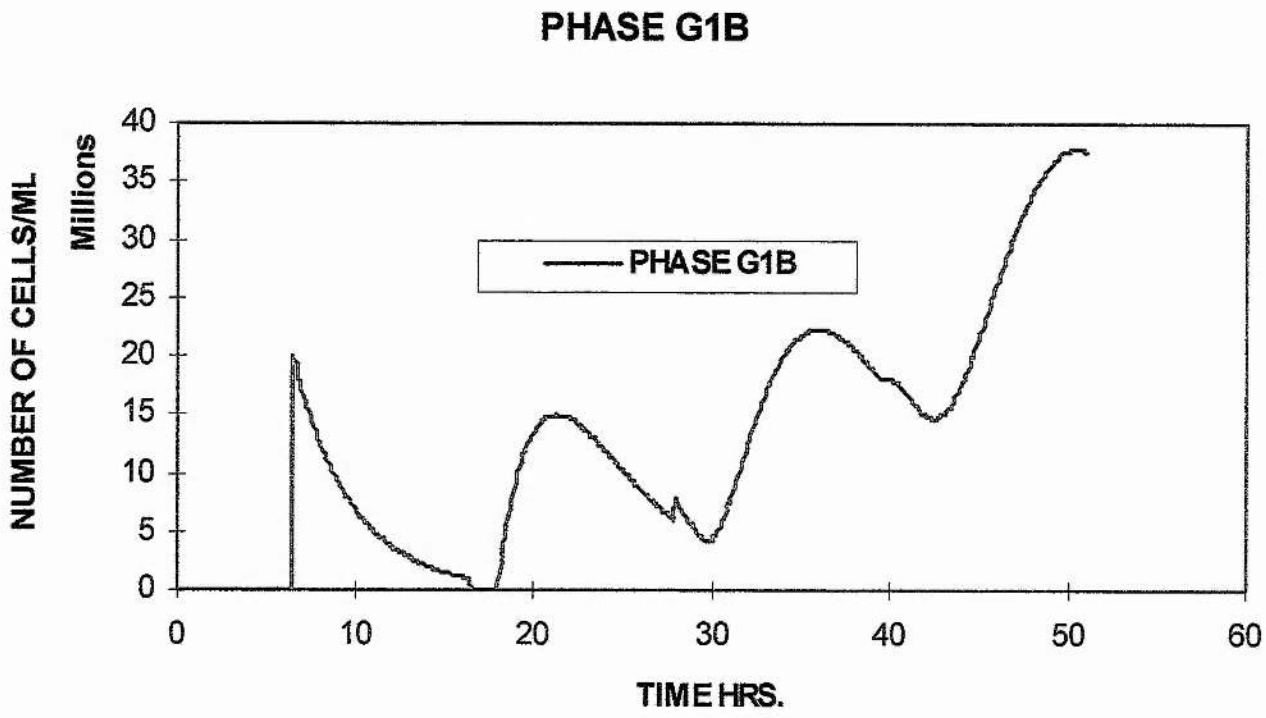

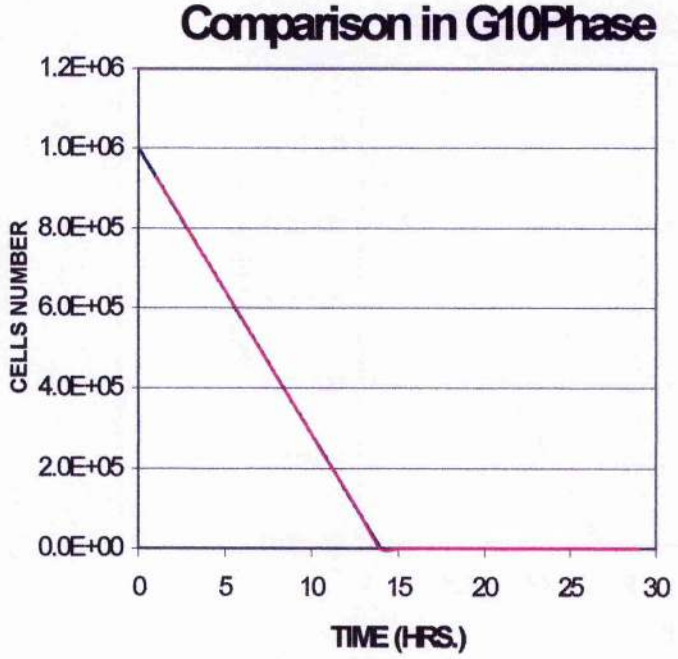

GRAPH 9
G10 Phase. Comparison between old and new versions of CelCyMUS. mm3211 Hybridome cell line released into the system

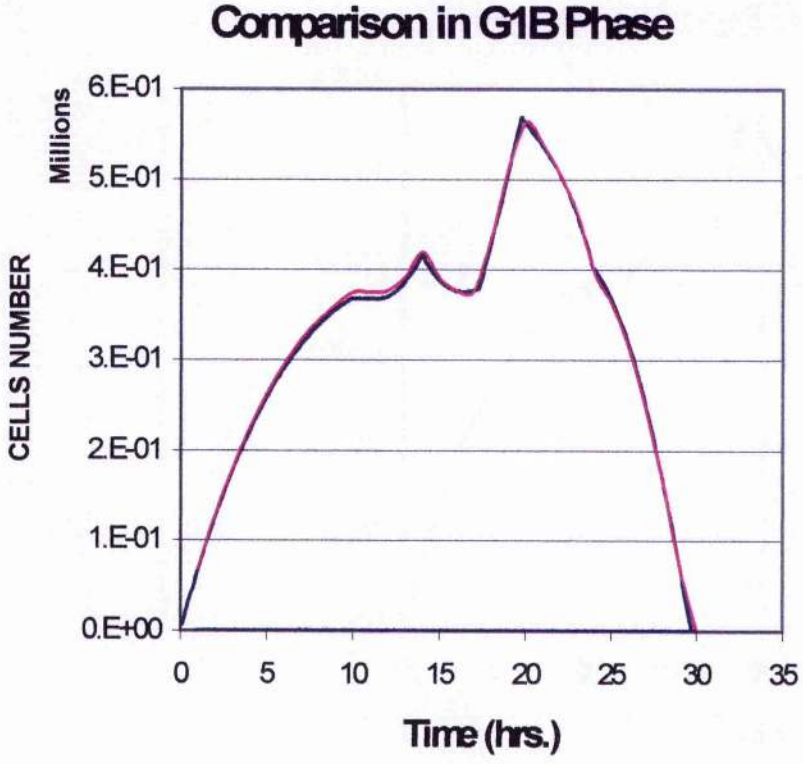

GRAPH 10G1B Phase . Comparison between old and new versions of CELCYMUS

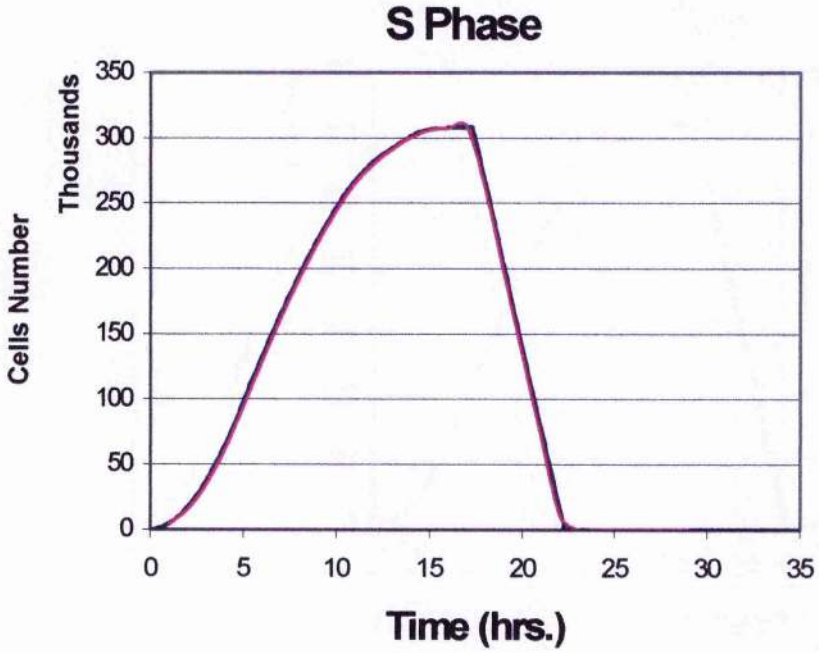

GRAPH 11

S phase. Comparing and testing reproducibility in the new model

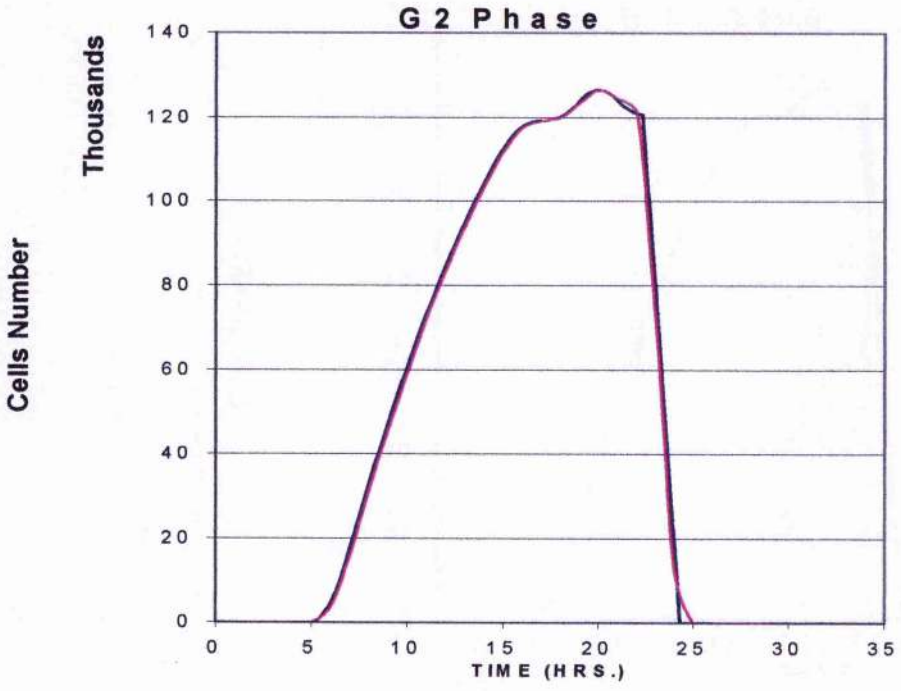

GRAPH 12

G2 Phase. Comparing and testing reproducibility in the new model

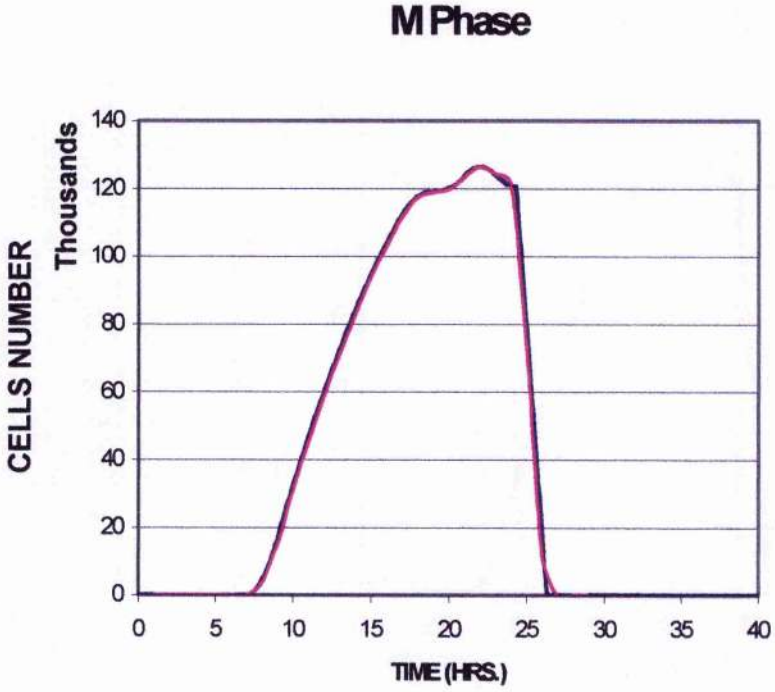

GRAPH 13

M Phase. Comparison between old and New version of CELCYMUS

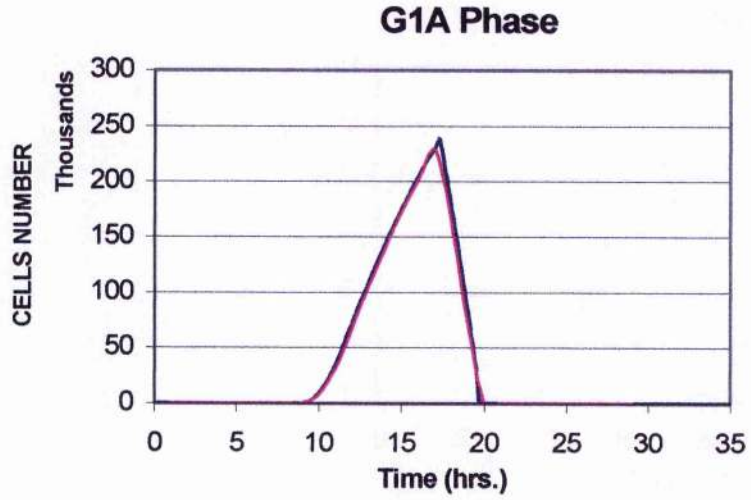

GRAPH 14

G1A Phase. Comparison between old and New version of CELCYMUS

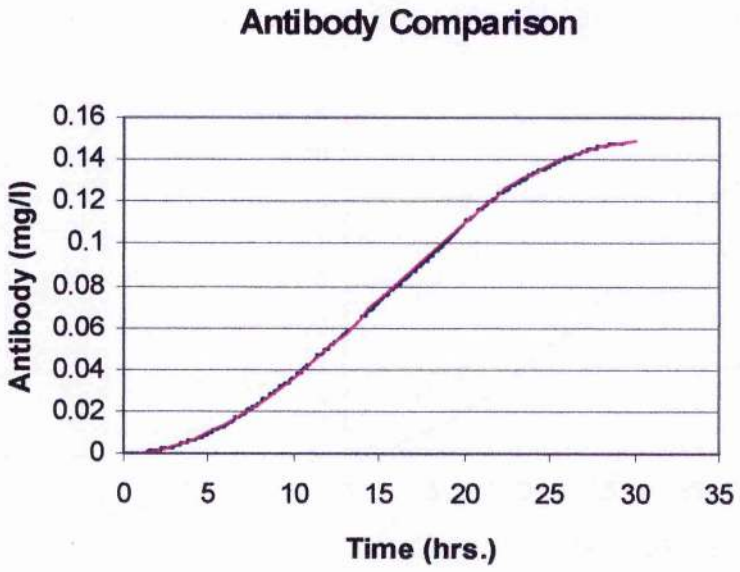

GRAPH 15.
Antibody Production in mm321 Hybridome cell line

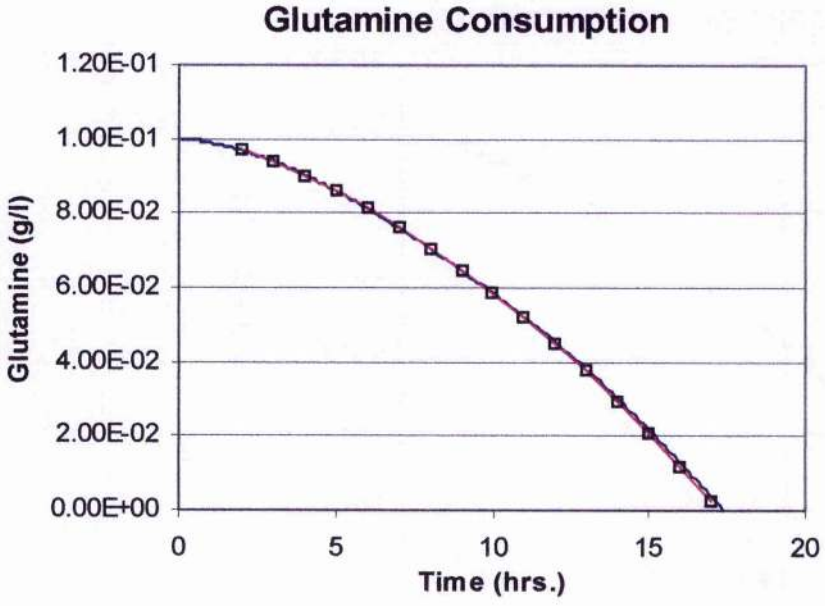

GRAPH 16
Glutamine Consumption in mm321 Hybridome cell line
Comparison in between old and new version of CELCYMUS

APPENDIX C

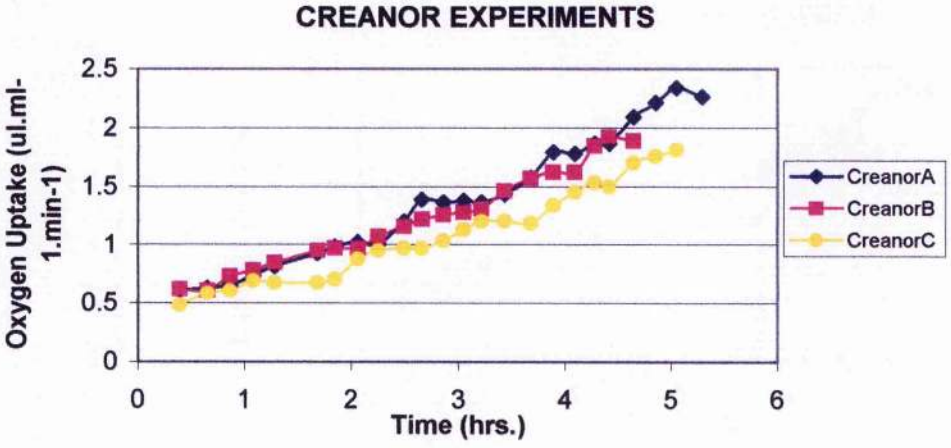

GRAPH 1
Oxygen Consumption. Simulations from Creanor experiments.

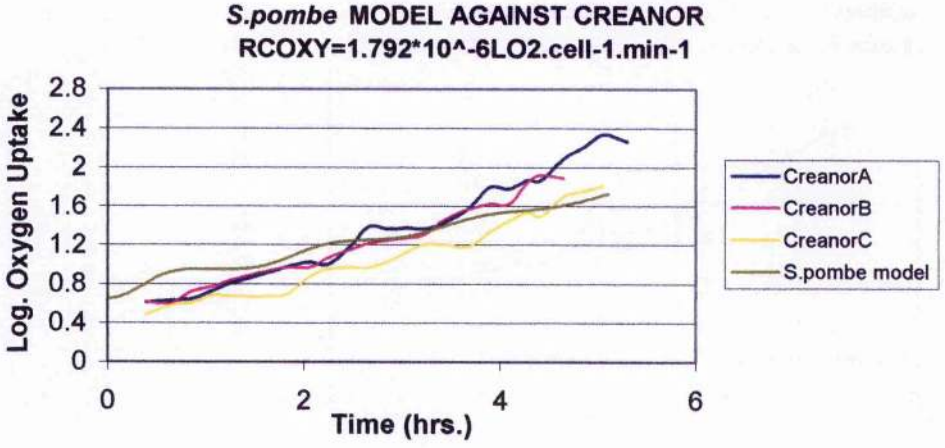

GRAPH 2
Comparison between experimental and simulated experiments

BATCH EXPERIMENTS. CELL NUMBER AND GLUCOSE CONSUMPTION

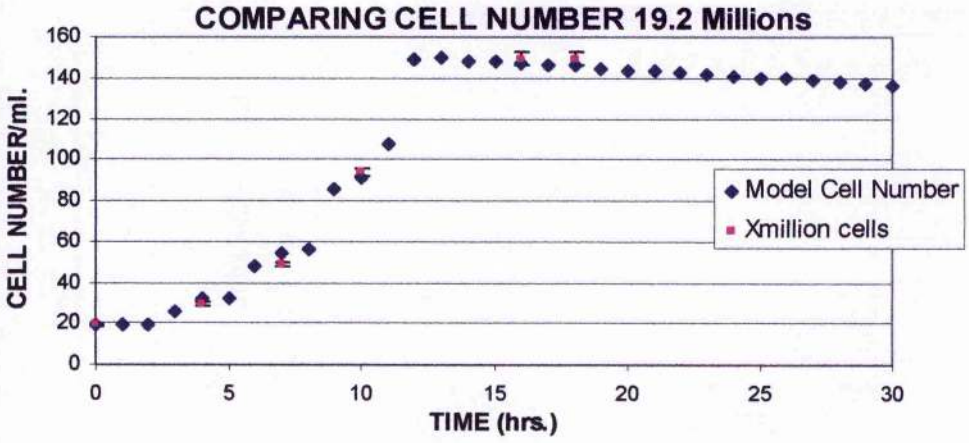

GRAPH 3

Initial Cell number 19.2 Million cells. Comparison with Fotuhi's experiments. Batch with 2% Glucose

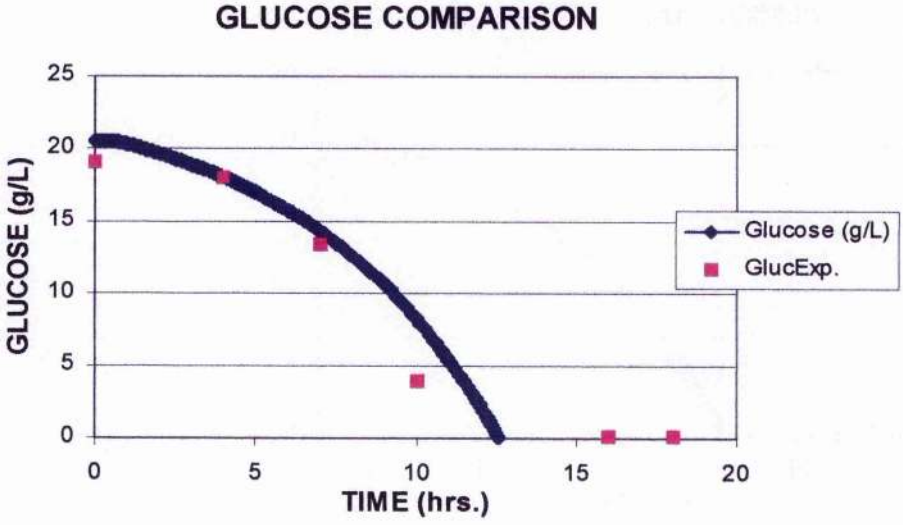

GRAPH 4

2%Glucose. Experimental and simulated consumption of Glucose.

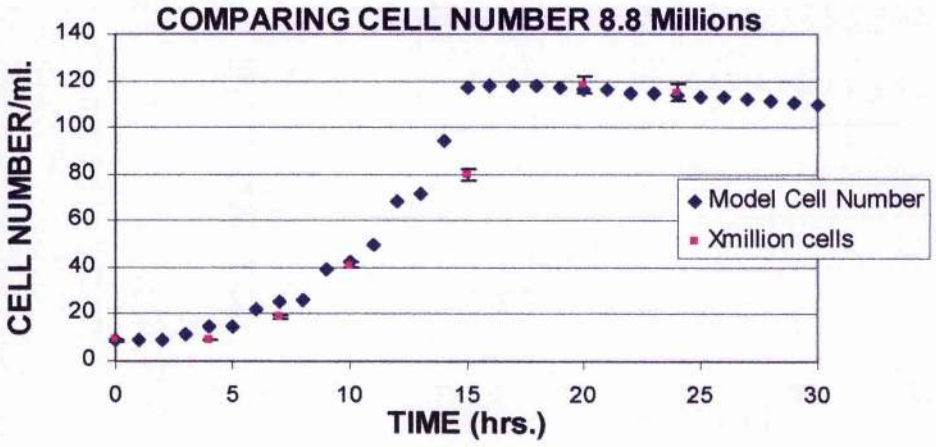

GRAPH 5

Initial Cell number 8.8 Million cells. Comparison with Fotuhi's experiments. Batch with 2% Glucose

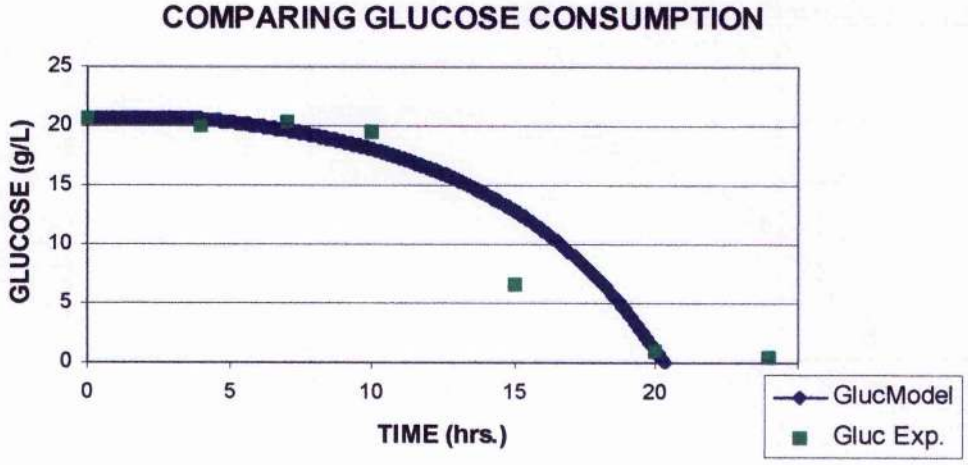

GRAPH 6

2%Glucose. Experimental and simulated consumption of Glucose.

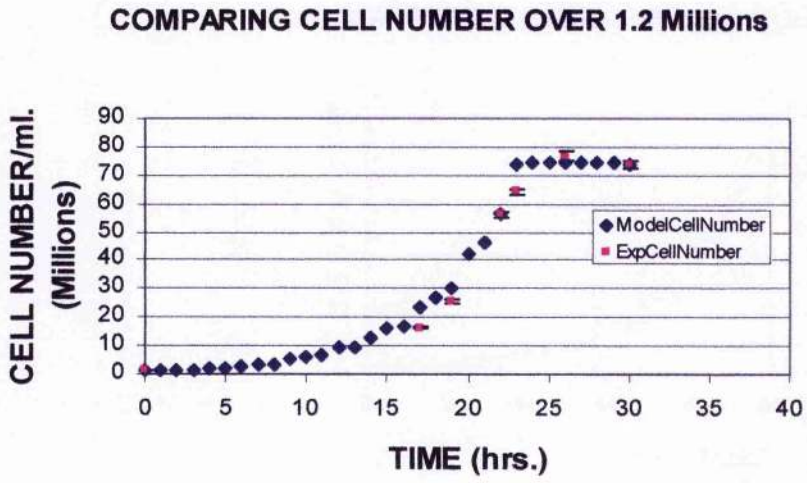

GRAPH 7

1.2 Million Cells. Initial cell number compared to Fotuhi's experiments

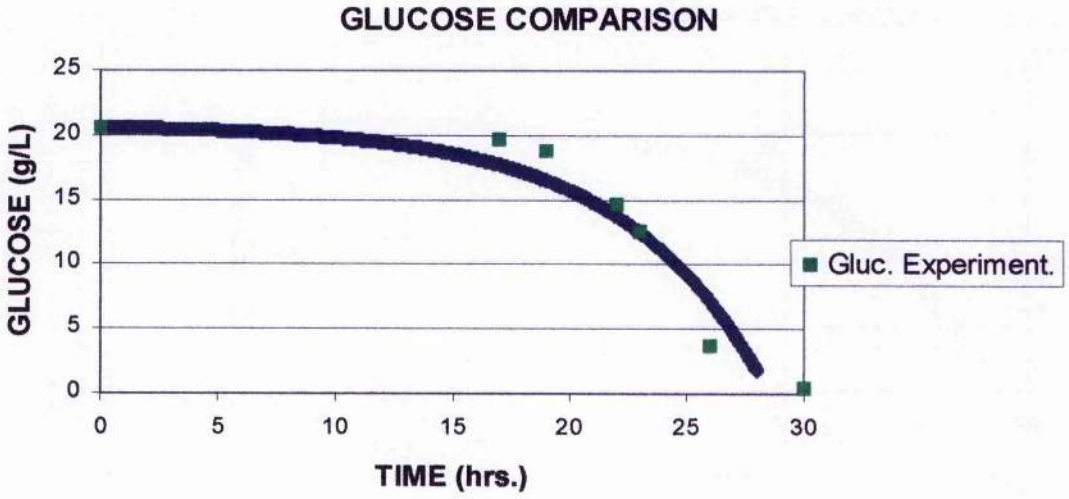

GRAPH 8

2%Glucose. Experimental and simulated consumption of Glucose.

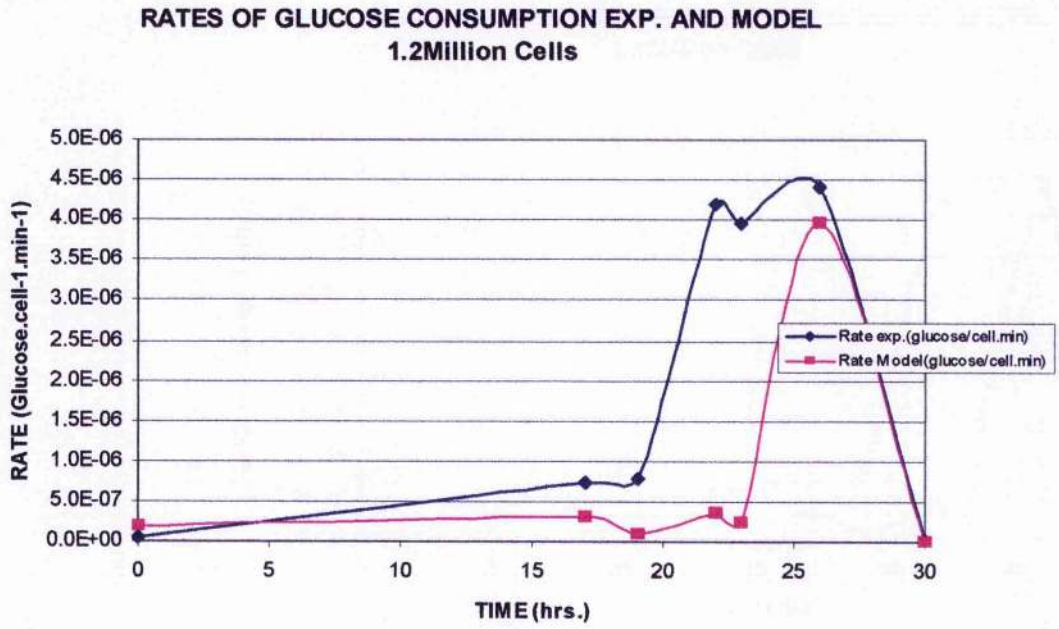

GRAPH 9

1.2 Million cells. Comparison with Fotuhi's experiments. Batch with 2% Glucose

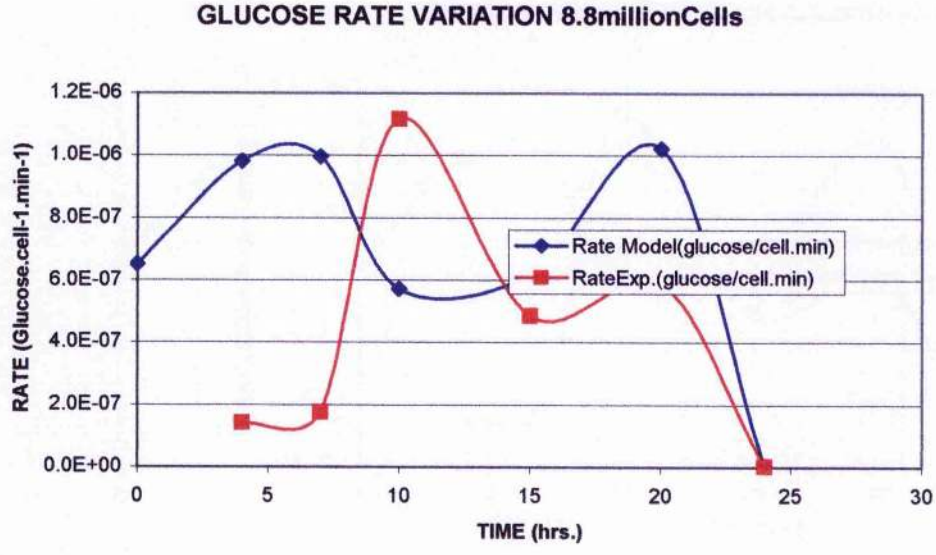

GRAPH 10

8.8 Million cells. Comparison with Fotuhi's experiments. Batch with 2% Glucose

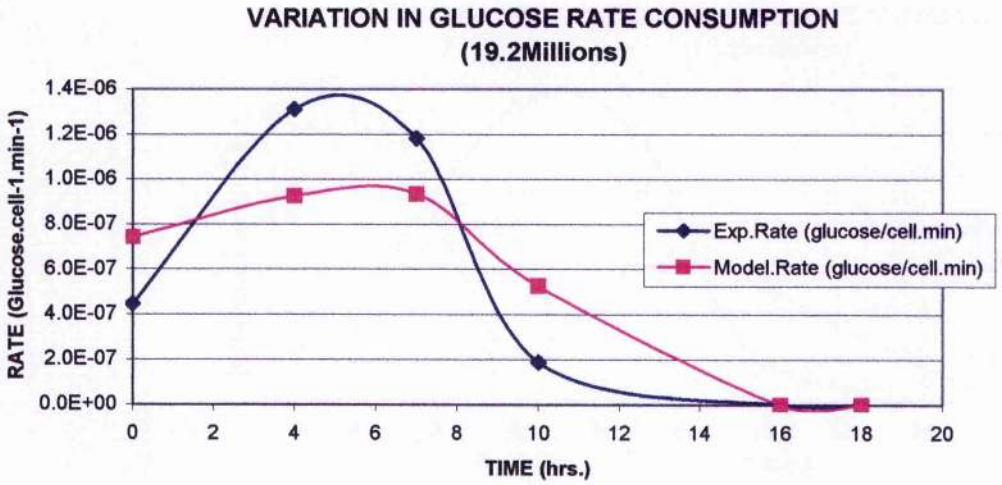

GRAPH 11

19.2 Million cells. Comparison with Fotuhi's experiments. Batch with 2% Glucose

EXPERIMENTAL AND SIMULATED REPEATED BATCH RESULTS

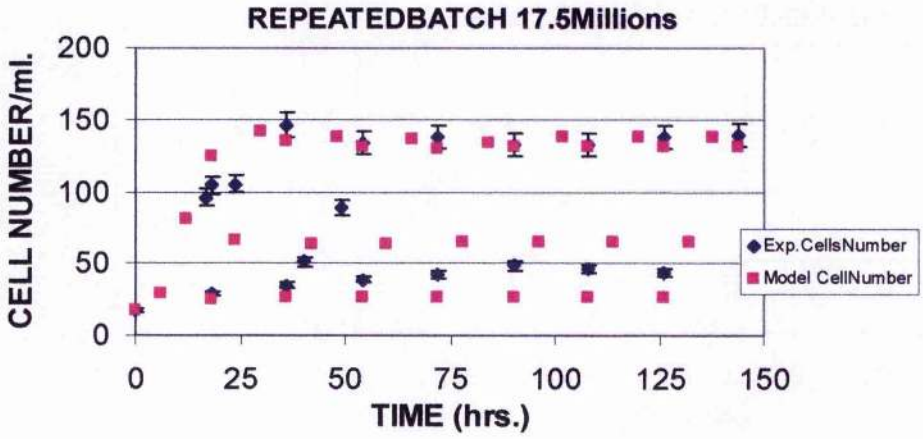

GRAPH 12
Cell number in repeated batch experiments compared to Fotuhi's 2002 (HF=80%, DCT= 18, Initial Cell number=17.5x10^6)

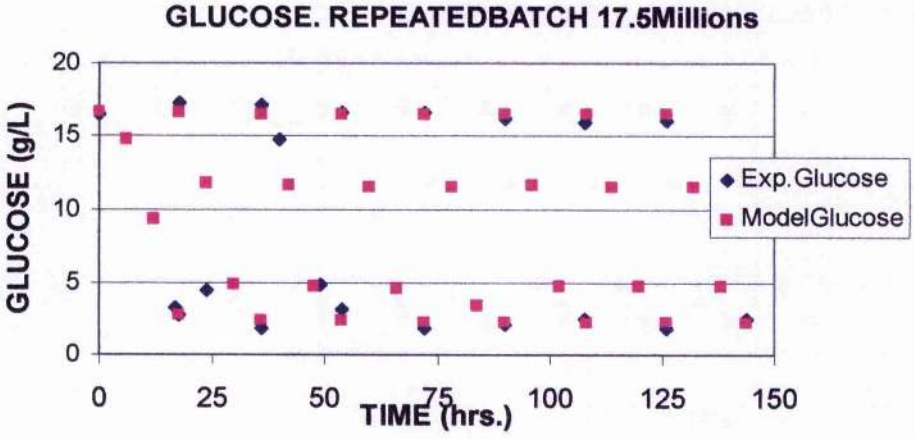

GRAPH 13
Glucose in medium repeated batch experiments compared to Fotuhi's 2002 (HF=80%, DCT= 18, Initial Glucose=20g/L)

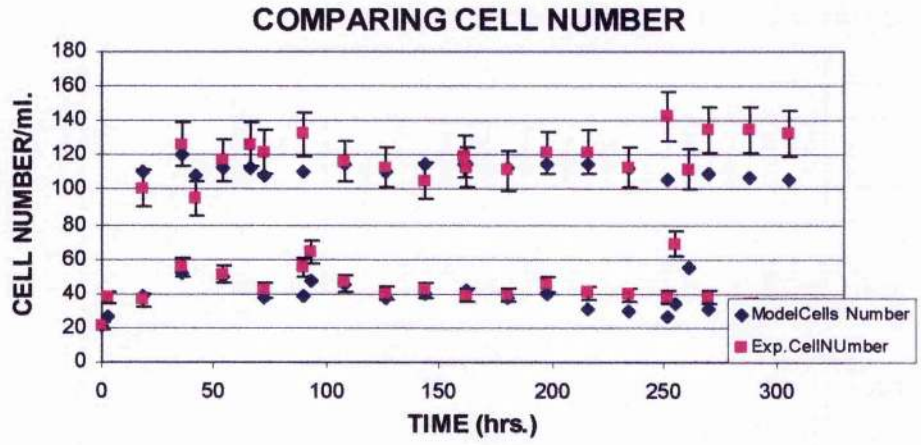

GRAPH 14

Cell number in repeated batch experiments compared to Fotuhi's 2002 (HF=80%, DCT= 18, Initial Cell number=$21x10^6$)

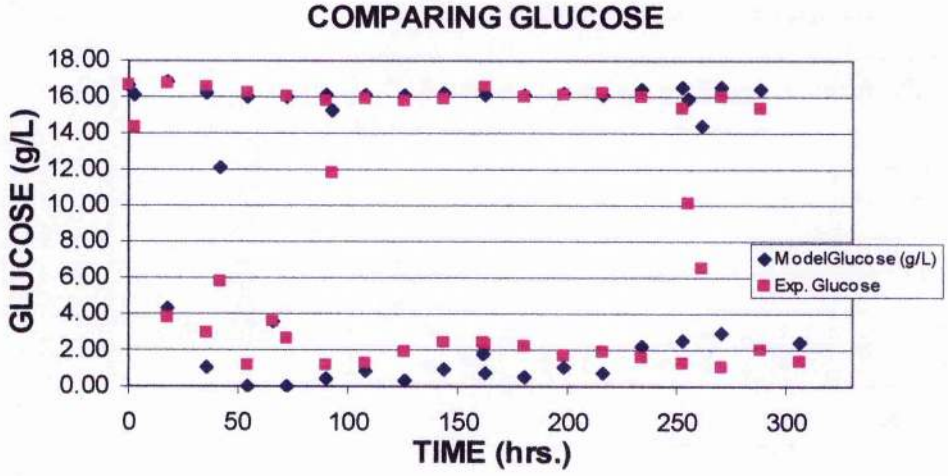

GRAPH 15

Glucose in medium. Repeated batch experiments compared to Fotuhi's 2002 (HF=80%, DCT=18, Initial Glucose=20g/L)

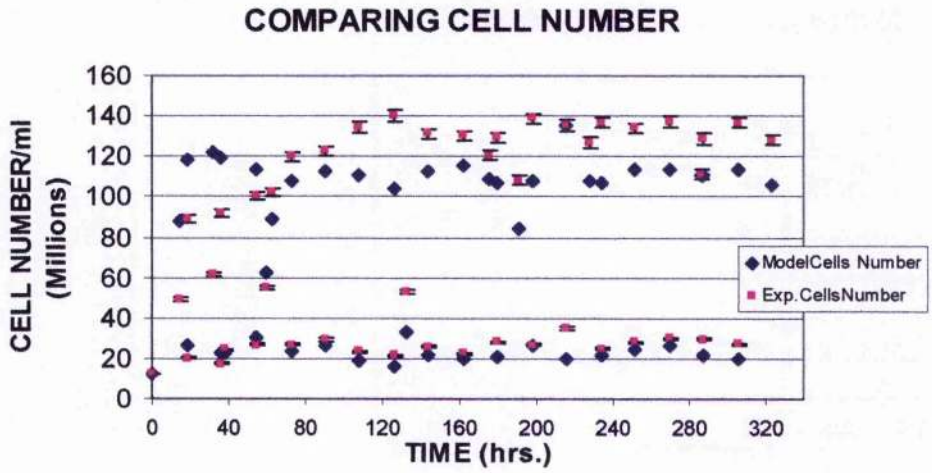

GRAPH 16
Cell number in repeated batch experiments compared to Fotuhi's 2002 (HF=80%, DCT= 18, Initial Cell number=$12.2x10^6$)

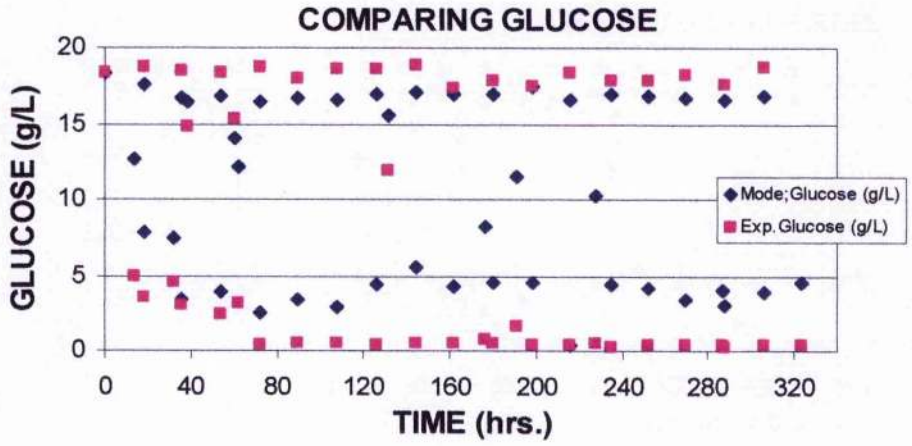

GRAPH 17
Glucose in medium. Repeated batch experiments compared to Fotuhi's 2002 (HF=80%, DCT= 18, Initial Glucose=20g/L)

APPENDIX D

Table 1: Cell Cycle times for *S.pombe* and its mutants

Strain	*N°Cycles analysed*	*BL (μm)*	*DL (μm)*	*CT (min)*	CV_{CT} *(%)*	CV_{DL} *(%)*	*Slope Ext/BL(μm/μm)*	*Slope CT/BL(min/μm)*	*CT difference between daughters(min)*	CV_{DA}*(%)*
WT(972)	164	$8.2^{0.52}$	$14.4^{0.8}_{5}$	148^{16}	10.8	5.9	-0.89	-19.1	12^{10}	3.2
WT(972-diploid)	190	$12.4^{0.8}_{8}$	$22.2^{1.6}_{0}$	159^{16}	10.4	7.2	-0.37	-8.8	15^{12}	3.0
Wee1-6	105	$4.7^{0.58}$	$7.9^{0.83}$	172^{34}	19.6	10.5	-0.97	-35.3	25^{29}	7.1
Wee1-6 diploid	105	$6.8^{0.59}$	11.9^{100}	160^{23}	14.4	8.4	-0.77	-19.9	14^{13}	3.9
Wee1-50	156	$5.0^{0.56}$	$8.2^{0.85}$	146^{30}	20.4	10.4	-0.55	-33.9	20^{21}	6.6
Wee1Δ	129	$5.0^{0.56}$	$8.4^{0.86}$	155^{30}	19.5	10.2	-1.01	-36.3	21^{19}	5.8
Cdc2-3w	137	$5.4^{0.48}$	$9.0^{0.69}$	143^{18}	12.4	7.7	-0.62	-20.9	16^{12}	6.1
Cdc2-1w	107	$5.5^{0.51}$	$9.1^{1.00}$	157^{27}	17.4	9.9	-0.46	-18.0	21^{15}	5.9
Cdc2-33wee1-6	40	$5.2^{0.42}$	$8.5^{0.56}$	217^{31}	14.3	6.6	-0.27	-46.1	36^{26}	5.4
Cdc2-3w cdc25Δ	115	$9.7^{0.77}$	$17.6^{1.2}_{6}$	159^{24}	15.3	7.2	-0.87	-21.3	24^{16}	4.3
Cdc2-3w cdc25Δpyp3Δ	80	$11.8^{1.1}_{0}$	$21.3^{1.9}_{7}$	153^{31}	20.0	9.2	-1.20	-17.8	27^{23}	4.0
Wee1-50 cdc25Δ	465	$9.9^{1.93}$	$18.2^{3.7}_{1}$	131^{47}	35.8	20.3	*	*	37^{37}	5.1
Cdc2-M35	116	$11.0^{0.9}_{6}$	$20.1^{1.5}_{1}$	219^{24}	10.8	7.5	-0.32	-15.1	20^{18}	4.7
Cdc2-33	148	$8.5^{0.48}$	$15.2^{0.7}_{6}$	197^{21}	10.5	5.0	-0.40	-26.5	18^{13}	3.2

Mean values plus s.d. as superscript. BL, birth length; DL, division length; CT, cycle time; CV, coefficient of variation; Ext, total extension (DL-BL); DA, assymetry between daughter cells . All at 35°C except for strains 9,10,14 at 29°C. Disruptions (Δ), were :ura4^{+} ura4-D18 in strains 6,11 12,13, which also had a leu1 marker. Strains 3 and 4 were from one film separated by BL in each cycle. All strains were h^{-} . Since BL and DL were measured in some oncomplete cycles, the s.e.m. will be less than the value to be derived from the s.d. and the number of complete cycles in column 2. The number of daughter cells in column 10 is less than that in column 2. For * in columns 8 and 9, see Fig.6.

FIGURE 1. MBO CONTROLLER

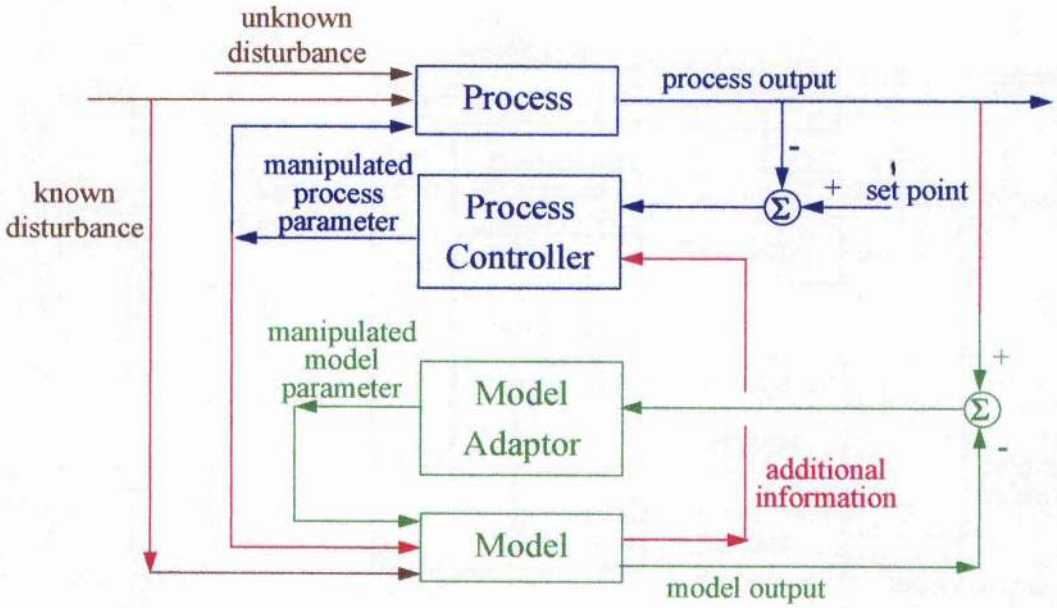

Schematic of the model-based observer (MBO) control strategy.

GRAPH 10. SIMULATION OF BATCH REACTOR 1% GLUCOSE

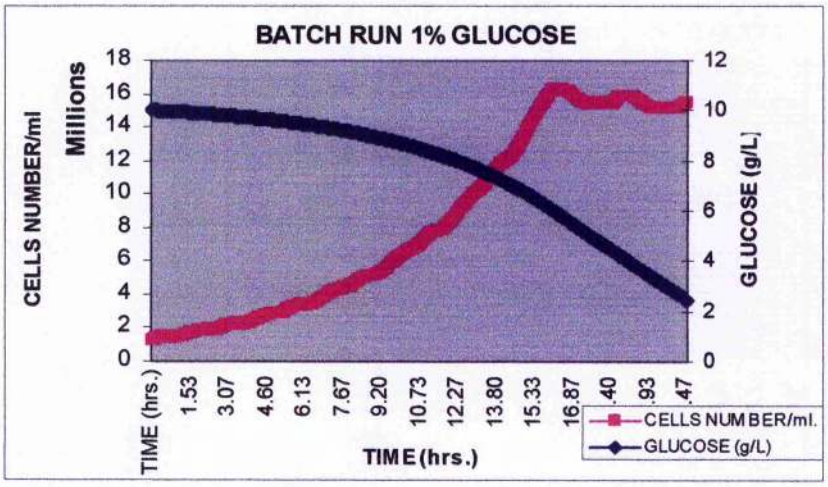

1.5 Million cell/ml at 1% glucose concentration against cell number

GRAPH 11. Cell number. Glucose 1%, Initial cell number 1.5 Million/ml

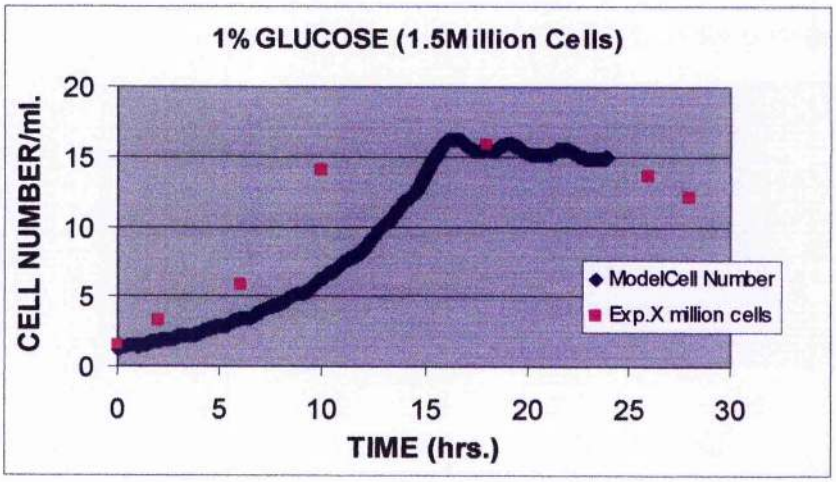

STUDYING POSSIBLE CHAOTIC GROWTH KINETICS

100 Cycles. Initial cell number = 17.5 Millions/ml. DCT = 18hr. HF = 80%

GRAPH 1. First 25 Batches

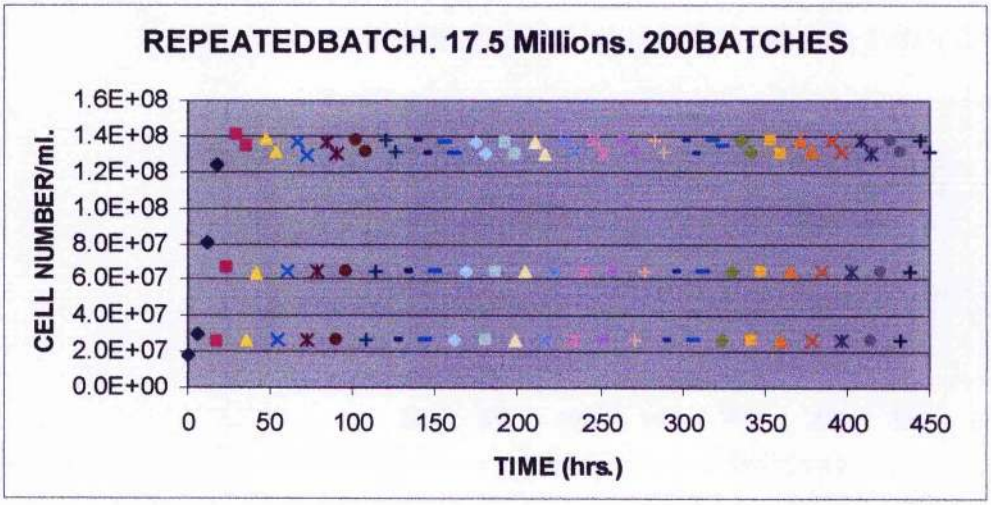

GRAPH 2. 25 - 50 Batches

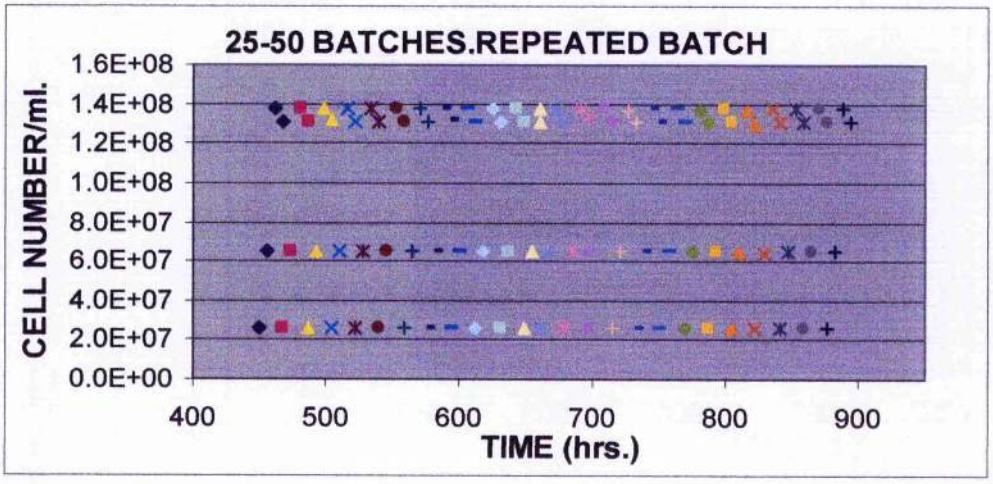

GRAPH 3. 50 – 75 Batches

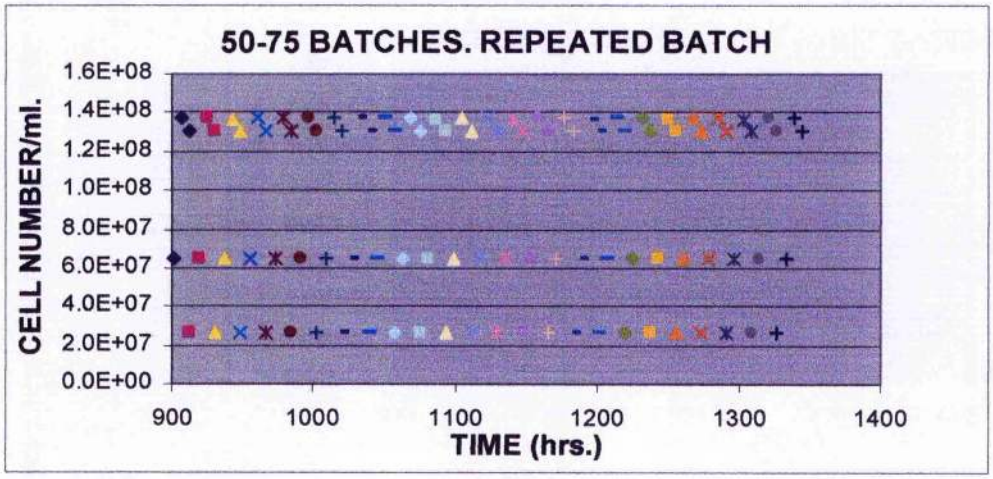

GRAPH 4. 75 – 100 BATCHES

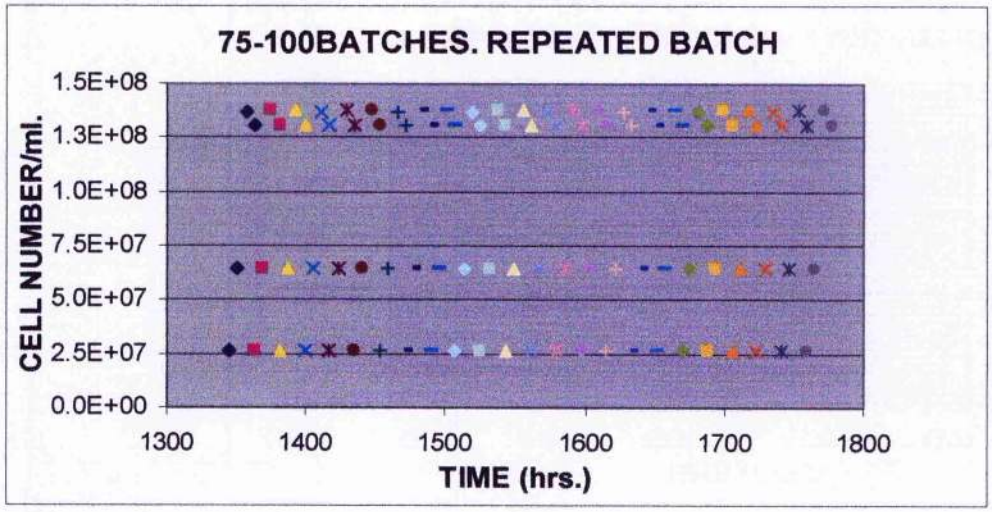

STUDYING POSSIBLE CHAOTIC GROWTH KINETICS

GRAPH 5. 200 Cycles. Initial cell number = 20 Millions/ml. DCT = 18hr. HF = 80%

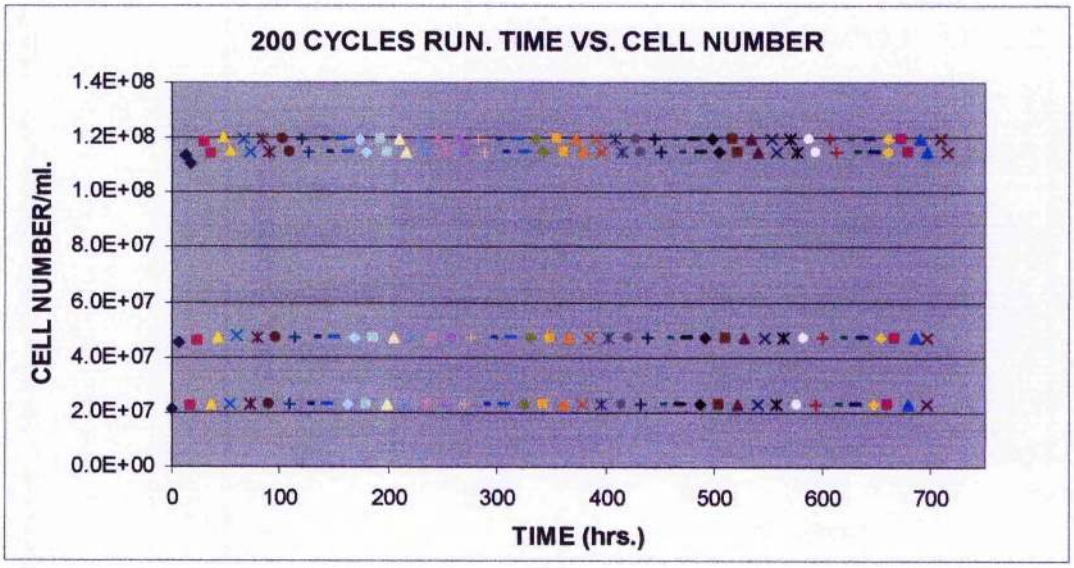

First 40 Batches in a repeated batch bioreactor

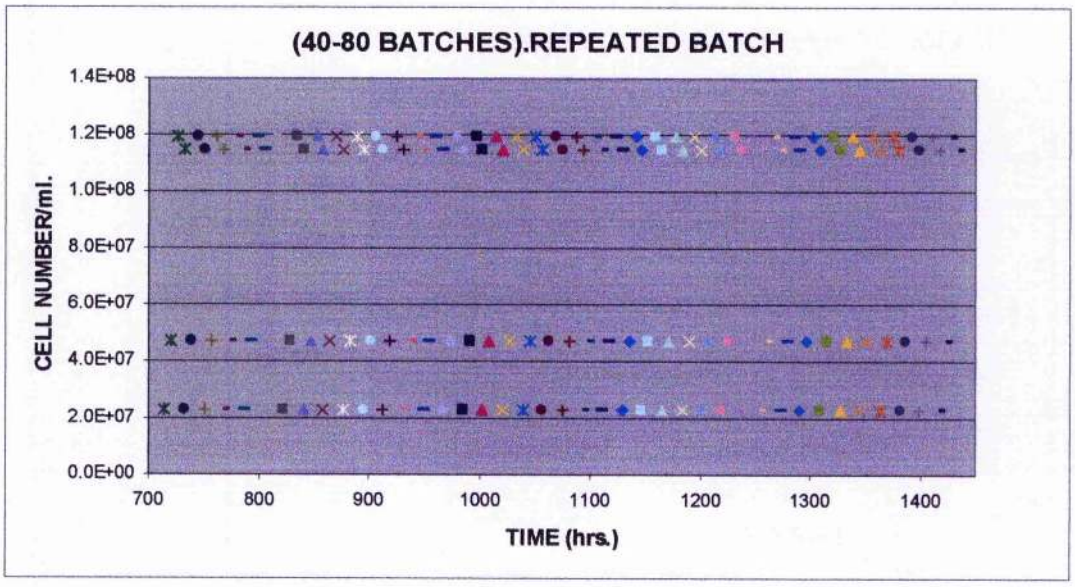

GRAPH 6. 40 – 80 Batches

GRAPH 7. 80 – 120 Batches

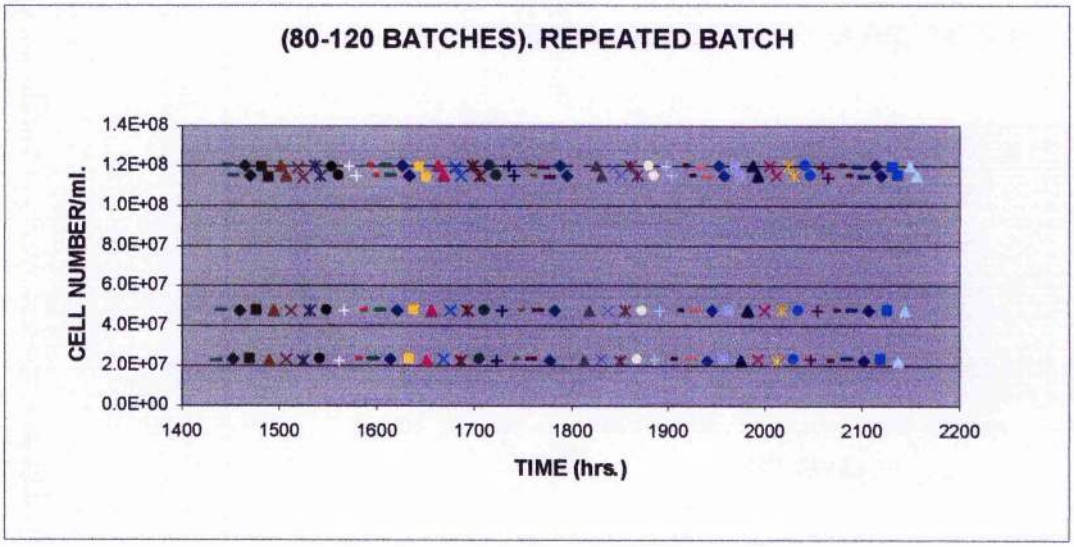

GRAPH 8. 120 – 160 Batches

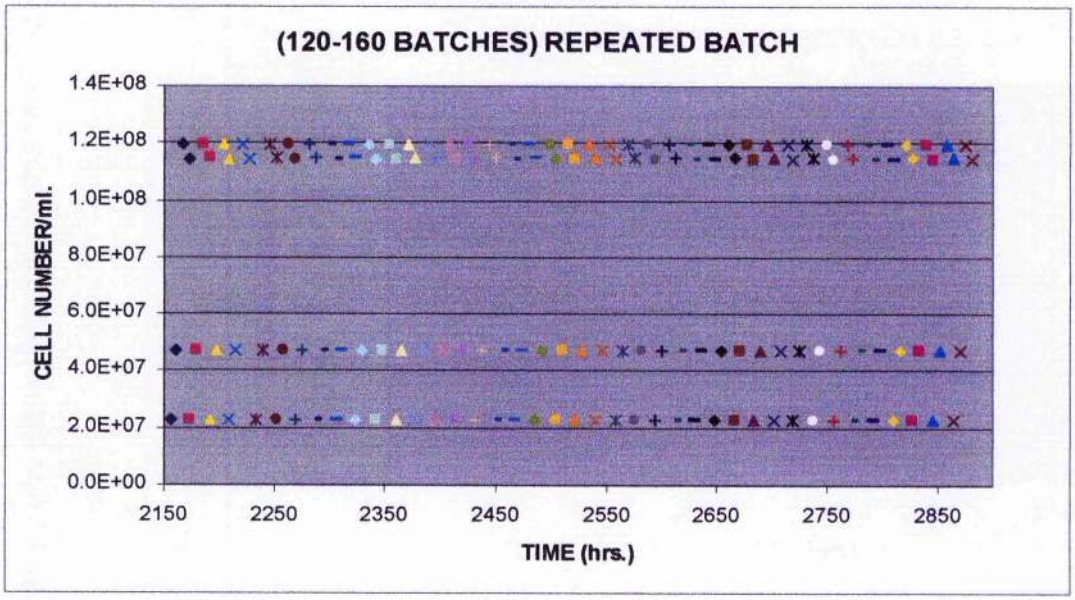

GRAPH 9. 160 – 200 Batch